Thermofluorimetric, magnetic and lateral flow aptamer based assays for point of care applications

Dissertation

der Mathematisch-Naturwissenschaftlichen Fakultät

der Eberhard Karls Universität Tübingen

zur Erlangung des Grades eines

Doktors der Naturwissenschaften

(Dr. rer. nat.)

vorgelegt von

Mostafa Mahmoud

aus Kairo, Ägypten

Tübingen

2020

Gedruckt mit Genehmigung der Mathematisch-Naturwissenschaftlichen Fakultät der Eberhard Karls Universität Tübingen.

Tag der mündlichen Qualifikation:	19.11.2020
Stellvertretender Dekan:	Prof. Dr. József Fortágh
1. Berichterstatter:	Prof. Dr. Stefan Laufer
2. Berichterstatter:	Prof. Dr. René Csuk

Advisors: Prof. Dr. Stefan Laufer
Prof. Dr. Hans-Peter Deigner

Mostafa Mahmoud

Abstract

Diagnostic assays are commonly performed in central laboratories. They rely on sophisticated analytical methods requiring expensive and bulky equipment as well as highly trained personnel. On the other hand, point of care offers an alternative for fast turnaround, simple and affordable diagnostics, thus enabling early medical intervention and a better clinical outcome. So far, point of care has failed to deliver on the small molecules front. This is due to the fact that most point of care assays are based on immunoassays. Based on antibodies, the quantification of small molecules remains a challenge due to their intrinsic properties and the unavailability of different binding epitopes. This limits available formats to competitive assay with its associated drawbacks e.g. inversely proportional signal and difficulty of labeling target molecules. In contrast, aptamers offer alternative detection formats that could enable the design of point of care for small molecules. Nevertheless, previous approaches lacked the required simplicity, sensitivity, multiplexing, or high-throughput. Although the first two are considered basic requirements, they are dependent and usually, a compromise has to be made on either. Building on this, this work aimed to tackle these bottlenecks through different strategies.

In the first project, aptamers were combined with a qPCR instrument for a bench-top high-throughput method for small molecules. Through measuring the melting point of the aptamer beacons, a quantification of ethanolamine was possible. Unlike ELISA and other antibody-based approaches, there are no washing or blocking steps. This is the first report on the quantification of small molecules based on measuring aptamer melting temperatures. Binding to the target results in a structure stabilization and a corresponding increase in the melting temperature. While the assay offers a high-throughput and sensitivity, it still is relatively complex in comparison to hand-held point of care (POC) assays. Therefore, my second project was focused on a hand-held POC with no readout devices necessary.

In the second project, the focus was to design a simple yet sensitive platform for small molecules (e.g. ethanolamine) in a low resource setting. To this aim, magnetic particles were functionalized with ethanolamine binding aptamers and used in a plastic capillary platform. The assay was based on the strand displacement format and 3 layers were built on the capillary surface. Firstly, the capillaries were coated with a layer of anchoring oligonucleotides. To this layer aptamer-magnetic particles were hybridized

resulting in the second layer. Additionally, to avoid free aptamers (i.e. not hybridized), oligonucleotide-magnetic particles were hybridized to the aptamers facing away from the capillary surface. When an ethanolamine containing sample is introduced, the magnetic particles are displaced and collected using a permanent magnet. This resulted in a visually detectable magnetic spot. The combination of simplicity and visual detection make this assay ideal for low resource settings.

While the first two platforms are theoretically capable of multiplexing, this remains experimentally challenging. For the qPCR instrument based method, one will need aptamers with significantly different melting temperatures. Alternatively, indirect multiplexing could be achieved through the use of short beacons competing for the target binding site. However, this requires full characterization of the aptamer's binding structure. On the other hand, the capillary platform will need color coding of the magnetic particles. This is experimentally challenging giving the present technologies. Based on the previous, the third project aimed at developing a POC with multiplexing capabilities. Accordingly, a duplex LFA was designed to quantify interleukin 6 (IL-6) and thrombin simultaneously. The platform consisted of red-emitting QD-thrombin binding aptamer and green-emitting QD-IL-6 binding antibody, combined with a lateral flow with a streptavidin test line and anti-mouse antibody as a control line. The readout setup based on a smartphone combined with a 3D-printed dark box with a built-in UV light. This enabled detecting both analytes on the same test line without the need for physical emission filters.

Advisors: Prof. Dr. Stefan Laufer
Prof. Dr. Hans-Peter Deigner

Mostafa Mahmoud

Kurzfassung

Diagnostische Tests werden üblicherweise in zentralen Labors durchgeführt. Sie stützen sich auf hochentwickelte Analysemethoden, die teure und sperrige Geräte sowie hochqualifiziertes Personal erfordern. Andererseits bietet der Point-of-Care eine Alternative für eine schnelle, einfache und erschwingliche Diagnostik und ermöglicht so eine frühzeitige medizinische Intervention und ein besseres klinisches Ergebnis. Bislang hat das Point-of-Care-System an der Front der kleinen Moleküle versagt. Dies ist darauf zurückzuführen, dass die meisten Point-of-Care-Assays auf Immunoassays basieren. Die Quantifizierung von kleinen Molekülen auf der Basis von Antikörpern bleibt aufgrund ihrer intrinsischen Eigenschaften und der Nichtverfügbarkeit verschiedener Bindungsepitope eine Herausforderung. Dies beschränkt die verfügbaren Formate auf kompetitive Assays mit den damit verbundenen Nachteilen, z.B. umgekehrt proportionales Signal und Schwierigkeit der Markierung von Zielmolekülen. Im Gegensatz dazu bieten Aptamere alternative Detektionsformate, die die Gestaltung von Point-of-Care für kleine Moleküle ermöglichen könnten. Dennoch fehlte den bisherigen Ansätzen die erforderliche Einfachheit, Sensitivität, Multiplexing oder Hochdurchsatz. Obwohl die ersten beiden als Grundvoraussetzungen betrachtet werden, sind sie voneinander abhängig und in der Regel muss bei beiden ein Kompromiss eingegangen werden. Darauf aufbauend zielte diese Arbeit darauf ab, diese Engpässe durch verschiedene Strategien anzugehen.

Im ersten Projekt wurden Aptamere mit einem qPCR-Instrument für ein Bench-Top-Hochdurchsatzverfahren für kleine Moleküle kombiniert. Durch die Messung des Schmelzpunktes der Aptamer-Beacons war eine Quantifizierung von Ethanolamin möglich. Im Gegensatz zum ELISA und anderen antikörperbasierten Ansätzen gibt es keine Wasch- oder Blockierungsschritte. Dies ist der erste Bericht über die Quantifizierung von kleinen Molekülen auf der Grundlage der Messung der Aptamer-Schmelztemperaturen. Die Bindung an das Target führt zu einer Stabilisierung der Struktur und einer entsprechenden Erhöhung der Schmelztemperatur. Obwohl der Assay einen hohen Durchsatz und eine hohe Empfindlichkeit bietet, ist er im Vergleich zu handgehaltenen Point-of-Care (POC)-Assays immer noch relativ komplex. Daher konzentrierte sich mein zweites Projekt auf einen handgehaltenen POC, für den keine Auslesegeräte erforderlich sind.

Im zweiten Projekt lag der Schwerpunkt auf der Entwicklung einer einfachen, aber empfindlichen Plattform für kleine Moleküle (z.B. Ethanolamin) in einem ressourcenar-

men Umfeld. Zu diesem Zweck wurden magnetische Partikel mit Ethanolamin-bindenden Aptameren funktionalisiert und in einer Kunststoff-Kapillar-Plattform verwendet. Der Assay basierte auf dem Strangverdrängungsformat und auf der Kapillaroberfläche wurden 3 Schichten aufgebaut. Zuerst wurden die Kapillaren mit einer Schicht aus verankernden Oligonukleotiden beschichtet. An diese Schicht wurden Aptamer-Magnetpartikel hybridisiert, wodurch die zweite Schicht entstand. Um freie (d.h. nicht hybridisierte) Aptamere zu vermeiden, wurden zusätzlich Oligonukleotid-magnetische Partikel an die von der Kapillaroberfläche abgewandten Aptamere hybridisiert. Wenn eine ethanolaminhaltige Probe eingeführt wird, werden die magnetischen Partikel verdrängt und mit einem Permanentmagneten aufgefangen. Dies führte zu einem visuell erkennbaren magnetischen Fleck. Durch die Kombination von Einfachheit und visueller Detektion ist dieser Assay ideal für den Einsatz bei geringen Ressourcen geeignet.

Obwohl die ersten beiden Plattformen theoretisch in der Lage sind, multiplexen zu können, bleibt dies experimentell herausfordernd. Für die auf dem qPCR-Instrument basierende Methode benötigt man Aptamere mit signifikant unterschiedlichen Schmelztemperaturen. Alternativ könnte indirektes Multiplexing durch die Verwendung von kurzen Beacons erreicht werden, die um die Zielbindungsstelle konkurrieren. Dies erfordert jedoch eine vollständige Charakterisierung der Bindungsstruktur des Aptamers. Auf der anderen Seite wird die Kapillarplattform eine Farbkodierung der magnetischen Partikel benötigen. Dies ist bei den derzeitigen Technologien experimentell eine Herausforderung. Auf der Grundlage des vorhergehenden, zielte das dritte Projekt auf die Entwicklung eines POC mit Multiplexing-Fähigkeiten ab. Dementsprechend wurde ein Duplex-LFA entworfen, um Interleukin 6 (IL-6) und Thrombin gleichzeitig zu quantifizieren. Die Plattform bestand aus rot-emittierendem QD-Thrombin-bindendem Aptamer und grün emittierendem QD-IL-6-bindendem Antikörper, kombiniert mit einem Lateral Flow mit einer Streptavidin-Testlinie und Anti-Maus-Antikörper als Kontrolllinie. Der Ausleseaufbau basiert auf einem Smartphone, kombiniert mit einer 3D-gedruckten dunklen Box mit eingebautem UV-Licht. Dies ermöglichte den Nachweis beider Analyten auf derselben Testlinie, ohne dass physikalische Emissionsfilter erforderlich waren.

Contents

Acknowledgments

I would like to start by expressing my deepest gratitude for Prof. Dr. Hans-Peter Deigner for giving me the opportunity to work in his group. He has offered me his time and support during my thesis, encouraged and guided me in order to pursue my ideas, presented me with various challenging projects, and helped keep my motivation when things were going rough. I thank him for the mentoring and for making this dissertation possible.

I would like to express my appreciation and gratitude for Prof. Dr. Stefan Laufer for his guidance and support without which this work would not have been possible.

Throughout the time of this work, many other friends and colleagues offered direct and indirect support which helped me round my ideas and shape them during my doctoral studies. I would like to deeply thank Christoph Ruppert for his friendship and sharing many personal and scientific subjects. Lars Kaiser for the fruitful scientific discussions and the motivating attitude. The HFU family for their personal support, namely: Marina Taichrib, Helena Herner, Helga Weinschrott, and Simone Rentschler.

Lastly, I thank my family for their believe and support through everything.

Chapter 1

Introduction

1.1 Background

There is a great demand for point of care platforms that are simple, sensitive and with multiplexing capabilities. Advances in the single components and the readout technology has failed to deliver on one or more fronts e.g. simplicity, sensitivity or throughput. This is usually due to the limitations imposed by the biological components in the platform. Although, monoclonal antibodies have provided high affinity molecular recognition element, yet the detection sensitives are majorly governed by the assay format.

Small molecules are a specially challenging target for simple point of care platforms. Their small size combined with the availability of only one binding epitope limits the immunoassay formats to a competitive assay. On the other hand, aptamers offer an alternative and unlimited possibilities for small molecules assay design.

In this dissertation, aptamers were used to design non conventional point of care assay platforms with focus on small molecules. This chapter will introduce the important components of point of care platforms as well as the bottlenecks and how this work contributes to solving them.

1.1.1 Small Molecules

There is no concrete description of the size and molecular weight limit of a certain molecule, in the literature, for it to be considered a small molecule. This depends mainly on the field of application where the molecules are being used[1]. According to (Ward et al., and Vanholder et al.),[2,3] small molecules are "organic, non-peptide compounds". However the criteria stated by (Dunn)[4] for small molecules are: first, "it is not directly encoded by the genome", second " it is synthesized by specific enzymes" and third "it is non polymeric". As for the molecular weight, the upper limits vary from 500 to 1000 Da[4–7]. Nevertheless, small molecules such as amino acids, lipids and sugars are of great importance in different aspects of disease pathology, treatment and are invaluable biomarkers. However, their detection and quantification using conventional immunoassays remains challenging owing to their innate properties e.g. small size, toxicity and the availability of only one epitope.

1.1.2 Point of care

Common approaches for the detection and quantification of biomarkers are dependent on central laboratories. They are mostly based on sophisticated instruments combined with highly trained personnel. Thus providing precise data for a better clinical decision and outcome. However, they are not suitable for on site analysis or when a fast turn around time is needed[8]. On the other hand, point of care tests were developed to overcome these limitations. Point of care testing refers to "a diagnostic test that is performed near the patient or treatment facility, has a fast turnaround time, and may lead to a change in patient management"[9]. Eventually providing faster results with no or minimum device requirements[10–15].

Lateral flow assays are the most commonly used POC devices e.g. pregnancy test. Lateral flow (immuno)assays (LF(I)As) are a class of immunochromatographic paper based assays. LFAs are simple, fast and cost efficient diagnostic tools. They have been developed for a variety of applications and targets including infectious agents (influenza viruses), metabolite disorders (diabetes), toxins (aflatoxin) and drugs (cocaine) as reviewed in[16]. LFAs generally consist of a sample pad, a conjugate pad, a detection area, and an absorbent pad. The detection area contains control and test lines with immobilized molecular recognition elements[17]. The molecular recognition element as well as

the assay format dictates the performance of a given LFA [18,19].

1.1.3 Molecular recognition and assay formats

The sensitive detection of a target molecule requires a molecular recognition element (MRE) with high affinity and specificity. Antibodies are the most commonly used molecular recognition element[20]. Their obvious advantages and variable assay formats they offer led to their implementation in various biosensors. LFAs are mostly designed using monoclonal antibodies in either a sandwich or a competitive format. However, in case of small molecules the format is limited to a competitive assay. Moreover, antibodies cannot be raised against toxic or non-immunogenic targets. This motivated the search for new MREs. Eventually in 1990[21,22], aptamers and their selection process (SELEX) were described.

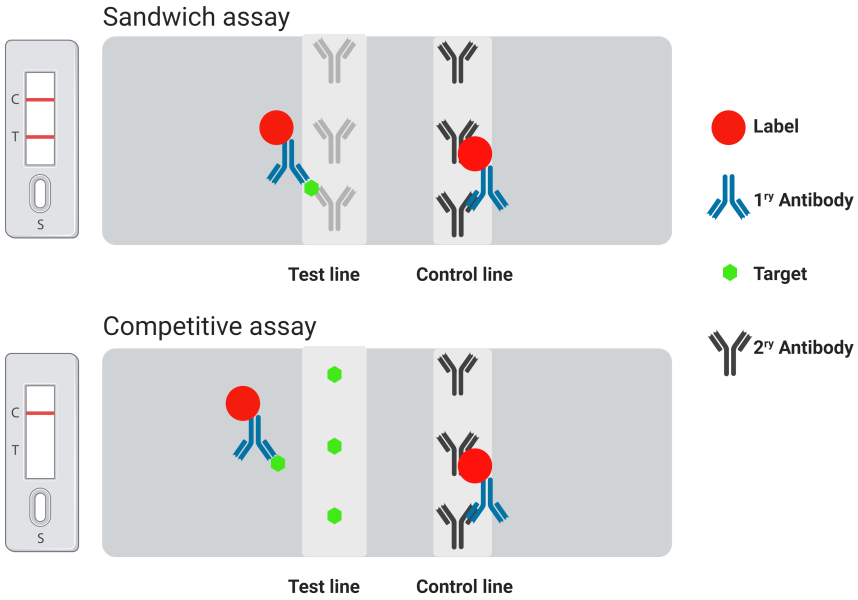

Figure 1.1: Schematic showing the sandwich and the competitive LFA format. Created with BioRender.com.

1.1.4 Aptamers

Aptamers are short DNA/RNA sequences capable of binding to targets with high specificity and affinity. They are selected in-vitro through a systematic evolution of ligands by exponential enrichment[21,22]. Although aptamers function similar to antibodies, they offer various advantages see table 1.1. Since their discovery, various aptamers have been selected against various targets e.g. proteins, metal ions, toxins, small molecules, viruses, bacteria and cells[23–26].

Table 1.1: Comparison between aptamers and antibodies as reviewed in[27,28].

	Aptamers	Antibodies
Production	In-vitro	In-vivo
Quality	No batch-to-batch variation	Batch-to-batch-variation
Target	From ions to cells	Immunogenic molecules
Stability	Thermally stable	Thermally unstable
Denaturation	Reversible	Irreversible
Size	6–30 kDa	150-180 kDa
Modifications	Easily modifiable	May lead to loss of activity

Ethanolamine binding aptamers

Ethanolamine is a small (61.08 g/mol) primary organic amine. It is essential for mammalian life as it forms the head of phosphatidylethanolamine (PE) and other lipids[29]. It is present as free mono-ethanolamine (MEA) in blood at varying concentrations (0-12 μM)[30]. Nevertheless, mammals cannot de novo synthesize MEA and only obtain it from their diet. Ethanolamine is linked with different biological and pathological processes and conditions. It can reverse low serum induced apoptosis[31], stimulate hepatocytes growth and proliferation in cell culture[32] and induce a cardio-protective effect by activating STAT-3[33]. On the other hand, it has a role in various diseases such as Alzheimer's[34], depression and bipolar disorder[35] and Parkinson's disease[36]. Moreover,

ethanolamine is toxic either through inhalation or upon skin contact[37]. Due to its small size and high polarity, MEA is difficult to separate using chromatographic techniques. This in turn hampers the development of a direct LC/MS quantification method[38]. Additionally no antibodies could be raised against MEA due to the lack of immunogenicity. This motivated the selection and optimization of a free MEA binding aptamer[39].

The ethanolamine binding aptamer initially selected by Mann et al. is a 96 nucleotide DNA aptamer. It Post SELEX optimization lead to shorter variants of the aptamer (16-42 nt)[39] without compromising the affinity (Kd = 9.6 nM for the 96 nt and the 42 nt) . The ethanolamine aptamers have been studied extensively and the binding structure[40,41] as well as the specificity[42] have been well characterized. The G rich aptamer folds into a parallel G-quadruplex conformation. Based on this knowledge, different ethanolamine aptamer sensors have been described to date[38,40,43]. Although very sensitive, most of these approaches were incompatible for a POC. table 1.2 shows the developed assays. Although the described assays are very sensitive, they still suffered from some limitations. The microarray developed by Heilkenbrinker et al.[40] used a strand displacement format combined with fluorescence readout. The assay was very sensitive, yet it needed 18 hours incubation time. On the other hand, the label free sensor based on electrochemical impedance developed by Liang et al.[43] needs only 1 hour to detect as low as 0.08 nM of MEA. Nevertheless, the sensor is quite complex and not suitable for low resource POC. Another assay made use of gold nanoparticles and strand displacement to indirectly detect MEA using LC/MS. However, LC/MS is not suitable as a POC.

Table 1.2: Summary of the assays described in the literature for MEA adapted from[44]

Method	Readout	LOD/ Incubation time	Linear range
Strand displacement Microarray	Fluorescence	10 pM/18 hours	-
Electrochemical impedance spectroscopy	Electrochemical	0.08 nM/1 hour	0.16–16 nM
Indirect LC/MS	LC/MS	1.2 nM -	5-5000 nM

Thrombin binding aptamers

Thrombin is a serine protease that plays an important role in hemostasis. It is the only enzyme that can cleave fibrinogen to insoluble fibrin. On the other hand, thrombin has a role as an anticoagulant in presence of thrombomodulin[45]. On the structural level, thrombin has an active catalytic site and two anion binding sites "exosites"[46]. These exosites finely modulate the thrombin function providing the high specificity of the proteolytic protein activity[47]. Although there are various synthetic antithrombin molecules, thrombosis and thromboembolism remains one of the major cause of disability and mortality[48]. This in term motivated the development of various thrombin binding apatmers[49–51].

Exosite I Thrombin binding aptamer (TBA) is a 15mer DNA aptamer that was selected in 1992 to bind thrombin[56]. TBA has been studied extensively through NMR spectroscopy[57–60] and x-ray crystallography[61–63]. These studies revealed the unique free and binding structure of TBA with high precision. TBA assumes an antiparallel G-quadruplex chair like structure. This structure was found to be preserved in the binding complex (fig. 1.2). TBA binds to thrombin's fibrinogen binding exosite I[54,64]. This information enabled other groups to select aptamers binding to thrombin's exosite II (HD22) (fig. 1.3)[55]. Interestingly most of the thrombin binding aptamers were developed for therapeutic applications. However, their extensive characterization lead to them being used as a model in various biosensors implementing aptamers[51].

Figure 1.2: X-ray structure of the complex between human alpha thrombin and thrombin binding aptamer. Image generated by PyMOL[52] using the PDB[53] entry 4DII[54].

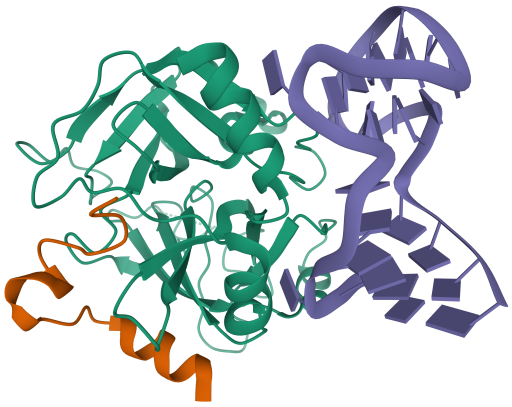

Figure 1.3: X-ray structure of human alpha thrombin in complex with HD22 aptamer bound to exosite II. Image generated by PyMOL[52] using the PDB[53] entry 4I7Y[55].

1.2 Research focus

The performance of POC still have not met the expected simplicity, sensitivity, specificity, multiplexing and throughput. The advances achieved in the technological components was hampered by limitations imposed by the biological ones (MRE). The introduction of aptamers offers an alternative MRE that offer new assay formats to fully meet the needs of POC. This can be achieved by making use of the aptamer conformational changes upon target binding. Various aptamer-based sensors have been described for protein detection[65]. On the other hand, aptamer based POC for small molecules are complex and based on sophisticated detection devices[24,65,66]. Moreover, they require various steps including washing and blocking steps[24]. In this research, different strategies were used to tackle the drawbacks and limitations of small molecules' POC. Namely, the simplicity, sensitivity, specificity, multiplexing and throughput. To this aim, model targets with corresponding well characterized aptamers were implemented in different assay formats.

1.2.1 An aptamer based thermofluorimetric assay for ethanolamine

This project aimed on the development of a small molecule assay that is simple, sensitive combined with high-throughput. To achieve this, instrumental analysis is a must. However, most ELISA based assays suffer from various limitations for small molecules detection including tedious washing and blocking steps as well as the need to label the analyte or immobilized it. Here, the assay was based on the aptamer conformational changes induced by target binding. Ethanolamine was chosen as an example target molecule combined with the ethanolamine binding aptamer. The assay is based on measuring the target dependent shift in the aptamer melting temperature using a qPCR instrument. To achieve this, a stem loop structure was designed from the ethanolamine binding aptamer (42 nt) by truncating it to 31 nt. This aptamer was further modified by adding a fluorophore and a quencher to form an aptamer beacon. The presence of ethanolamine would lead to stabilization of the folded structure and consequently to a shift in the melting temperature. Thus allowing the quantification of as low as 1.5 nM ethanolamine using only 2 µL sample. This assay provides the high-throughput and sensitivity for a transfer to a POC. However, the assay is not yet simple enough for low resource settings.

1.2.2 Data for homogeneous thermofluorimetric assays for ethanolamine using aptamers and a PCR instrument

This article describes the methods and data analysis approaches used to develop the thermofluorimetric assay in the first project. An aptamer beacon was designed and the secondary structure was simulated using mfold. Furthermore, different structurally similar targets were tested. The beacons were further compared to intercalating dyes e.g. SYBR green. The data could be used to reproduce the experimental approach or develop other platforms using aptamers.

1.2.3 Visual aptamer-based capillary assay for ethanolamine using magnetic particles and strand displacement

The aim of this project was to introduce a simpler and faster assay compared to the thermofluorimetric assay. However, this meant that the assay should be performed without the need of any instruments. This in turn meant that the throughput will have to be compromised. Therefore, this project aimed for higher specificity and applicability to real sample analysis. To this aim, a visual capillary based assay for ethanolamine (EA) was designed. The capillary tubes are coated with three layers in this order (a) short oligonucleotides complementary to the aptamer (EA-comp.); (b) magnetic particles (Dynabeads) coated with EA-binding aptamer (EA-aptamer), and (c)lastly with short oligonucleotide-coated magnetic particles (EA-comp.). This was to make sure that ethanolamine binding will lead to a displaced magnetic particle. Ethanolamine binding leads to displaced magnetic particles. The realeased particles are collected using a permanent magnet forming brown/black spot proportional to the EA amount in the sample. The assay had a visual limit of detection of 5 nM in buffer, spiked serum samples and tap water samples. The simplicity of this platform as well as the need for only 5 minutes of incubation and no readout device makes it ideal as a POC for small molecules.

1.2.4 Combining aptamers and antibodies: lateral flow quantification for thrombin and interleukin-6 with smartphone readout

The third project aimed at developing a POC with multiplexing capabilities. Therefore, a duplex LFA for IL-6 and Thrombin was designed. This platform combined ap-

tamers and antibodies to simultaneously detect two clinically relevant targets. In this assay two different quantum dots (QD) were used. A red emitting QD was conjugated to the thrombin binding aptamer (TBA) and a green emitting QD was conjugated to anti human IL-6 monoclonal antibody (mouse). This was combined with corresponding biotin labelled thrombin aptamer (HD22) and a biotin labelled IL-6 antibody. The lateral flow had a streptavidin test line and an anti-mouse antibody. In presence of IL-6 or thrombin, signal will be detected on the test line due to sandwich formation and subsequent attachment through the biotin labeled detection molecule. Additionally excess green emitting IL-6 QDs will be captured by the anti-mouse antibody forming a green signal on the control line. The readout system is based on a smartphone combined with a dark box with built in UV light. Images captured by the smartphone could either be quantified using an application or visually inspected by splitting RGB components. The performance of the smartphone based readout system is comparable to the BioImager (Analytik Jena). The assay was able to detect IL-6 and thrombin in spiked serum samples with an LOD of 0.625 and 2 pmole respectively, providing a simple platform for duplex quantification of clinically relevant biomarkers.

Chapter 2

An aptamer based thermofluorimetric assay for ethanolamine

Status: Published

Reprinted (adapted) with permission from Mahmoud M, Laufer S, Deigner H-P. An aptamer based thermofluorimetric assay for ethanolamine. Biochimie. 2019;158:233-7.

Biochimie 158 (2019) 233–237

Contents lists available at ScienceDirect

Biochimie

journal homepage: www.elsevier.com/locate/biochi

Research paper

An aptamer based thermofluorimetric assay for ethanolamine

Mostafa Mahmoud [a, b], Stefan Laufer [b], Hans-Peter Deigner [a, c, *]

[a] Furtwangen University, Institute of Precision Medicine, Jakob-Kienzle-Straße 17, 78054, Villingen-Schwenningen, Germany
[b] Department of Pharmaceutical and Medicinal Chemistry, Institute of Pharmaceutical Sciences, Eberhard Karls Universität Tübingen, Auf der Morgenstelle 8, 72076, Tübingen, Germany
[c] Fraunhofer Institute IZI, Leipzig, EXIM Department, Schillingallee 68, D-18057, Rostock, Germany

ARTICLE INFO

Article history:
Received 25 September 2018
Accepted 21 January 2019
Available online 25 January 2019

Keywords:
Aptamer
Aptamer-assay
Thermofluorimetric method

ABSTRACT

There is a great need for fast, simple and precise diagnostic assays capable of direct quantification of biomarkers in complex biological matrices. Yet, the commonly used techniques such as ELISA/Immunoassays are tedious and involve various steps *e.g.* blocking, washing and signal development. Moreover, most of these assays have very limited ability of detecting small molecules and have hardly any multiplexing capabilities. The gold standard and alternative, mass-spectrometry, however, depends upon expensive hardware and is incompatible with point of care (POC) diagnostics. As opposed to POC assays for proteins or larger targets where variable formats are readily available.

Here, we present a simple, versatile and fast one-step assay for detecting a small molecule, ethanolamine as example. The assay makes use of commonly available qPCR machines to detect target-concentration dependent shifts in the melting temperatures of aptamer beacons. The method allows detection of ethanolamine in the low nM range without requiring tedious elaboration of assay conditions as required for molecular beacons at room temperature. If generalizable, it may change the situation of small molecule assays significantly.

1. Introduction

The reliable detection and quantification of small molecules, such as metabolites and signalling molecules found endogenously in living organisms or toxins as well as contaminants found in the environment, independent of HPLC and mass spectrometry remains a challenge. The use of HPLC systems requires expensive equipment and well-trained personnel. On the other hand, biosensors or assays based on antibodies for small molecules lack the high throughput and suffer from drawbacks usually associated with the assay format *e.g.* lack of immunogenicity, the need for labelling in competitive formats or the requirement for two binding epitopes for sandwich formats [1]; these requirements, however, are hardly compatible with small molecule targets. In contrast, aptamer-based biosensors can address these drawbacks. They are advantageous over antibodies in terms of cost, stability, reversibility of denaturation, sensitivity, and specificity [2]. Methods based on aptamers for protein detection and quantification vary a lot and offer various approaches such as fluorescence sensors, electrochemical sensors, aptamer arrays and aptamer-gold nanoparticles sensors [3]. Further developments in protein label-free detection include methods based on surface plasmon resonance (SPR) [4,5] and quartz crystal microbalance (QCM) [6]. However, due to difference in mass and size, most aptamer-based biosensors for small molecules mentioned in the literature need a complex setup and a sophisticated detection method to achieve high throughput performance [2,3,7]. Moreover, they usually require immobilization of aptamers and/or washing and incubation steps [3].

Aptamers are RNA/DNA sequences capable of binding to target molecules specifically and with high affinity. They were first introduced in 1990 [8] through an in-vitro selection process known as systemic evolution of ligands by exponential enrichment (SELEX). Various aptamers against small molecules have been reported in the literature [9]. The uniqueness of aptamers relates to conformational changes associated with binding. Aptamers adopt different conformational structures based on internal base pairings *e.g.* stem loops, G-quadruplexes and pseudoknots [10]. These

* Corresponding author. Furtwangen University, Institute of Precision Medicine, Jakob-Kienzle-Straße 17, 78054, Villingen-Schwenningen, Germany.
E-mail addresses: deigner@hs-furtwangen.de, hans-peter.deigner@hs-furtwangen.de (H.-P. Deigner).

https://doi.org/10.1016/j.biochi.2019.01.014
0300-9084/

structures are either stabilized or destructed upon target binding. Indeed, this feature of nucleic acids has been used to design molecular beacons to signal the presence of specific target nucleic acid sequence [11]. Based on this concept, Hamaguchi et al. [12] developed an aptamer beacon where target induced conformational change enabled detection and quantification of thrombin using a fluorophore on one end of the hairpin structure and a quencher on the other [12]. This homogeneous assay format does not require immobilization of the biorecognition molecules on solid support thus evading the dependence on the relatively slow diffusion kinetics faced by common bioassays but driving the bioreaction by its fast binding kinetics [13]. One of the major drawbacks faced by solid phase assays and biosensors, the dependence on mass transport rather than the fast assay kinetics [14].

Differential scanning fluorimetry has been used to identify low-molecular-weight ligands that bind and stabilize purified proteins [15] and the governing thermodynamics has been extensively studied [16]. It has been recently shown [17,18] that quantifying proteins using thermofluorimetric analysis is possible. The method, however, depends on a DNA intercalating dye as a reporter molecule *e.g.* SYBR green. SYBR green has associated drawbacks and limitations which include the shift of melting temperature of the DNA depending on the dye concentration and preferential binding to DNA fragments with higher GC content [19,20]. SYBR green is also known to compete with target binding leading to imprecise estimation of the melting temperature. This competition of SYBR green and similar intercalating dyes, has been applied to target quantification through fluorescence signal change upon target binding [20–23]. Notably, quantification here is through the fluorescence signal and peak height and not through the melting temperature shift. A similar principle has been applied for the quantification of cyclic adenosine monophosphate with an antibody-oligonucleotide [24] construct.

In this work, we present a simple and sensitive method for the detection and quantification of ethanolamine based on the shift of the melting temperature of aptamer beacons. The presence of the target leads to either stabilization of the aptamer structure leading to a shift in the melting temperature. The method can be combined with any qPCR machine capable of capturing a melting profile and yields fast results within minutes of analysis time. In comparison to a common FRET experiment, it is simpler, faster and more reproducible. Moreover, the use of the melting profile shifts the focus on the melting temperature rather than change in fluorescence signal alone. This minimizes the effect of fluorescent background and fluctuations in signal due to non-optimum folding of the aptamers or structure switching related with uncontrolled temperatures as opposed to PCR machine. To our knowledge, this is the first report on using aptamer beacons melting temperature shift to quantify a small molecule.

2. Materials and methods

2.1. Materials

Aptamer beacons (with 5′ Fluorescein and 3′ DABCYL) were synthesized and purified by Integrated DNA Technologies (Coralville, IA). Ethanolamine, phenylethylamine, oxytetracycline and SYBR® Green I (10,000× in DMSO) were purchased from Sigma-Aldrich (Darmstadt, Germany).

The following are the sequences of the used aptamers all of which had 5′ Fluorescein and 3′ DABCYL and with no labels for use with SYBR green.

Ethanolamine binding aptamer EA#14.3K42: ATACCAGCTTATT CAATTTGAGGCGGGTGGGTGGGTTGAATA

Ethanolamine binding aptamer EA#14.3K31: ATTCAATTTGAG GCGGGTGGGTGGGTTGAAT

Scrambled sequence used as ethanolamine negative: CACGG CATGGTTCATACTTAAGGGCGTCGTG

2.2. Methods

2.2.1. CD spectra

CD spectroscopy was performed using a Jasco J-720 CD spectropolarimeter. The spectra were acquired at room temperature at a rate of 20 nm/min from 220 to 320 nm using a 1 mm cells. Measurements were carried out in the ethanolamine binding buffer (20 mM TRIS, 100 mM NaCl, 5 mM KCl, 2 mM $MgCl_2$, 1 mM $CaCl_2$, 0.02% Tween® 20 at pH 7.6) at an aptamer concentration of 10 μM and ethanolamine 1 mM. The spectra were background corrected and smoothed with 10 accumulations per sample.

2.2.2. Melting temperature profiles

To account for signal variation and scattering of the data, the on-plate redundancy was at least 4 identical wells per parameter. Additionally, each experiment was repeated at least 3 times to assess both reproducibility and inter-assay variation.

The concentration of the aptamer beacon was fixed at 0.5 μM in all experiments except for the experiments with SYBR green (10×) and the corresponding melting analysis using aptamer beacons at the same concentrations (0.5, 1, 2 and 4 μM). The beacons were pipetted in a 96 wells PCR plate at a volume of 20 μL in ethanolamine binding buffer [25] consisting of (20 mM TRIS, 100 mM NaCl, 0.02% Tween® 20 at pH 7.6).

The analyte concentration of ethanolamine, phenylethylamine, ethanol and propylamine was varied from (5–100 nM) and were added in a volume of 2 μL per well. Additionally, 1 μM concentration of phenylethylamine, ethanol and propylamine was tested.

2.2.3. PCR protocol

The PCR machine (LightCycler® 480, Roche) was set to heat first till 99 °C (rate 4.4 °C/Sec) followed by holding for 5 min to ensure the complete denaturing of any DNA base pairings. Then, the fluorescence was measured from 95 °C to 20 °C with the SYBR Green filter (465 nm excitation and 510 nm emission) and a rate of 0.11 °C/Sec.

2.2.4. Data analysis

Data analysis (plotting and fitting using one site binding equation) was performed using GraphPad Prism version 7.00 for Windows, GraphPad Software, La Jolla California USA, www.graphpad.com and JMP®, Version *<13.1>*. SAS Institute Inc., Cary, NC, 1989–2007. The raw data obtained from the PCR (Figs. 4, 6 and 8) [26] was used to generate first derivative graphs for each individual experiment (Figs. 5, 7 and 9) [26]. These first derivatives were fitted using a Gaussian distribution with the following equation Y=Amplitude*exp(-0.5*((X-Mean)/SD)^2). The resulting Tm (defined as the Mean in the equation) was then plotted against the concentration (Figs. 2 and 3) to produce the calibration curves.

3. Results

3.1. Structure prediction and CD spectra

Ethanolamine aptamer was used to show the case of increasing the melting temperature through binding to the target molecule. For this we choose the 42 nucleotides sequence (EA#14.3K42) [25] which is a truncated version of the original (EA#14.3) 96 nucleotides aptamer [25]. This was further modified by adding a

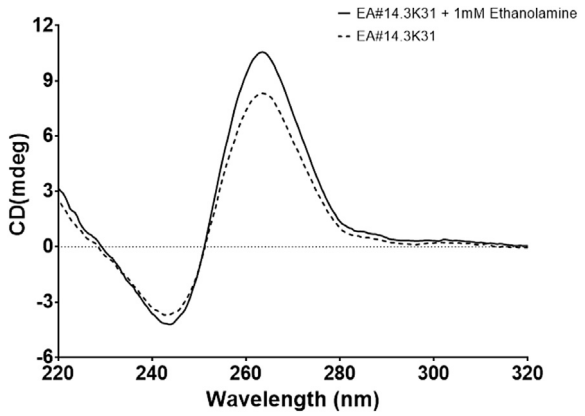

Fig. 1. CD spectra of EA#14.3K31. The dash curve denotes 10 μM aptamer prepared in ethanolamine binding buffer and the solid line denotes 10 μM aptamer in ethanolamine binding buffer after addition of 1 mM ethanolamine.

fluorophore (fluorescein) on the 5′ end and a quencher (DABCYL) on the 3′ end. The folding structure was predicted using mfold (see Fig. 1 in Ref. [26]). The structure did not show a perfect stem loop folding. Therefore, we decided to modify the sequence by truncating it to 31 nucleotides (see Fig. S2 in Ref. [26]) to improve the folding. Moreover, this allowed us to check the effect of small modifications on the binding parameters and kinetics. As a non-binding control, we chose a scrambled sequence consisting of 31 nucleotides showing a secondary structure similar to the ethanolamine aptamer (see Fig. 3 in Ref. [26]). Our results show that the structural conformation needs only a proximity of the fluorophore and the quencher to work which may be provided by other means than the stem loop *e.g.* short complementary strands. As well as that a modified structure is still capable of binding to the target; this is in agreement with previously published work, where it was shown that a 16 nucleotide is sufficient for binding [25].

It has been shown that the ethanolamine aptamer G rich consensus region adopts a G-quartet structure [27] and that this sequence is responsible for the binding [25]. This has been shown by Cheng et al. [28] using CD spectroscopy measurements which revealed a parallel quadruplex structure with a positive ellipticity maximum around 260 nm and a negative minimum around 240 nm. As seen in Fig. 1, the CD spectra of EA#14.3K31 are consistent with previously published results and confirm the formation of a parallel G-quadruplex structure. Upon addition of ethanolamine, the positive band at 263.5 nm increases and the negative band at 243.5 decreases, this indicates the ability of the ethanolamine to induce the G-quadruplex structure.

3.2. Melting profiles of beacons and SYBR green

We further tested SYBR green as a candidate intercalating dye (see Fig. 10 a and b in Ref. [26]), the melting profile, however, could not be captured for the aptamer concentrations used (0.5, 1, 2 and 4 μM and 10× SYBR green). The beacons, however, showed well defined melting peaks (see Fig. 10 c and d in Ref. [26]). This effect could be attributed to the preferential binding of SYBR green to DNA fragments with higher GC content [19,20]. The ethanolamine aptamers (EA#14.3K42 and EA#14.3K31) show low content of GC in the stem loop, hindering capturing of the melting curve using SYBR green. This limits the use of SYBR green to aptamer structures with high GC content in the stem loop. On the other hand, structures with high GC content or modifiable to contain higher GC content in the stem loop region could be used with SYBR green. These modifications, however, could interfere with binding activity of the aptamer and lead to loss of sensitivity.

3.3. Ethanolamine binding response

As seen in Fig. 2, the addition of ethanolamine increased the melting temperature in comparison to the negative controls. The

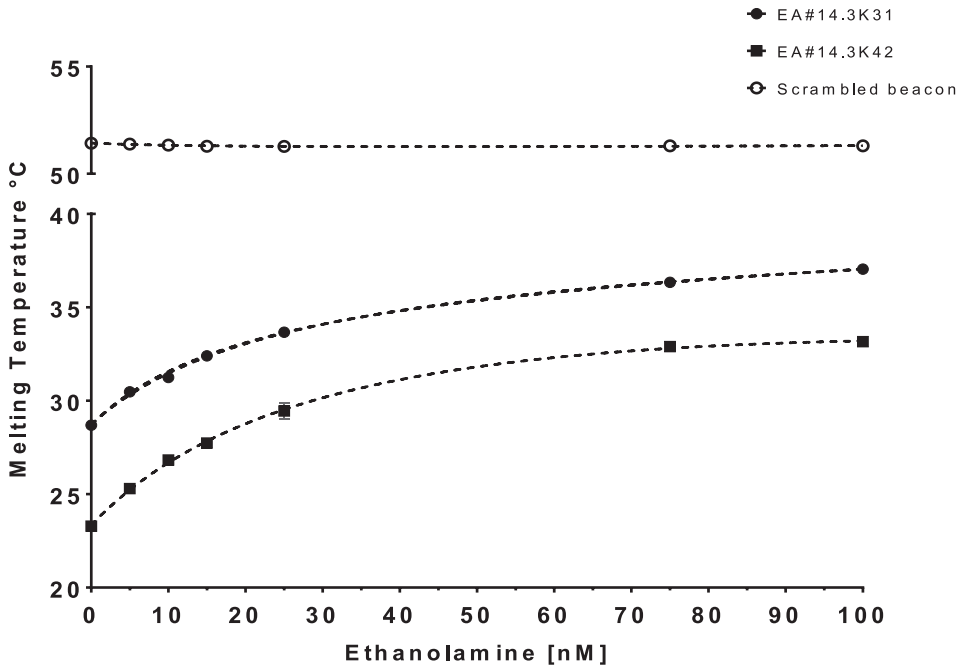

Fig. 2. Melting temperature °C plotted against the concentration of ethanolamine. The points represent the average of at least 4 experiments with on plate redundancy of 4 wells. The error bars represent the standard error of the mean, some error bars are smaller than the symbol size. Two aptamer beacons have been used, the EA#14.3K42 is 42 nt whereas the EA#14.3K31 is 31 nt and a scrambled sequence as a no binding control. The lines represent the best fit using one site total binding equation Y=Bmax*X/(Kd + X) + NS*X + Background.

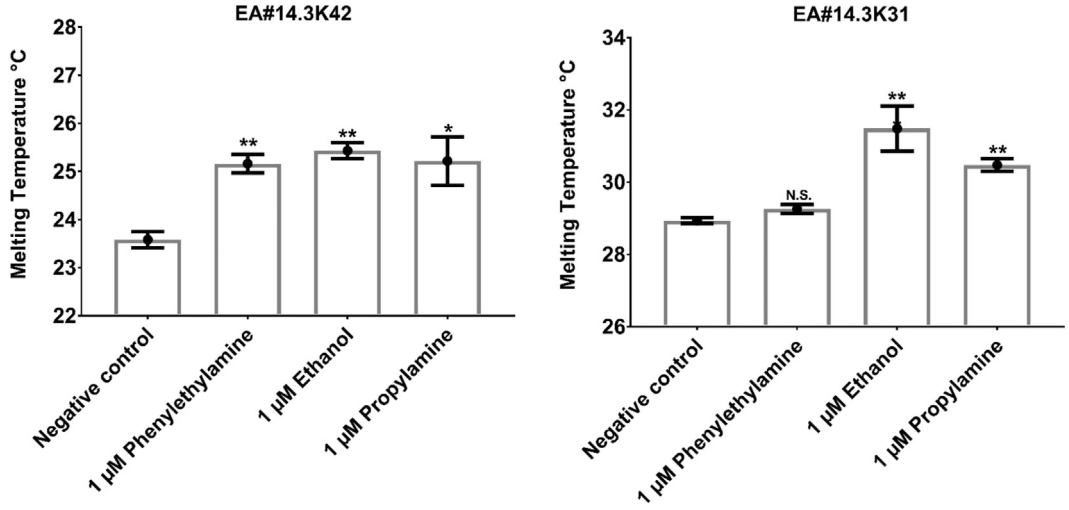

Fig. 3. Melting temperature °C of the aptamer EA#14.3k42 and EA#14.3K31 in buffer (negative control) and after the addition of 1 μM of structurally similar molecules to ethanolamine. P values were generated by ANOVA using the Dunnett Test for multiple comparisons to one control (N.S. $P > 0.05$ * $P \leq 0.05$ **$P \leq 0.01$).

limit of detection (LOD = blank mean value + $3^{*}SD_{blank}$) for the EA#14.3K42 42 nt aptamer version was 2.2 ± 0.378 nM and the EA#14.3K31 31 nt version was 1.5 ± 0.615 nM. The estimated Kd value was 26.6 ± 4.4 nM and 28.8 ± 3.4, respectively (see Fig. 12 in Ref. [26]). We could show that small modification in the structure of the aptamer does not affect the binding (provided that the binding sequence is still included). The approach shows promising results that could be potentially transferred to other aptamers for small molecules. A paper published previously [25] reported a 10 pM limit of detection using an aptamer microarray based on EA#14.3 aptamer (96 nt) version, however, using 100 μL sample volume and 18 h incubation time. In comparison, the assay presented here uses 2 μL sample volume and no incubation needed.

3.4. Specificity of the assay

Additionally, the response of the assay to the structurally similar molecules such as phenylethylamine, ethanol and propylamine has been tested. It has been shown that phenylethylamine binds the 96 nt aptamer (EA#14.3) by affinity elution test at about 50% of the ethanolamine binding [29]. The study revealed that the aptamers bind as well to molecules, which contain a freely accessible ethyl- or methylamine group [29]. Our results (see Figs. 11, 12, 13 in Ref. [26]), show that in the assay concentration range, both the EA#14.3K42 and the EA#14.3K31 display no significant binding to phenylethylamine, ethanol or propylamine. Both aptamer versions showed significant binding to both ethanol and propylamine (1 μM) (Fig. 3) which is in agreement with previously published results [29]. However, upon increasing the concentration of phenylethylamine significantly (1 μM), only the EA#14.3K42 42 nucleotides aptamer displayed a significant change in comparison to the control (Fig. 3). This could be related to the aptamer length, since the version tested in the previous publication was 96 nucleotides which may exhibit less specificity.

4. Discussion

Our findings pave the way for establishing assays for small molecules in combination with PCR machines or any similar device capable of capturing the melting profile. In general, quantification is performed by a) measuring a standard curve recording concentration-dependent optical signals across a suitable temperature range to identify melting temperatures at given conditions; b) measure unknown concentrations of the target by recording the melting temperature(s) and c) processing the measured melting temperature by an algorithm providing a best fit function for assigning melting temperatures to target molecule concentrations. Further dyes and quencher pairs should be tested and might lead to optimization of the approach. As for long aptamer sequences, where a beacon structure could be troublesome or difficult to synthesize, an indirect format could be tested. This format will then employ an unlabelled binding aptamer and an aptamer beacon competing for the binding region. Through capturing the melting temperature of such probe, the target could be quantified. Similarly, the method could also give insights on the binding thermodynamics and mechanisms. Using different beacon probes binding to different regions of the aptamer and capturing their melting temperature binding regions could be revealed. This, however, will need further development and a different experimental setup. An important limitation is the specificity of the ethanolamine aptamers and the abundance of both ethanolamine (0–12 μM) and ethanolamine containing molecules in serum such as phosphatidylethanolamine and other lipids [30]. In fact, this complicates the transfer of the assay to serum or other complex media.

The method also has great multiplexing potential. Since aptamers for different targets are of different length, they are expected to have different melting temperatures. At present, the limitation is, that different aptamers are selected in different buffers and need different salt concentration to be able to bind to their targets. This, however, could be overcome through testing the aptamers of interest to the multiplex assay and finding a common binding buffer.

An onsite point of care diagnostic device could be designed to make full use of the concept presented here, generalizability provided. Based on the advances made in PCR on chip technology [31], a simple miniaturization of the assay should be possible to achieve. The challenges and bottlenecks faced by miniaturized PCR assays, *e.g.* the need for non-metallic heating elements not to interfere with the enzymes for the PCR reaction, would not be the case here. The assay is based on profiling the melting temperature and no polymerase reaction is involved. Applications for such a device would include but not be limited to clinical diagnostics, environmental testing, contamination for food and water and testing for

drugs of abuse, confirmation in experiments determining additional thermostable target molecules provided.

Author contributions

M. Mahmoud performed the lab-experiments, analyzed data, prepared the figures and contributed to writing the manuscript; S. Laufer contributed to the planning and to manuscript writing; HPD contributed to the study design, analysis of experimental data and to manuscript writing.

Competing interests

M. Mahmoud and HPD are co-inventors on a European patent application (EP18175561.2 submitted 01 June 2018) covering the assay described in this article.

Acknowledgments

The authors thank Ms. Natascha Bartlick and Prof. Dr. Thilo Stehle, Interfaculty Institute of Biochemistry, University of Tübingen for circular dichroism equipment. The support from Steinbeis Transfer Center Personalized Medicine is highly appreciated (grant number 201801007).

References

[1] A.Y. Rubina, E.I. Dementieva, A.A. Stomakhin, E.L. Darii, S.V. Pan'kov, V.E. Barsky, S.M. Ivanov, E.V. Konovalova, A.D. Mirzabekov, Hydrogel-based protein microchips: manufacturing, properties, and applications, Biotechniques 34 (2003) 1008–1014, 1016-1020, 1022.
[2] S.Y. Toh, M. Citartan, S.C.B. Gopinath, T.-H. Tang, Aptamers as a replacement for antibodies in enzyme-linked immunosorbent assay, Biosens. Bioelectron. 64 (2015) 392–403.
[3] J. Liu, Z. Cao, Y. Lu, Functional nucleic acid sensors, Chem. Rev. 109 (2009) 1948–1998.
[4] P. Singh, SPR biosensors: historical perspectives and current challenges, Sensor. Actuator. B Chem. 229 (2016) 110–130.
[5] Z. Wang, T. Wilkop, D. Xu, Y. Dong, G. Ma, Q. Cheng, Surface plasmon resonance imaging for affinity analysis of aptamer-protein interactions with PDMS microfluidic chips, Anal. Bioanal. Chem. 389 (2007) 819–825.
[6] M. Liss, B. Petersen, H. Wolf, E. Prohaska, An aptamer-based quartz crystal protein biosensor, Anal. Chem. 74 (2002) 4488–4495.
[7] J. Wang, Z. Cao, Y. Jiang, C. Zhou, X. Fang, W. Tan, Molecular signaling aptamers for real-time fluorescence analysis of protein, IUBMB Life 57 (2005) 123–128.
[8] A.D. Ellington, J.W. Szostak, In vitro selection of RNA molecules that bind specific ligands, Nature 346 (1990) 818–822.
[9] M. McKeague, M.C. DeRosa, Challenges and opportunities for small molecule aptamer development, J. Nucleic Acids 2012 (2012) 20.
[10] C. Frauendorf, A. Jaschke, Detection of small organic analytes by fluorescing molecular switches, Bioorg. Med. Chem. 9 (2001) 2521–2524.
[11] S. Tyagi, F.R. Kramer, Molecular beacons: probes that fluoresce upon hybridization, Nat. Biotechnol. 14 (1996) 303–308.
[12] N. Hamaguchi, A. Ellington, M. Stanton, Aptamer beacons for the direct detection of proteins, Anal. Biochem. 294 (2001) 126–131.
[13] E.F. Ullman, Chapter 2.3 - homogeneous immunoassays, in: D. Wild (Ed.), The Immunoassay Handbook, fourth ed., Elsevier, Oxford, 2013, pp. 67–87.
[14] W. Kusnezow, Y.V. Syagailo, I. Goychuk, J.D. Hoheisel, D.G. Wild, Antibody microarrays: the crucial impact of mass transport on assay kinetics and sensitivity, Expert Rev. Mol. Diagn 6 (2006) 111–124.
[15] F.H. Niesen, H. Berglund, M. Vedadi, The use of differential scanning fluorimetry to detect ligand interactions that promote protein stability, Nat. Protoc. 2 (2007) 2212.
[16] G.A. Holdgate, W.H.J. Ward, Measurements of binding thermodynamics in drug discovery, Drug Discov. Today 10 (2005) 1543–1550.
[17] J. Hu, J. Kim, C.J. Easley, Quantifying aptamer-protein binding via thermofluorimetric analysis, Anal. Method: Adv. Method Appl. 7 (2015) 7358–7362.
[18] J. Kim, J. Hu, A.B. Bezerra, M.D. Holtan, J.C. Brooks, C.J. Easley, Protein quantification using controlled DNA melting transitions in bivalent probe assemblies, Anal. Chem. 87 (2015) 9576–9579.
[19] H. Gudnason, M. Dufva, D.D. Bang, A. Wolff, Comparison of multiple DNA dyes for real-time PCR: effects of dye concentration and sequence composition on DNA amplification and melting temperature, Nucleic Acids Res. 35 (2007) e127-e127.
[20] P.T. Monis, S. Giglio, C.P. Saint, Comparison of SYTO9 and SYBR Green I for real-time polymerase chain reaction and investigation of the effect of dye concentration on amplification and DNA melting curve analysis, Anal. Biochem. 340 (2005) 24–34.
[21] C. Yang, J. Bie, X. Zhang, C. Yan, H. Li, M. Zhang, R. Su, X. Zhang, C. Sun, A Label-free Aptasensor for the Detection of Tetracycline Based on the Luminescence of SYBR Green I, Spectrochim. Acta A: Mol. Biomol. Spectr. 202 (2018) 382–388.
[22] D. Monchaud, C. Allain, M.-P. Teulade-Fichou, Development of a fluorescent intercalator displacement assay (G4-FID) for establishing quadruplex-DNA affinity and selectivity of putative ligands, Bioorg. Med. Chem. Lett 16 (2006) 4842–4845.
[23] Y.-P. Xing, C. Liu, X.-H. Zhou, H.-C. Shi, Label-free detection of kanamycin based on a G-quadruplex DNA aptamer-based fluorescent intercalator displacement assay, Sci. Rep. 5 (2015) 8125.
[24] J. Hu, C.J. Easley, Homogeneous assays of second messenger signaling and hormone secretion using thermofluorimetric methods that minimize calibration burden, Anal. Chem. 89 (2017) 8517–8523.
[25] A. Heilkenbrinker, C. Reinemann, R. Stoltenburg, J.G. Walter, A. Jochums, F. Stahl, S. Zimmermann, B. Strehlitz, T. Scheper, Identification of the target binding site of ethanolamine-binding aptamers and its exploitation for ethanolamine detection, Anal. Chem. 87 (2015) 677–685.
[26] M. Mahmoud, S. Laufer, H.-P. Deigner, Data for Homogeneous Thermofluorimetric Assays for Ethanolamine Using Aptamers and a PCR Instrument, Data in Brief, submitted for publication.
[27] C. Xiaohong, L. Xiangjun, B. Tao, Z. Rui, X. Shaoxiang, S. Dihua, Specific DNA G-quadruplexes bind to ethanolamines, Biopolymers 91 (2009) 874–883.
[28] X. Cheng, X. Liu, T. Bing, R. Zhao, S. Xiong, D. Shangguan, Specific DNA G-quadruplexes bind to ethanolamines, Biopolymers 91 (2009) 874–883.
[29] C. Reinemann, R. Stoltenburg, B. Strehlitz, Investigations on the specificity of DNA aptamers binding to ethanolamine, Anal. Chem. 81 (2009) 3973–3978.
[30] D.S. Wishart, D. Tzur, C. Knox, R. Eisner, A.C. Guo, N. Young, D. Cheng, K. Jewell, D. Arndt, S. Sawhney, C. Fung, L. Nikolai, M. Lewis, M.-A. Coutouly, I. Forsythe, P. Tang, S. Shrivastava, K. Jeroncic, P. Stothard, G. Amegbey, D. Block, D.D. Hau, J. Wagner, J. Miniaci, M. Clements, M. Gebremedhin, N. Guo, Y. Zhang, G.E. Duggan, G.D. MacInnis, A.M. Weljie, R. Dowlatabadi, F. Bamforth, D. Clive, R. Greiner, L. Li, T. Marrie, B.D. Sykes, H.J. Vogel, L. Querengesser, HMDB: the human metabolome database, Nucleic Acids Res. 35 (2007) D521–D526.
[31] C. Zhang, D. Xing, Miniaturized PCR chips for nucleic acid amplification and analysis: latest advances and future trends, Nucleic Acids Res. 35 (2007) 4223–4237.

Chapter 3

Data for homogeneous thermofluorimetric assays for ethanolamine using aptamers and a PCR instrument

Status: Published

Reprinted (adapted) with permission from Mahmoud M, Laufer S, Deigner H-P. Data for homogeneous thermofluorimetric assays for ethanolamine using aptamers and a PCR instrument. Data in Brief. 2019;24:103946.

Data in brief 24 (2019) 103946

Contents lists available at ScienceDirect

Data in brief

journal homepage: www.elsevier.com/locate/dib

Data Article

Data for homogeneous thermofluorimetric assays for ethanolamine using aptamers and a PCR instrument

Mostafa Mahmoud [a, b], Stefan Laufer [b], Hans-Peter Deigner [a, c, *]

[a] Furtwangen University, Institute of Precision Medicine, Jakob-Kienzle-Straße 17, 78054, Villingen-Schwenningen, Germany
[b] Department of Pharmaceutical and Medicinal Chemistry, Institute of Pharmaceutical Sciences, Eberhard Karls Universität Tübingen, Auf der Morgenstelle 8, 72076 Tübingen, Germany
[c] Fraunhofer Institute IZI, Leipzig, EXIM Department, Schillingallee 68, D-18057, Rostock, Germany

ARTICLE INFO

Article history:
Received 1 March 2019
Received in revised form 20 March 2019
Accepted 15 April 2019
Available online 23 April 2019

ABSTRACT

The data presented in this article describe the quantitative detection of small molecules e.g. ethanolamine through the shifts in the melting temperatures of aptamer beacons presented in the research article entitled “An aptamer based thermofluorimetric assay for ethanolamine” [1]. The data include prediction and optimization of the folding structure of the aptamers. Moreover, the data from using intercalating dyes such as SYBR green is included for comparison. The presented data could be used for the design of other small molecules sensing platforms using aptamers.

DOI of original article: https://doi.org/10.1016/j.biochi.2019.01.014.
* Corresponding author. Furtwangen University, Institute of Precision Medicine, Jakob-Kienzle-Straße 17, 78054, Villingen-Schwenningen, Germany.
E-mail address: deigner@hs-furtwangen.de (H.-P. Deigner).

https://doi.org/10.1016/j.dib.2019.103946

Specifications table

Subject area	*Chemistry*
More specific subject area	*Analytical biochemistry*
Type of data	*Figures and graphs*
How data was acquired	*PCR LightCycler® 480, Roche*
Data format	*Analyzed*
Experimental factors	*The concentration of the aptamer beacon was fixed at 0.5 μM in all experiments except for the experiments with SYBR green (10x) and the corresponding melting analysis using aptamer beacons at the same concentrations (0.5, 1, 2 and 4 μM). The beacons were pipetted in a 96 wells PCR plate at a volume of 20 μL in ethanolamine binding buffer consisting of (20 mM TRIS, 100 mM NaCl, 0.02% Tween® 20 at pH 7.6).*
Experimental features	*The PCR machine (LightCycler® 480, Roche) was set to heat first till 99 °C (rate 4.4 °C/Sec) followed by holding for 5 minutes to ensure the complete denaturing of any DNA base pairings. Then, the fluorescence was measured from 95 °C to 20 °C with the SYBR Green filter (465 nm excitation and 510 nm emission) and a rate of 0.11 °C/Sec.*
Data source location	*Villingen-Schwenningen, Germany*
Data accessibility	*All data used and generated is included in this article and in its Supplementary Material*
Related research article	*M. Mahmoud, S. Laufer, H.P. Deigner, An aptamer based thermofluorimetric assay for ethanolamine, Biochimie, 158 (2019) 233–237.*

Value of the data

- The data could be used for optimizing homogeneous aptamer assays for small molecules
- The data could give insights on aptamers thermodynamic and kinetic properties
- The described methods are essential for simple and rapid detection of small molecules

1. Data

The obtained data show the optimization and validation of a thermofluorimetric assay for ethanolamine using ethanolamine binding aptamers and a PCR machine [1]. The assay was performed in a homogeneous format with no pre-activation of the aptamers and low volume of target (2 μL). The concentration of the aptamer beacon was fixed at 0.5 μM in all experiments except for the experiments with SYBR green (10×) and the corresponding melting analysis using aptamer beacons at the same concentrations (0.5, 1, 2 and 4 μM). The beacons were pipetted in a 96 wells PCR plate at a volume of 20 μL in ethanolamine binding buffer [4] consisting of (20 mM TRIS, 100 mM NaCl, 0.02% Tween® 20 at pH 7.6). The analyte concentration of ethanolamine, phenylethylamine, ethanol and propylamine was varied from (5–100 nM) and were added in a volume of 2 μL per well. Additionally, 1 μM concentration of phenylethylamine, ethanol and propylamine was tested.

1.1. Structure prediction and optimization of the aptamers folding

The aptamer folding structure in the given buffer conditions was predicted using mfold [2]. The aptamer 42 nucleotides EA#14.3K42 [3] (Fig. 1) did not show optimal stem loop folding. Therefore, the sequence was modified by truncation to produce a 31-nucleotide aptamer EA#14.3K31 (Fig. 2). The G-rich binding sequence [4] was conserved during this truncation. A scrambled sequence consisting of 31 nucleotides showing a secondary structure similar to the ethanolamine aptamer was added as a non-binding aptamer (Fig. 3). The aptamers were then modified with A fluorophore (Fluorescein) on the 5′ end and a quencher (DABCYL) on the 3′ end to produce a beacon [3].

1.2. Melting profiles and thermofluorimetric analysis

The three aptamers EA#14.3K42, EA#14.3K31 and the scrambled sequence were prepared in the ethanolamine binding buffer [4] in a 96 well PCR plates at a volume of 20 μL per well. Afterwards, the sample was added to the wells at a volume of 2 μL per well and directly measured in the PCR machine. The obtained data from the PCR machine for each plate was averaged (Figs. 4, 6 and 8) and then the first derivative with second order smoothing (4 neighbours) was produced (Figs. 5, 7 and 9. Then the Model

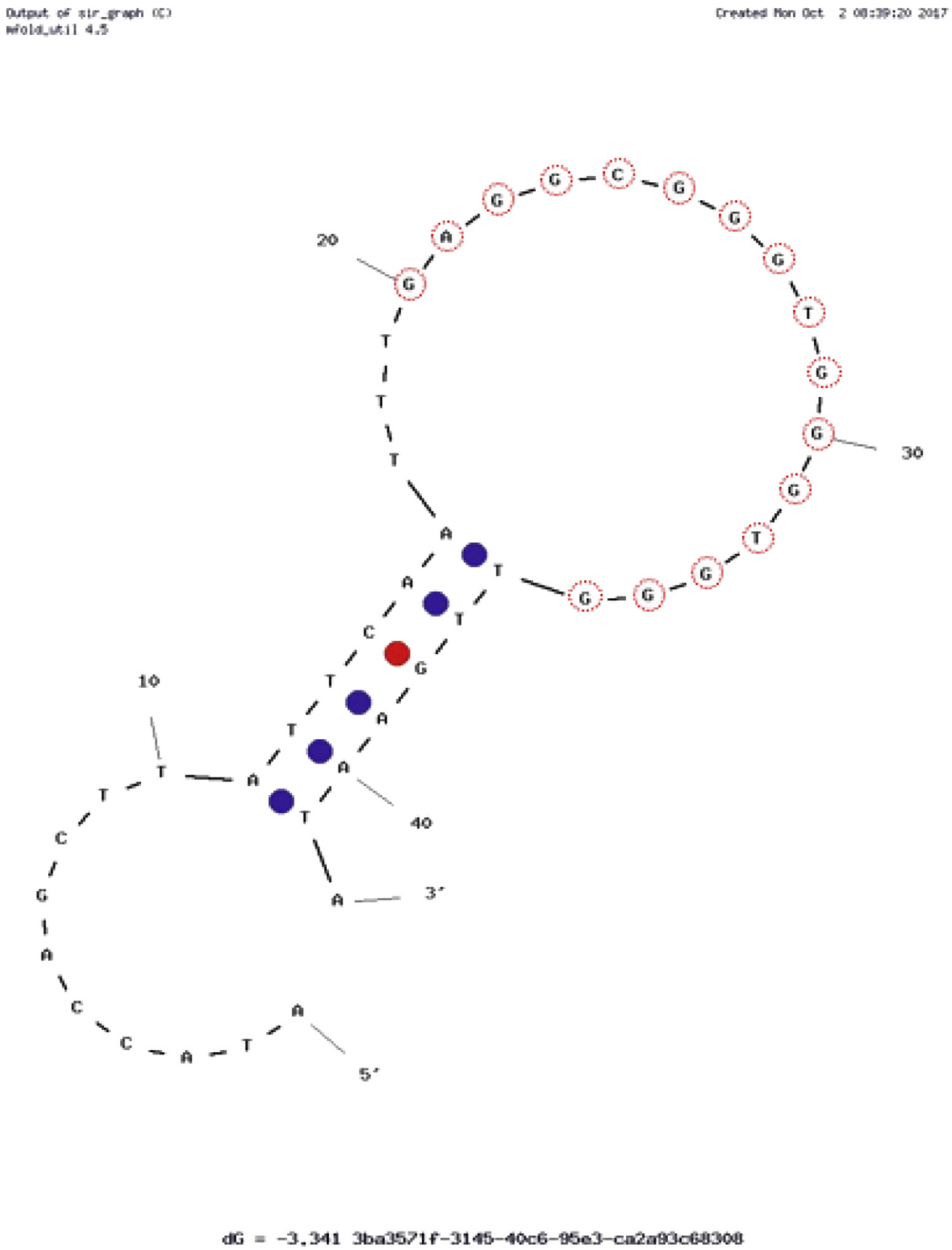

Fig. 1. The predicted secondary structure of the ethanolamine aptamer 42 nucleotides (EA#14.3K42) [4] a truncated version of the original 96nt (EA#14.3) [5] aptmaer. A fluorophore (Fluorescein) was added to the 5′ end and a quencher (DABCYL) to the 3′ end to produce a beacon. Folding simulated using mfold [2]. The G-rich consensus sequence is marked by red circles.

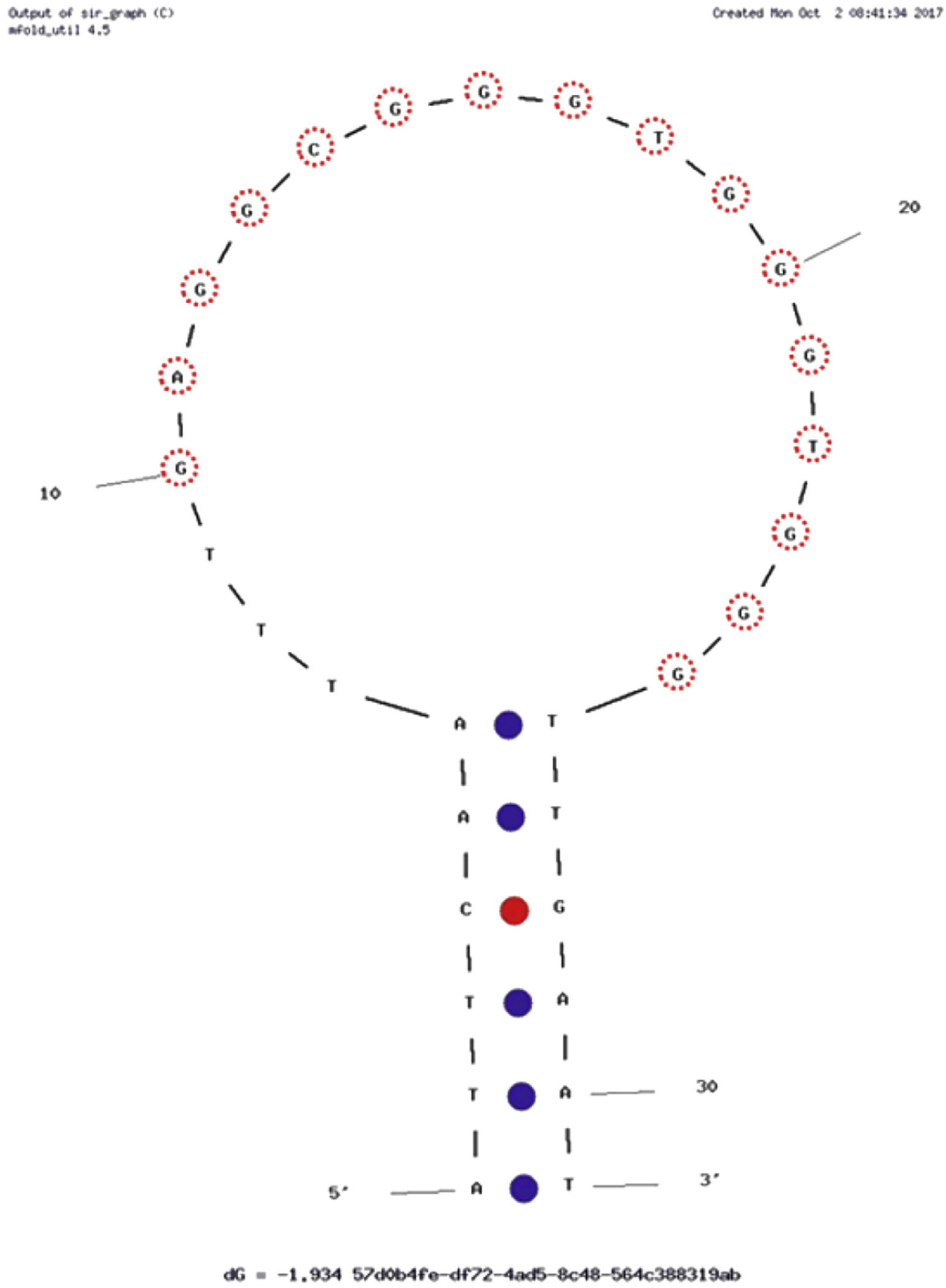

Fig. 2. The predicted secondary structure of the modified ethanolamine aptamer EA#14.3K31 a truncated version of the EA14.3K42 aptamer. A fluorophore (Fluorescein) was added to the 5′ end and a quencher (DABCYL) to the 3′ end to produce a beacon. Folding generated using mfold [2]. The G-rich consensus sequence is marked by red circles.

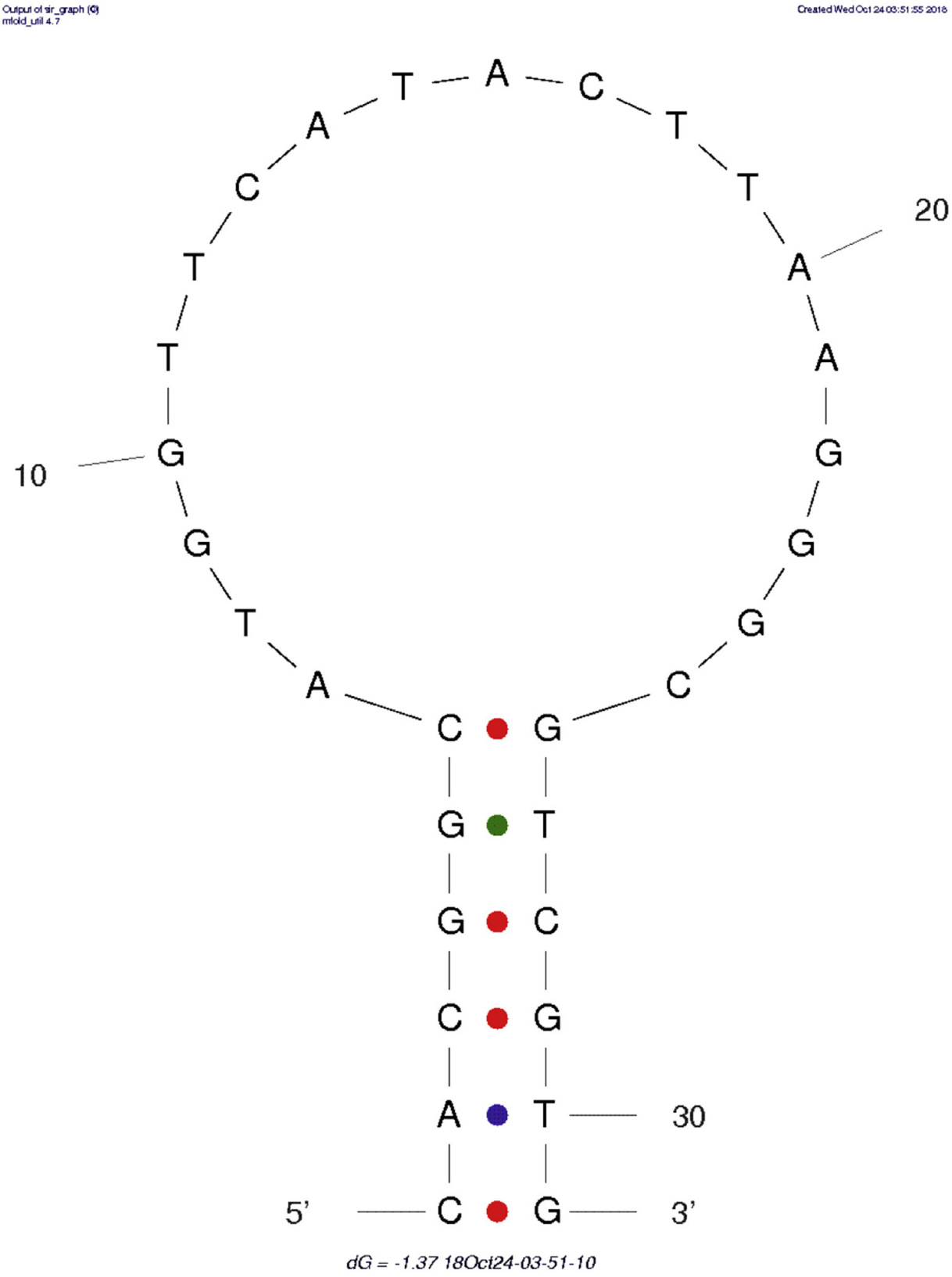

Fig. 3. The predicted secondary structure of the scrambled aptamer used as negative control for the ethanolamine 31 nucleotides modified aptamer. A fluorophore (Fluorescein) was added to the 5′ end and a quencher (DABCYL) to the 3′ end to produce a beacon. Folding generated using mfold [2].

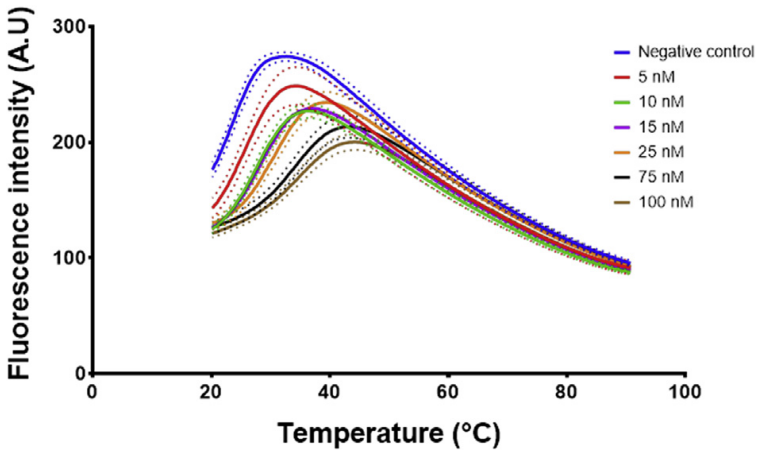

Fig. 4. Signal data from the qPCR machine showing fluorescence intensity against temperature °C. The lines represent the average of at least 4 wells, the dots represent the SD. Each well had 20 μL of ethanolamine aptamer EA14.3K42 at 0.5 μM concentration. 2 μL of ethanolamine (0–100 nM) were added to each well before measuring in the PCR.

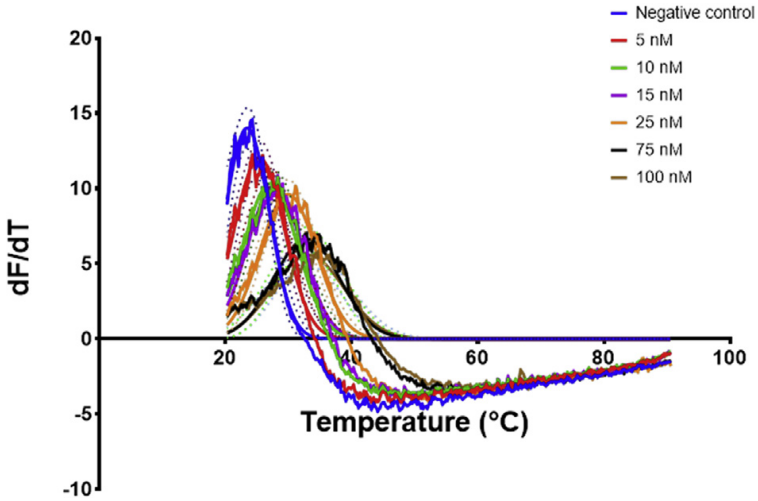

Fig. 5. The first derivative of the signal measured over temperature obtained from Fig. 4. The curve was generated using graphpad prism First derivative with 2nd order smoothing (4 neighbours) then Model (Gaussian distribution) Y=Amplitude*exp(-0.5*((X-Mean)/SD)^2) was fitted to the data points and the mean defined the Tm, the Tm was then plotted against the concentration to produce the calibration curve. The lines represent the fitting and the dots represent the 95% confidence bands of the fit.

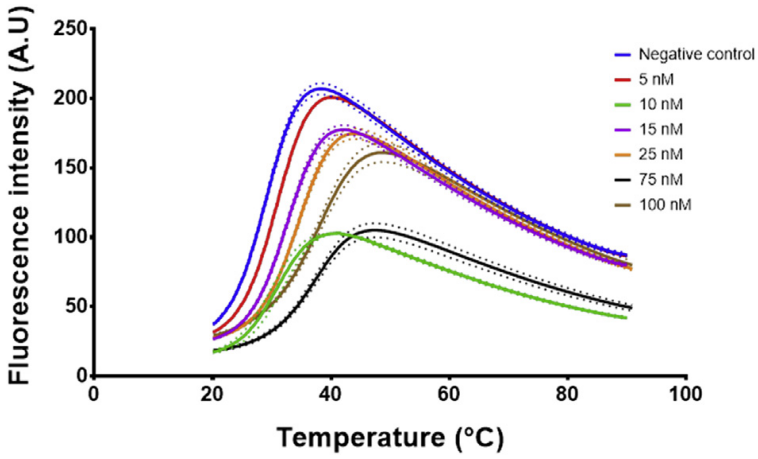

Fig. 6. Signal data from the qPCR machine showing fluorescence intensity against temperature °C. The lines represent the average of at least 4 wells, the dots represent the SD. Each well had 20 μL of ethanolamine aptamer EA14.3K31 at 0.5 μM concentration. 2 μL of ethanolamine (0–100 nM) were added to each well before measuring in the PCR.

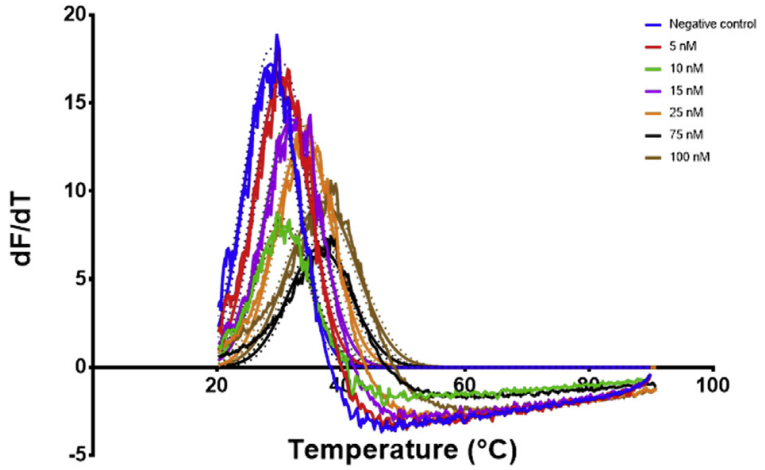

Fig. 7. The first derivative of the signal measured over temperature obtained from Fig. 6. The curve was generated using graphpad prism First derivative with 2nd order smoothing (4 neighbours) then Model (Gaussian distribution) Y=Amplitude*exp(-0.5*((X-Mean)/SD)^2) was fitted to the data points and the mean defined the Tm, the Tm was then plotted against the concentration to produce the calibration curve. The lines represent the fitting and the dots represent the 95% confidence bands of the fit.

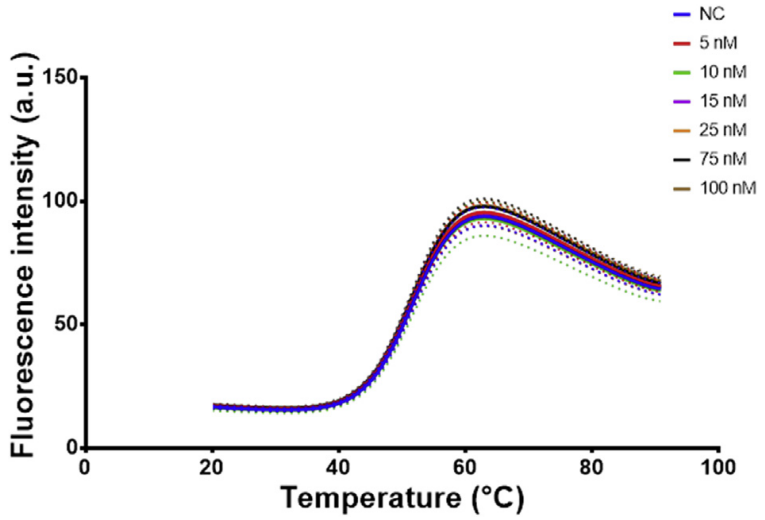

Fig. 8. Signal data from the qPCR machine showing fluorescence intensity against temperature °C. The lines represent the average of at least 4 wells, the dots represent the SD. Each well had 20 μL of scrambled ethanolamine aptamer sequence at 0.5 μM concentration. 2 μL of ethanolamine (0–100 nM) were added to each well before measuring in the PCR.

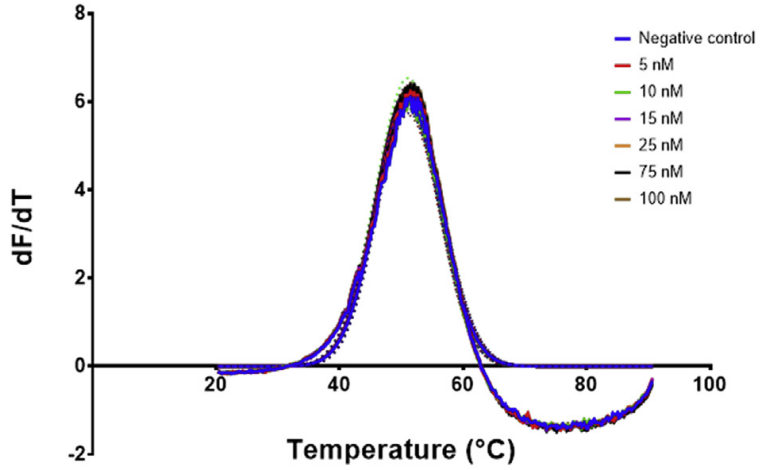

Fig. 9. The first derivative of the signal measured over temperature obtained from Fig. 8. The curve was generated using graphpad prism First derivative with 2nd order smoothing (4 neighbours) then Model (Gaussian distribution) Y=Amplitude*exp(-0.5*((X-Mean)/SD)^2) was fitted to the data points and the mean defined the Tm, the Tm was then plotted against the concentration to produce a calibration curve. The lines represent the fitting and the dots represent the 95% confidence bands of the fit.

(Gaussian distribution) Y=Amplitude*exp(-0.5*((X-Mean)/SD)2) was fitted to the data points and the mean defined the Tm.

Similarly, SYBR green a DNA intercalating dye [6] was used at 10× concentration and a varying amount of the non-labelled aptamers (0.5, 1, 2 and 4 μM) was used to capture the melting profile (Fig. 10a and b). The data obtained was handled slightly different and the negative first derivative was produced for the SYBR green experiments. These results were compared to the melting profiles of aptamer beacons at the same concentrations (0.5, 1, 2 and 4 μM) (Fig. 10c and d).

1.3. Specificity of the assay and ethanolamine binding response

To further verify the specificity of the response of the ethanolamine aptamers, the response to various structurally similar compounds e.g. Phenyethylamine, ethanol and propylamine was tested. The obtained melting temperatures from the first derivative fit was plotted against the corresponding concentrations of the analyte to produce the calibration curves (Figs. 11–13).

The kinetic parameters were determined using the one site binding equation Y=Bmax*X/(Kd + X). The melting temperatures were background corrected and plotted against the concentration of the ethanolamine to produce the curve (Fig. 14).

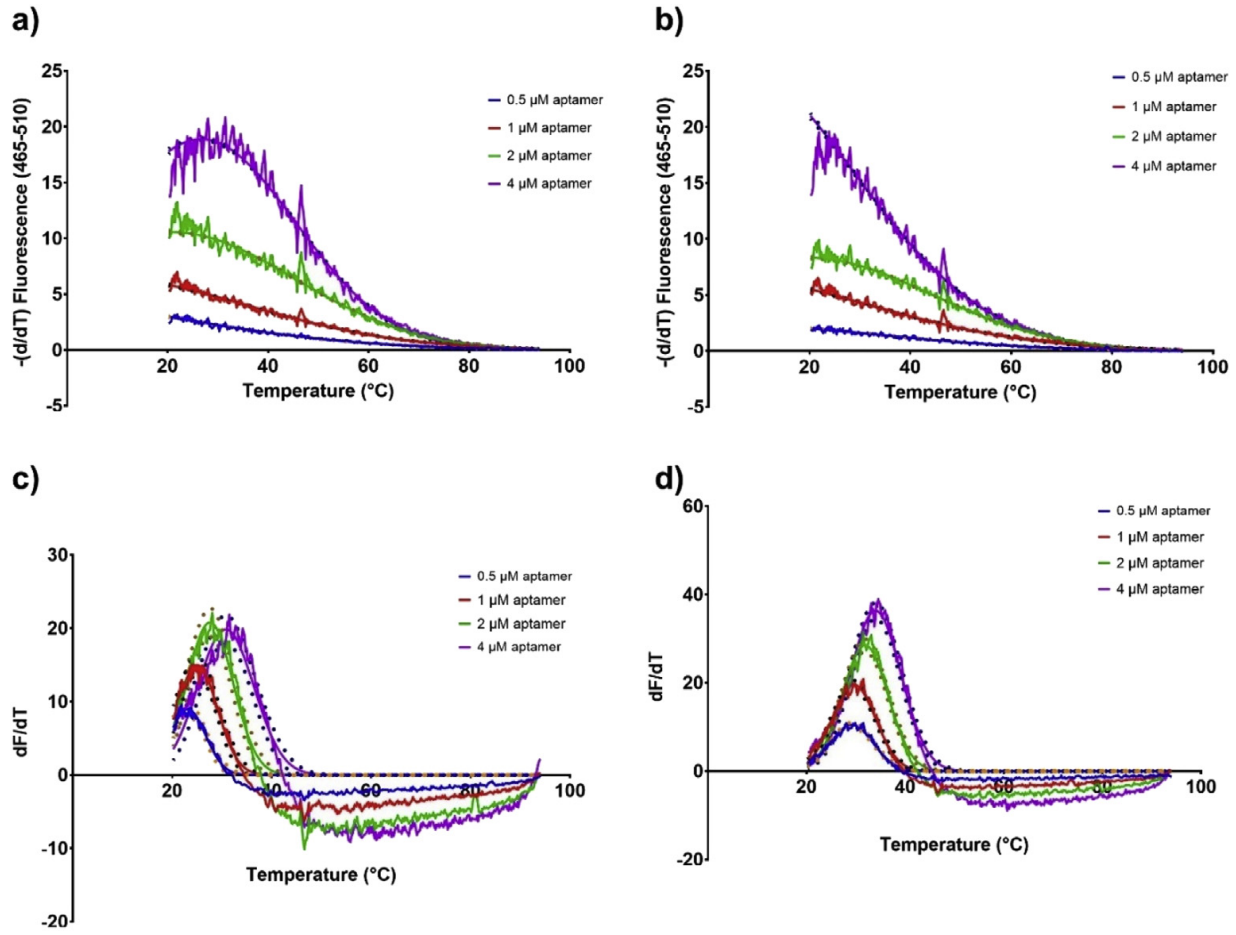

Fig. 10. a) melting profile of different concentrations of EA#14.3K42 aptamer using 10× SYBR green b) melting profile of different concentration of the EA#14.3K31 aptamer using 10× SYBR green c) melting profile of different concentrations of EA#14.3K42 aptamer beacon d) melting profile of different concentrations of the EA#14.3K31 aptamer beacon. The lines are the fit using the Model (Gaussian distribution) Y=Amplitude*exp(-0.5*((X-Mean)/SD)^2) and the dots represent the 95% CI of the fit. The aptamer beacons show sharper well-defined peaks in comparison to the use of the SYBR green.

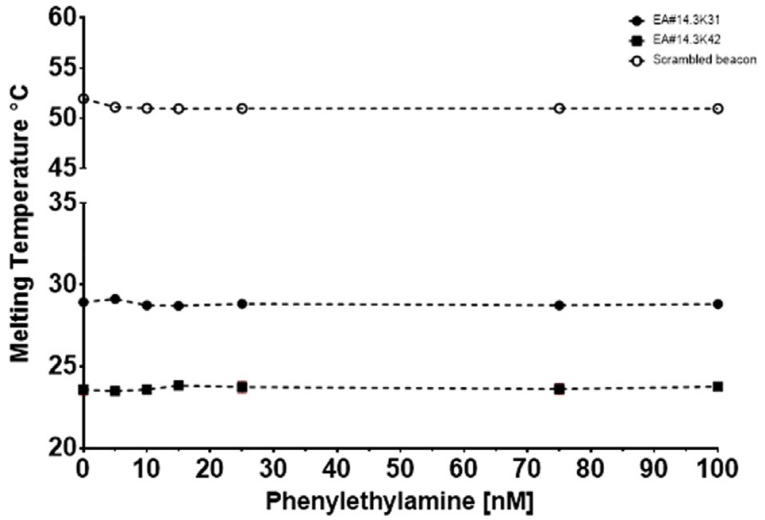

Fig. 11. Melting temperature ◦C plotted against the concentration of phenylethylamine. The points represent the average of at least 3 experiments with on plate redundancy of 3 wells. The error bars represent the standard deviation, some error bars are smaller than the symbol size. Two aptamer beacons were used the EA#14.3K42 is 42nt whereas the EA#14.3K31 is 31nt and a scrambled sequence as a no binding control.

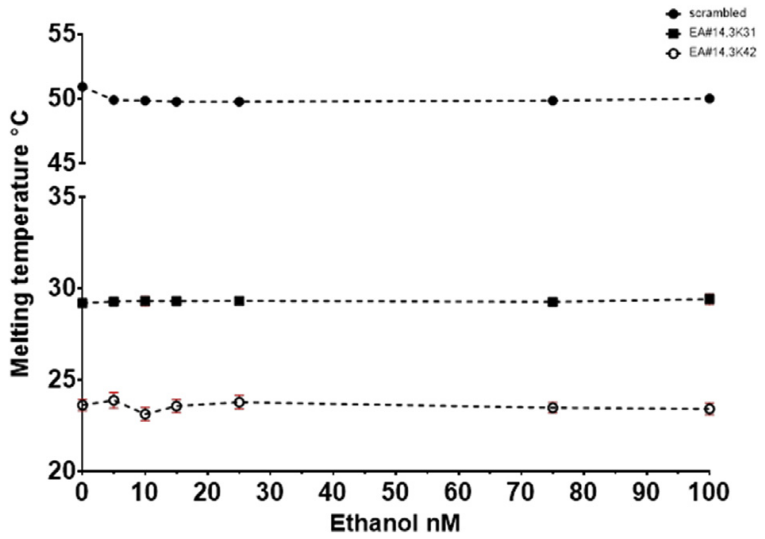

Fig. 12. Melting temperature ◦C plotted against the concentration of Ethanol. The points represent the average of at least 2 experiments with on plate redundancy of 3 wells. The error bars represent the standard deviation, some error bars are smaller than the symbol size. Two aptamer beacons were used the EA#14.3K42 is 42nt whereas the EA#14.3K31 is 31nt and a scrambled sequence as a no binding control.

2. Experimental design, materials and methods

2.1. Materials

Aptamer beacons (with 5′ Fluorescein and 3′ DABCYL) were synthesized and purified by Integrated DNA Technologies (Coralville, IA). Ethanolamine, phenylethylamine, oxytetracycline and SYBR® Green I (10,000× in DMSO) were purchased from Sigma-Aldrich (Darmstadt, Germany).

The following are the sequences of the used aptamers all of which had 5′ Fluorescein and 3′ DABCYL and with no labels for use with SYBR green.

Ethanolamine binding aptamer EA#14.3K42: ATACCAGCTTATTCAATTTGAGGCGGGTGGGTGGGTTGAATA.

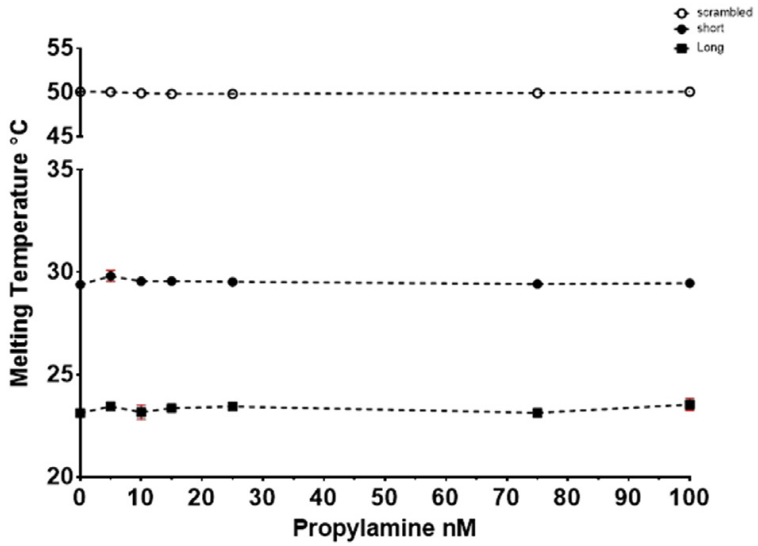

Fig. 13. Melting temperature °C plotted against the concentration of Propylamine. The points represent the average of at least 2 experiments with on plate redundancy of 3 wells. The error bars represent the standard deviation, some error bars are smaller than the symbol size. Two aptamer beacons were used the EA#14.3K42 is 42nt whereas the EA#14.3K31 is 31nt and a scrambled sequence as a no binding control.

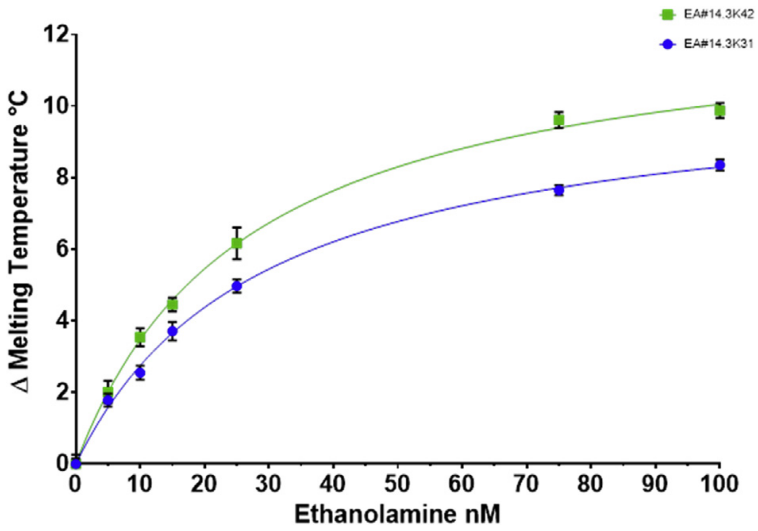

Fig. 14. ΔTm °C plotted against the concentration of ethanolamine. The points represent the average of at least 4 experiments with on plate redundancy of 4 wells. The error bars represent the standard error of the mean, some error bars are smaller than the symbol size. Two aptamer beacons were used the EA#14.3K42 is 42nt whereas the EA#14.3K31 is 31nt. The lines represent the best fit using one site binding equation Y=Bmax*X/(Kd + X).

Ethanolamine binding aptamer EA#14.3K31: ATTCAATTTGAGGCGGGTGGGTGGGTTGAAT.
Scrambled sequence used as ethanolamine negative: CACGGCATGGTTCATACTTAAGGGCGTCGTG.

2.2. Methods

2.2.1. Melting temperature profiles

To account for signal variation and scattering of the data, the on-plate redundancy was at least 4 identical wells per parameter. Additionally, each experiment was repeated at least 3 times to assess both reproducibility and inter-assay variation.

The concentration of the aptamer beacon was fixed at 0.5 μM in all experiments except for the experiments with SYBR green (10×) and the corresponding melting analysis using aptamer beacons at

the same concentrations (0.5, 1, 2 and 4 μM). The beacons were pipetted in a 96 wells PCR plate at a volume of 20 μL in ethanolamine binding buffer [25] consisting of (20 mM TRIS, 100 mM NaCl, 0.02% Tween® 20 at pH 7.6).

The analyte concentration of ethanolamine, phenylethylamine, ethanol and propylamine was varied from (5–100 nM) and were added in a volume of 2 μL per well. Additionally, 1 μM concentration of phenylethylamine, ethanol and propylamine was tested.

2.2.2. PCR protocol

The PCR machine (LightCycler® 480, Roche) was set to heat first till 99 °C (rate 4.4 °C/Sec) followed by holding for 5 minutes to ensure the complete denaturing of any DNA base pairings. Then, the fluorescence was measured from 95 °C to 20 °C with the SYBR Green filter (465 nm excitation and 510 nm emission) and a rate of 0.11 °C/Sec.

2.2.3. Data analysis

Data analysis (plotting and fitting using one site binding equation) was performed using GraphPad Prism version 7.00 for Windows, GraphPad Software, La Jolla California USA, www.graphpad.com and JMP®, Version <*13.1*>. SAS Institute Inc., Cary, NC, 1989–2007. The raw data obtained from the PCR (Figs. 4, 6 and 8) was used to generate first derivative graphs for each individual experiment (Figs. 5, 7 and 9). These first derivatives were fitted using a Gaussian distribution with the following equation Y=Amplitude*exp(-0.5*((X-Mean)/SD)2.

Acknowledgements

The support from Steinbeis Transfer Center Personalized Medicine is highly appreciated (grant number 201801007).

Transparency document

Transparency data associated with this article can be found in the online version at https://doi.org/10.1016/j.dib.2019.103946.

Appendix A. Supplementary data

Supplementary data to this article can be found online at https://doi.org/10.1016/j.dib.2019.103946.

References

[1] M. Mahmoud, S. Laufer, H.P. Deigner, An aptamer based thermofluorimetric assay for ethanolamine, Biochimie 158 (2019) 233–237.
[2] M. Zuker, Mfold web server for nucleic acid folding and hybridization prediction, Nucleic Acids Res. 31 (2003) 3406–3415.
[3] N. Hamaguchi, A. Ellington, M. Stanton, Aptamer beacons for the direct detection of proteins, Anal. Biochem. 294 (2001) 126–131.
[4] A. Heilkenbrinker, C. Reinemann, R. Stoltenburg, J.-G. Walter, A. Jochums, F. Stahl, S. Zimmermann, B. Strehlitz, T. Scheper, Identification of the target binding site of ethanolamine-binding aptamers and its exploitation for ethanolamine detection, Anal. Chem. 87 (2015) 677–685.
[5] D. Mann, C. Reinemann, R. Stoltenburg, B. Strehlitz, In vitro selection of DNA aptamers binding ethanolamine, Biochem. Biophys. Res. Commun. 338 (2005) 1928–1934.
[6] P.T. Monis, S. Giglio, C.P. Saint, Comparison of SYTO9 and SYBR Green I for real-time polymerase chain reaction and investigation of the effect of dye concentration on amplification and DNA melting curve analysis, Anal. Biochem. 340 (2005) 24–34.

Chapter 4

Visual aptamer-based capillary assay for ethanolamine using magnetic particles and strand displacement

Status: Published

Reprinted (adapted) with permission from Mahmoud, M., Laufer, S. & Deigner, HP. Microchim Acta (2019) 186: 690.

Microchimica Acta
https://doi.org/10.1007/s00604-019-3795-9

ORIGINAL PAPER

Visual aptamer-based capillary assay for ethanolamine using magnetic particles and strand displacement

Mostafa Mahmoud[1,2] · Stefan Laufer[2] · Hans-Peter Deigner[1,3]

Received: 12 July 2019 / Accepted: 7 September 2019

Abstract

This work describes an aptamer-based capillary assay for ethanolamine (EA). It is making use of strand displacement format and magnetic particles. The capillary tubes are coated with three layers, viz. (a) first with short oligonucleotides complementary to the aptamer (EA-comp.); (b) then with magnetic particles (Dynabeads) coated with EA-binding aptamer (EA-aptamer), and (c) with short oligonucleotide-coated magnetic particles (EA-comp.). On exposure to a sample containing ethanolamine, the DNA-coated magnetic particles are released and subsequently collected and spatially separated using a permanent magnet. This results in the formation of a characteristic black/brown spots. The assay has a visual limit of detection of 5 nM and only requires 5 min of incubation. Quantification is possible through capture and analysis of digital (RGB) photos in the 5 to 75 nM EA concentration range. Furthermore, results from tap water and serum spiked with EA samples showed that the platform performs well in complex samples and can be applied to real sample analysis. The combined use of plastic capillaries, visual detection and passive flow make the method suited for implementation into a point-of-care device.

Keywords Aptamer-assay · Small molecules · Capillary flow · Visual detection · Magnetic particles · RGB images

Introduction

The quantification of small molecules remains a considerably challenging task requiring complex setups as well as highly trained personnel e.g. mass spectrometry [1, 2]. Their detection is hampered by their intrinsic properties such as their small size and the availability of only one epitope for binding. Thus, most immunoassays still do not provide a fast turn-around time and lack the sensitivity required for diagnostics [3, 4]. Moreover, the tedious steps included e.g. washing, blocking and signal development hinders the transfer of these assays to point of care (POC) devices [5]. On the other hand, aptamers stand out as a promising alternative to antibodies due to their stability, fast binding kinetics and the reversibility of the binding [6, 7].

Aptamers are single stranded DNA/RNA sequences selected in-vitro through a process known as SELEX [8, 9]. They have been selected for various targets such as proteins, small molecules, toxins and single ions [6, 10, 11]. The fast binding kinetics and the easy simple modifications of aptamers enables the development of non-conventional POC devices [12–14]. Additionally, they have been explored to replace antibodies in some lateral flow assays as simple point of care devices [7].

Lateral flow assays are a class of paper- or fiber-based POC platforms. Lateral flow immunoassays (LFIA) are simple, fast and can provide reliable results within few minutes; however, their performance with regard to small molecules is still insufficient. Some of the principal drawbacks associated with LFA are the non-specific interactions to the membrane material, inversible relation between signal and target concentration (competitive format) and the unfavorable optical properties of the membranes [7, 15, 16]. A typical LFA assay consists of a porous membrane, molecular recognition elements

Electronic supplementary material The online version of this article (https://doi.org/10.1007/s00604-019-3795-9) contains supplementary material, which is available to authorized users.

✉ Hans-Peter Deigner
dei@hs-furtwangen.de

[1] Institute of Precision Medicine, Furtwangen University, Jakob-Kienzle-Straße 17, 78054 Villingen-Schwenningen, Germany

[2] Department of Pharmaceutical and Medicinal Chemistry, Institute of Pharmaceutical Sciences, Eberhard Karls Universität Tübingen, Auf der Morgenstelle 8, 72076 Tübingen, Germany

[3] EXIM Department, Fraunhofer Institute IZI, Leipzig, Schillingallee 68, D-18057 Rostock, Germany

Published online: 09 October 2019

(MRE) e.g. antibodies or aptamers as well as a test/control lines with corresponding MRE depending on the assay format e.g. sandwich or competitive [17]. Moreover, a reporter molecule/particle for signal generation such as gold nanoparticles, quantum dots, fluorescent or magnetic beads [15].

Magnetic beads are Micro or Nano-sized particles containing iron or iron oxide. Magnetic mono-sized particles provide a large and uniform surface area for attaching functional molecules e.g. antibodies, enzymes, DNA or aptamers. This can be achieved through various covalent and non-covalent strategies [18]. Superparamagnetic beads can be separated exceptionally fast using external magnetic forces. This allows for a hybrid assay which is fast due to the easy and efficient mixing and spatial separation for including washing steps when needed. These properties made magnetic beads suitable for use in various application such as cell preparation, immunoassays, bio-separation and targeted drug delivery [19]. They have been implemented in LFA assays as reporter molecules and were detected either visually [20] or by a magnetic reader [17, 21].

The EA aptamer was selected and optimized by Mann et al. [22]. This system was selected for this work, as it is well characterized and the aptamer binding structure as well as the specificity has been extensively studied [23–25]. The aptamer binds to EA in a G-quadruplex conformation [24]. Ethanolamine is a small organic amine that plays a crucial role in both health and disease [26]. It has been associated with various conditions such as Parkinson's disease [27], depression and bipolar disorder [28], and Alzheimer's disease [29]. On the other hand, it has a protective role in low serum induced apoptosis [30], as a cardioprotective agent [31], and a role in proliferation of hepatocytes [32]. It is also known to have toxic effects on humans upon inhalation or contact [33]. Nevertheless, it is not possible to directly detect EA through LC/MS [34]. This motivated the development of different sensors for the detection of EA e.g. fluorescence, electrochemical, indirect LC/MS and thermofluorimetric [23, 34–36]. They are based on either strand displacement or the G-quadruplex binding conformation of the aptamer. However, they need bulky equipment and highly trained personnel. This makes them unsuitable for the direct implementation as POC assays.

This work presents an assay system based on strand displacement [23] and magnetic microbeads in a capillary platform. This system mimics a lateral flow system; however, the signal is directly proportional to the analyte concentration, spatial separation allows for adding washing steps if needed and separation of signal from background. Streptavidin coated magnetic particles were used for the simple and direct immobilization of biotin labelled oligonucleotides [37]. The capillary tubes were coated with 3 layers. First, short oligonucleotides complementary to EA aptamer (EA-comp.) were immobilized to the capillary surface followed by aptamer-magnetic beads. This resulted in hybridization of the aptamer magnetic beads to the oligonucleotides. A third layer consisting of oligonucleotide-magnetic particles was hybridized to the free aptamers (facing away from the capillary surface); this was to avoid any free non-hybridized aptamers and to ensure that strand displacement results in a magnetic particle release from the surface. The minimum manipulation needed, low sample volume as well as the visual detection are ideal for using the system as POC assay.

Materials and methods

Materials

Oligonucleotides were synthesized and purified by Integrated DNA Technologies (Coralville, IA, www.idtdna.com).

Ethanolamine, phenylethylamine, propylamine, ethanol and human serum were purchased from Sigma-Aldrich (Darmstadt, Germany, www.sigmaaldrich.com).

Magnetic particles 1 µm (Dynabeads™ MyOne™ Streptavidin C1 product number: 65002) and DNA coating solution (product number: 17250) were purchased from Thermo Fischer Scientific (Sankt Leon-Rot, Germany, www.thermofisher.com).

Untreated Polyethylene Terephthalate Glycol (PETG) capillary tubes measuring 0.85*1.55*75 mm (1216 M98) were purchased from Thomas Scientific (Swedesboro, USA, www.thomassci.com).

Neodymium magnet cubes measuring 5 mm × 5 mm × 5 mm with the grade N45 were purchased from Amazon EU S.à r.l. (Munich, Germany, www.amazon.de).

The following are the sequences for the used aptamers:

Name	Sequence	Modification
EA binding aptamer (EA-apt)	5′- ATACCAGCTTATTCAATTTGAGGCGGGTGGGTGGGTTGAATA −3’	3’ Biotin
Non-binding sequence (EA-neg.)	5′- CACGGCATGGTTCCATACTTAAGGGCGTCGTGGTTGGGTGGG-3’	3’ Biotin
Complementary strand Et 1 0_3 (EA-comp.)	5′- CCACCCACCC-3’	3’ Biotin
Complementary strand for negative sequence ET 10_nt (EA-cnt)	5′- CCCACCCAAC-3’	3’ Biotin

Methods

Oligonucleotides and aptamers coupling to streptavidin coated magnetic beads

Streptavidin-coupled Dynabeads® 1 μm magnetic beads were diluted to 1 mg.ml^{-1} in 1x phosphate buffered saline (PBS) pH 7.4 and used at this concentration throughout all experiments.

The coupling procedure was performed according to the manufacture protocol as follows: a volume of 50 μL (10 mg.ml^{-1}) particles was diluted in 450 μL PBS buffer in an 0.5 ml Eppendorf tube. The particles were washed a total of 3 washes with PBS solution. Afterwards, a volume of 10 μL of the buffer was replaced by 10 μL biotin labelled oligonucleotide at a concentration of 100 μM and incubated overnight on a shaker. The particles were washed again 3 times with PBS solution and the first supernatant was collected for evaluating the reaction efficiency.

Coating the capillaries with oligonucleotides

The capillary tubes were coated with the EA-comp. Using the DNA coating solution according to the manufacture protocol.

A 25 μM oligonucleotide solution was prepared and an equal volume of the DNA coating solution was added in a glass container, the capillaries were filled with about 20 μL of the solution and a red mark was made as a filling line. After an overnight incubation, the capillaries were washed three times with 25 μL PBS using a syringe. Then the tubes were left to dry at room temperature for 2 h.

Development of the test platform

The EA-comp. Coated capillary tubes were filled with 20 μL EA-apt. Functionalized magnetic particles using capillary forces. The tubes were incubated overnight afterwards washed three times with a PBS pH 7.4 solution.

The aptamer-magnetic beads coated capillaries were then filled with complementary oligonucleotides (EA-comp. and EA-cnt) functionalized magnetic beads solution and incubated overnight followed by a 3 times PBS wash. The tubes were left to dry at room temperature for 2 h prior to use.

Quantification of oligonucleotides immobilization and hybridization efficiency

Nanophotometer (Nanophotometer® P-class, P-360, Implen GmbH) was used to determine the amount of immobilized oligonucleotides; 1 μl of the supernatant was transferred to the nanodrop and a triplicate measurement were recorded per sample. The same measurements were done with non-reacted oligonucleotides as a control to the total absorption.

Similarly, the EA-apt. Functionalized magnetic particles were reacted with the EA-comp. Oligonucleotide and after separation the supernatant was collected and analyzed. This gave insights on the ability of the complementary strands to hybridize to the aptamers and the effect of steric hinderance.

Characterization of the magnetic beads

Characterization of the particles was performed using light microscopy. Images were capture for three samples a) magnetic beads conjugated with EA apt., b) a mixture of magnetic beads conjugated with EA-apt. and reacted with the magnetic beads conjugated with the EA-comp., and c) the mixture in b) after reacting with 200 nM ethanolamine for 5 min. A volume of 5 μL was then transferred to a glass microscope slide and images were captured using light microscopy with 40x magnification.

Ethanolamine binding response and specificity of the assay

The capillary platform was filled with a different concentration of ethanolamine (0 to 200 nM) solution. The capillaries were filled with 20 μL of ethanolamine diluted in PBS buffer and incubated for 5 min. A permanent neodymium magnet was placed above the filling line (marked in red on the capillaries) and the solution was removed using a syringe.

As controls to the specificity of the response, the capillaries were challenged with structurally similar (ethanol, propylamine and phenylethylamine) molecules. Each experiment was repeated at least 3 times to account for signal variation and assess the reproducibility of the response.

Serum samples were diluted to a 10% concentration using PBS buffer and spiked with ethanolamine to a concentration of 25 nM and 75 nM. Tap water was used to prepare PBS buffer and then used to prepare 25 nM and 75 nM ethanolamine solutions.

After completion of the assay, the capillaries were fixed to a plain sheet of paper and images were captured using a smartphone for further analysis.

Data and image analysis

Images were analyzed using the ImageJ image processing program [38]. The magnetic spots (brown/black) were measured for area using the analysis command. The spot area was chosen as the analysis parameter as this is minimally affected by differences in exposure or brightness of the images. The spot area (pixel^2) was plotted against the concentration to produce the calibration plots. In this case, no calibration was needed as all the capillaries were captured in the same image. However, to be able compare the response of the ethanolamine in buffer, serum and tap water the area was measured in (pixel^2) and then converted to mm^2. This was done by

calibrating the number of pixels corresponding to the known length of the capillary (75 mm). The same was applied to the structurally similar molecules (ethanol, propylamine and phenylethylamine). Then the area of the spots in mm^2 were plotted against the concentration of EA for comparison.

Data analysis (plotting, fitting using linear and non-linear regression analysis and statistical significance) was performed using GraphPad Prism version 8.02 for Windows, GraphPad Software, La Jolla California USA, www.graphpad.com.

Results and discussion

Immobilization and hybridization efficiency

The immobilization of the biotin labelled oligonucleotides and aptamers to the magnetic particles was confirmed using absorption values at 260 nm. The absorption values before (0.064 and 0.067) and after the reaction (0.029 and 0.028) were compared to estimate the DNA amount immobilized on the surface of the beads. The amount of EA-apt. Immobilized was 515 pmol per mg bead and 560 pmol per mg beads for the EA-comp. This corresponds to 515 nM EA-apt. and 560 nM EA-comp.. These amounts agree with the manufacture specification of 500 pmol per mg beads.

To assess the functionality of the immobilized oligonucleotides, the EA-apt. Functionalized magnetic particles were reacted with the EA-comp. and the absorbance values before (0.067) and after the reaction (0.048) were compared. The hybridization efficiency of the EA-comp. to the EA-apt. Functionalized beads was 55%, this can be attributed to the steric effects exerted by the magnetic particles.

To further characterize the particles, light microscopy was used to capture images of the magnetic particles. The EA-apt. Conjugated magnetic particles (Fig. S4), shows a monodisperse magnetic particles. Upon reacting with the EA-comp. Conjugated particles (Fig. S5) the particles formed clusters due to the hybridization of the DNA. The addition of ethanolamine 200 nM to the hybridized particles lead to the strand displacement reaction and in the redispersion of the formed clusters (Fig. S6).

Assessment of the capillary coating and non-specific interactions

The capillary tubes were coated with the complementary oligonucleotides EA-comp. and EA-nct. Using DNA coating solution. The coated tubes were first reacted with the EA-apt. and EA-neg. Functionalized beads. Afterwards the tubes were reacted with magnetic beads functionalized with the corresponding complementary oligonucleotide (EA-comp. and EA-nct.). This resulted in three layers attached to the capillary surface.

As seen in (Fig. S1), non-specific adsorptions to the capillaries were minimal, three different controls a) EA-apt. Coated capillaries and EA-nct functionalized beads with no-complementarity, b) EA-comp. Coated capillaries with streptavidin coated magnetic beads and c) non-coated capillaries and EA-apt. Functionalized magnetic beads were used to assess the specificity. Minimum non-specific adsorption can be seen in the case of the coated tubes and functionalized particles with no complementary oligonucleotide (Fig. S1a).

Ethanolamine binding response

The assay is based on strand displacement as the target bind to the aptamers releasing the magnetic particles and their subsequent capture for visual detection. As seen in Fig. 1, the amount of magnetic particles released after the incubation with ethanolamine is proportional to the concentration of ethanolamine in the sample solution. The assay has a visual limit of detection of 5 nM within 5 min. Negative control reacted with buffer only showed no displacement of the particles, and no magnetic spots were visually detected.

Further quantitative analysis was carried out using images captured using a smartphone and ImageJ analysis software. The resulting calibration plot (Fig. 2) was fitted using one site total binding eq. $Y=Bmax*X/(Kd+X)+NS*X+$ Background, Kd was 33.93 ± 16.31 nM. The assay showed a linear range between 5 and 75 nM (Fig. 2 inset). Previous studies [23] reported a Kd value of 9.6 ± 1.4 nM and a limit of detection of 10 pM using the full length aptamer (96 nt), an incubation time of 18 h and fluorescence readout. Using

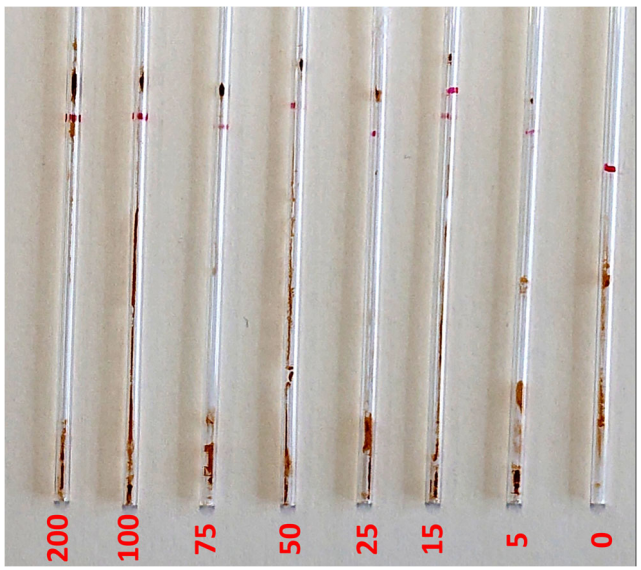

Fig. 1 shows the capillaries after reacting with ethanolamine samples (5 to 200 nM) and buffer only (0). The black/brown spots are the displaced magnetic particles after collection using a permanent magnet. For making the photos and further analysis the solution was completely withdrawn from the capillaries and the capillaries were glued to a blank paper sheet

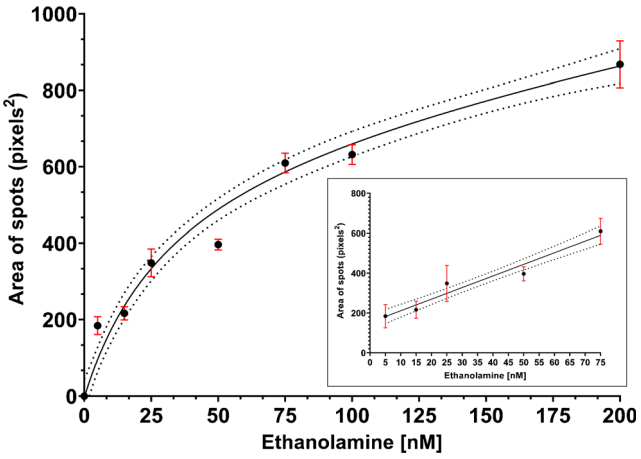

Fig. 2 Plot of spots' area (pixel^2) against ethanolamine concentration in the sample. The spots area from the capillaries (Fig. 1) was measured using ImageJ software. The points show the mean value and the error bars represent the standard deviation $n = 3$. The line represents the best fit using one site total binding eq. Y=Bmax*X/(Kd + X) + NS*X + Background, r2 = 0.9872. The inset shows the linear response of the assay from 5 to 75 nM; the line represents the best fit with the eq. Y = 5.826*X + 153.0 r2 = 0.9336. The dashed lines represent the 95% CI of the best fitting lines

electrochemical impedance spectroscopy, Liang et al. [35] could detect 0.08 nM ethanolamine.

Specificity of the assay

Various controls were implemented to further confirm the specificity of the assay response. Non-binding aptamers (EA-neg.) showed no displacement of the strands, and no magnetic spots were visually detected at ethanolamine concentration of 100 and 200 nM (Fig. S2).

Studies on the specificity of the ethanolamine aptamers found that they react to various molecules containing ethyl- or methylamine groups [25]. Structurally similar molecules (phenylethylamine, propylamine and ethanol) all showed no visually detected spots in the assay range. However, increasing the concentrations substantially (1 μM) lead to displacement of magnetic particles and formation of a magnetic spot (Fig. 3 and fig. S3) which agrees with previously published findings [23, 36].

Detection of ethanolamine in complex samples

The capillary platform was challenged with tap water and 10% serum samples containing 25 and 75 nM ethanolamine. The response (Fig. 4) showed that the effect of the matrix is minimal, and the results were comparable to the response in buffer (analyzed using ANOVA comparing to one control (buffer) no significant difference was observed. P value 0.8463) (Fig. 5). This showed that the platform can be applied to real samples for visual detection of ethanolamine.

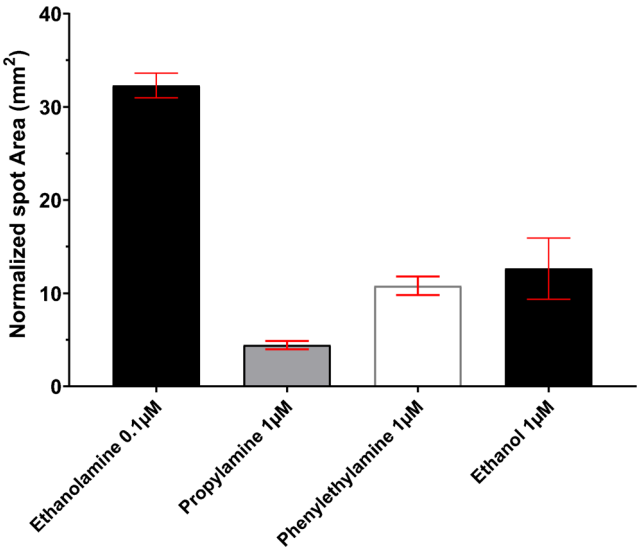

Fig. 3 normalized spot area against EA structurally similar molecules. The plot shows the response of 0.1 μM ethanolamine and 1 μM propylamine, phenylethylamine and ethanol. The error bars represent the standard deviation $n = 4$

Comparison with published EA assays

Various approaches have been described for the detection and quantification of ethanolamine (Table 1). Based on strand displacement, Heilkenbrinker et al. [23] developed a competitive microarray for EA using a fluorescence readout. The assay could detect EA as low as 10 pM EA, however, it needed 18 h incubation time. Moreover, the inverse relation between the analyte concentration and signal limited the use of complex sample matrix in this system.

Making use of the G-quadruplex binding conformation of the EA aptamer, Liang et al. [35] developed a label free

Fig. 4 shows the capillaries after reacting with ethanolamine samples (0, 25 and 75 nM) spiked in tap water and 10% serum respectively. The black/brown spots are the displaced magnetic particles after collection using a permanent magnet. For making the photos and further analysis the solution was completely withdrawn from the capillaries and the capillaries were glued to a blank paper sheet

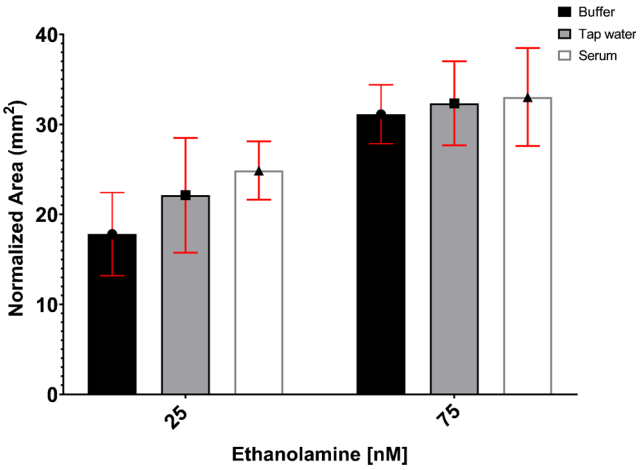

Fig. 5 the response of the assay after incubation with Ethanolamine in **a**) buffer, **b**) tap water and **c**) 10% serum. $n = 3$ and error bars represent the standard deviation. Statistical significance was evaluated using ANOVA comparing to one control (buffer) no significant *difference was observed*

electrochemical impedance spectroscopy sensor. The sensor detected 0.08 nM ethanolamine in 1-h incubation time with high specificity in real samples. However, this system still needed a bulky instrument to measure electrochemical impedance and is not suitable for low cost settings.

Another approach described by Lee et al. [34] combined gold nanoparticles and strand displacement coupled with LC/MS to indirectly quantify EA. The displaced adenine rich strand was hydrolyzed and quantified through LC/MS, indirectly detecting EA (LOD 1.2 nM). The method offered an alternative platform for molecules not suitable for direct LC/MS analysis. However, it is based on LC/MS and is not suitable for a POC application.

Using Thermofluorimetric analysis [36], the melting temperature shifts of EA aptamer beacons was used to quantify EA. Using a PCR instrument EA was quantified through stabilization of the aptamer beacons with a limit of detection 1.5 nM. The homogeneous assay format combined with PCR provided high throughput analysis of EA using 2 μL sample volume and no incubation. However, the assay is based on a PCR instrument and requires well trained personnel.

In comparison to previously published methods, the magnetic capillary assay requires minimum manipulation and no readout device. The use of magnetic beads allows reaching an LOD of 5 nM within 5 min. The combined use of plastic capillaries, visual detection and passive flow make the assay suitable as a POC device.

Conclusion

This work presents an assay for detecting ethanolamine, based on strand displacement and magnetic separation. Platform generation was achieved through the multilayer immobilization of the aptamer-magnetic particles. The inclusion of magnetic particles allows for spatial separation of signal from background and subsequent visual detection. The spatial separation of the magnetic particles from the solution decreases the matrix effect and allows the direct analysis of complex or colored samples. Additionally, the use of magnetic particles in a multilayer format allowed increasing the specificity for the small molecule target. This is due to steric hinderance exerted by the particles on interfering molecules e.g. proteins or lipids leading to a size exclusion effect (sieving). The assay's limit of detection (5 nM) and dynamic range (5–75 nM) were in good agreement with aptamer based LFA based on visual detection reviewed in [39]. The assay was performed in plastic capillaries and can be used as a standalone device or can be incorporated in test cassettes for POC applications. It has a great potential in various fields where fast yes/no or semi-quantitative simple assays are needed; applications include but are not limited to clinical diagnostics, environmental assay, water and food contamination, drugs of abuse and doping.

The possibility of regenerating the platform and the magnetic particles must be investigated further. Nevertheless, as the aptamer coated magnetic particles are displaced from the surface, these can be collected, and the bound target washed off, an option which, however, has not been confirmed experimentally in this study. Some of the assay drawbacks are related to the specificity of the aptamers used. The principle,

Table 1 summary of different assays for the detection of ethanolamine

Method	Readout	Target/Aptamer	Limit of Detection/ Incubation time	Linear range	Ref.
Strand displacement Microarray	Fluorescence	EA/ 96 nucleotide DNA aptamer	10 pM 18 h	–	[23]
Electrochemical impedance spectroscopy	Electrochemical	EA/ 42 nucleotide DNA aptamer	0.08 nM 1 h	0.16–16 nM	[35]
Indirect LC/MS	LC/MS	EA/34 nucleotide DNA aptamer	1.2 nM-	5–5000 nM	[34]
Thermofluorimetric Analysis	PCR melting curve	EA/ 42 and 31 nucleotide DNA aptamer beacons	1.5 nM-	–	[36]
Magnetic capillary assay	Visual/RGB photos analysis	EA/ 42 nucleotide DNA aptamer	5 nM 5 min	5–75 nM	This work

however, can be transferred to other aptamers after carefully designing a strand-displacement assay. The assay can also be developed as a qualitative method with a preset cut-off value for fast detection of analytes. It thus meets a great need for POC assays in low resource settings.

Acknowledgements The authors thank Ms. Evelyn Halitzki for experimental support.

Author contributions M. Mahmoud performed the lab-experiments, analyzed data, prepared the figures and contributed to writing the manuscript; S. Laufer contributed to the planning and to manuscript writing; HPD contributed to the study design, analysis of experimental data and to manuscript writing.

Compliance with ethical standards This article does not contain any studies involving human participants performed by any of the authors.

Conflict of interests The authors declare no competing interests.

References

1. Fechner P, Bleher O, Ewald M, Freudenberger K, Furin D, Hilbig U, Kolarov F, Krieg K, Leidner L, Markovic G, Proll G, Proll F, Rau S, Riedt J, Schwarz B, Weber P, Widmaier J (2014) Size does matter! Label-free detection of small molecule-protein interaction. Anal Bioanal Chem 406(17):4033–4051
2. McKeague M, DeRosa MC (2012) Challenges and opportunities for small molecule aptamer development. J Nucleic Acids 2012: 20–20. https://doi.org/10.1155/2012/748913
3. Rubina AY, Dementieva EI, Stomakhin AA, Darii EL, Pan'kov SV, Barsky VE, Ivanov SM, Konovalova EV, Mirzabekov AD (2003) Hydrogel-based protein microchips: manufacturing, properties, and applications. Biotechniques 34(5):1008–1014 1016-1020, 1022
4. Brandhorst G, Oellerich M, Maine G, Taylor P, Veen G, Wallemacq P (2012) Liquid chromatography-tandem mass spectrometry or automated immunoassays: what are the future trends in therapeutic drug monitoring? Clin Chem 58(5):821–825. https://doi.org/10.1373/clinchem.2011.167189
5. Singh P (2016) SPR biosensors: historical perspectives and current challenges. Sensors Actuators B Chem 229:110–130. https://doi.org/10.1016/j.snb.2016.01.118
6. Toh SY, Citartan M, Gopinath SCB, Tang T-H (2015) Aptamers as a replacement for antibodies in enzyme-linked immunosorbent assay. Biosens Bioelectron 64(0):392–403. https://doi.org/10.1016/j.bios.2014.09.026
7. Chen A, Yang S (2015) Replacing antibodies with aptamers in lateral flow immunoassay. Biosens Bioelectron 71:230–242. https://doi.org/10.1016/j.bios.2015.04.041
8. Tuerk C, Gold L (1990) Systematic evolution of ligands by exponential enrichment: RNA ligands to bacteriophage T4 DNA polymerase. Science (New York, NY) 249(4968):505–510
9. Ellington AD, Szostak JW (1990) In vitro selection of RNA molecules that bind specific ligands. Nature 346(6287):818–822. https://doi.org/10.1038/346818a0
10. Radom F, Jurek PM, Mazurek MP, Otlewski J, Jeleń F (2013) Aptamers: molecules of great potential. Biotechnol Adv 31(8): 1260–1274. https://doi.org/10.1016/j.biotechadv.2013.04.007
11. Tombelli S, Minunni M, Mascini M (2005) Analytical applications of aptamers. Biosens Bioelectron 20(12):2424–2434
12. Zhang W, Liu QX, Guo ZH, Lin JS (2018) Practical application of aptamer-based biosensors in detection of low molecular weight pollutants in water sources. Molecules 23(2):344
13. Mehlhorn A, Rahimi P, Joseph Y (2018) Aptamer-based biosensors for antibiotic detection: a review. Biosensors 8(2):54
14. Hasanzadeh M, Shadjou N, de la Guardia M (2017) Aptamer-based assay of biomolecules: recent advances in electro-analytical approach. TrAC Trends Anal Chem 89:119–132. https://doi.org/10.1016/j.trac.2017.02.003
15. Posthuma-Trumpie GA, Korf J, van Amerongen A (2009) Lateral flow (immuno)assay: its strengths, weaknesses, opportunities and threats. A literature survey. Anal Bioanal Chem 393(2):569–582. https://doi.org/10.1007/s00216-008-2287-2
16. Jauset-Rubio M, Svobodová M, Mairal T, McNeil C, Keegan N, El-Shahawi MS, Bashammakh AS, Alyoubi AO, O'Sullivan CK (2016) Aptamer lateral flow assays for ultrasensitive detection of β-Conglutin combining recombinase polymerase amplification and tailed primers. Anal Chem 88(21):10701–10709. https://doi.org/10.1021/acs.analchem.6b03256
17. Jacinto MJ, Trabuco JRC, Vu BV, Garvey G, Khodadady M, Azevedo AM, Aires-Barros MR, Chang L, Kourentzi K, Litvinov D, Willson RC (2018) Enhancement of lateral flow assay performance by electromagnetic relocation of reporter particles. PLoS One 13(1):e0186782. https://doi.org/10.1371/journal.pone.0186782
18. Jonkheijm P, Weinrich D, Schröder H, Niemeyer CM, Waldmann H (2008) Chemical strategies for generating protein biochips. Angew Chem Int Ed 47(50):9618–9647. https://doi.org/10.1002/anie.200801711
19. Colombo M, Carregal-Romero S, Casula MF, Gutierrez L, Morales MP, Bohm IB, Heverhagen JT, Prosperi D, Parak WJ (2012) Biological applications of magnetic nanoparticles. Chem Soc Rev 41(11):4306–4334. https://doi.org/10.1039/c2cs15337h
20. Tang D, Sauceda J, Lin Z, Ott S, Basova E, Goryacheva I, Biselli S, Lin J, Niessner R, Knopp D (2009) Magnetic nanogold microspheres-based lateral-flow immunodipstick for rapid detection of aflatoxin B2 in food. Biosens Bioelectron 25(2):514–518
21. Granade TC, Workman S, Wells SK, Holder AN, Owen SM, Pau C-P (2010) Rapid detection and differentiation of antibodies to HIV-1 and HIV-2 using multivalent antigens and magnetic Immunochromatography testing. Clin Vaccine Immunol 17(6): 1034–1039. https://doi.org/10.1128/cvi.00029-10
22. Mann D, Reinemann C, Stoltenburg R, Strehlitz B (2005) In vitro selection of DNA aptamers binding ethanolamine. Biochem Biophys Res Commun 338(4):1928–1934. https://doi.org/10.1016/j.bbrc.2005.10.172
23. Heilkenbrinker A, Reinemann C, Stoltenburg R, Walter J-G, Jochums A, Stahl F, Zimmermann S, Strehlitz B, Scheper T (2015) Identification of the target binding site of ethanolamine-binding aptamers and its exploitation for ethanolamine detection. Anal Chem 87(1):677–685. https://doi.org/10.1021/ac5034819
24. Cheng X, Liu X, Bing T, Zhao R, Xiong S, Shangguan D (2009) Specific DNA G-quadruplexes bind to ethanolamines. Biopolymers 91(10):874–883. https://doi.org/10.1002/bip.21272
25. Reinemann C, Stoltenburg R, Strehlitz B (2009) Investigations on the specificity of DNA aptamers binding to ethanolamine. Anal Chem 81(10):3973–3978. https://doi.org/10.1021/ac900305y
26. Patel D, Witt SN (2017) Ethanolamine and phosphatidylethanolamine: Partners in Health and Disease. Oxidative Med Cell Longev 2017:18–18. https://doi.org/10.1155/2017/4829180
27. Wang S, Zhang S, Liou L-C, Ren Q, Zhang Z, Caldwell GA, Caldwell KA, Witt SN (2014) Phosphatidylethanolamine deficiency disrupts α-synuclein homeostasis in yeast and worm models of

Parkinson disease. Proc Natl Acad Sci 111(38):E3976–E3985. https://doi.org/10.1073/pnas.1411694111
28. Modica-Napolitano JS, Renshaw PF (2004) Ethanolamine and phosphoethanolamine inhibit mitochondrial function in vitro: implications for mitochondrial dysfunction hypothesis in depression and bipolar disorder. Biol Psychiatry 55(3):273–277. https://doi.org/10.1016/S0006-3223(03)00784-4
29. Farooqui AA, Rapoport SI, Horrocks LA (1997) Membrane phospholipid alterations in Alzheimer's disease: deficiency of ethanolamine Plasmalogens. Neurochem Res 22(4):523–527. https://doi.org/10.1023/a:1027380331807
30. Matas D, Juknat A, Pietr M, Klin Y, Vogel Z (2007) Anandamide protects from low serum-induced apoptosis via its degradation to ethanolamine. J Biol Chem 282(11):7885–7892. https://doi.org/10.1074/jbc.M608646200
31. Kelly RF, Lamont KT, Somers S, Hacking D, Lacerda L, Thomas P, Opie LH, Lecour S (2010) Ethanolamine is a novel STAT-3 dependent cardioprotective agent. Basic Res Cardiol 105(6):763–770. https://doi.org/10.1007/s00395-010-0125-0
32. Sasaki H, Kume H, Nemoto A, Narisawa S, Takahashi N (1997) Ethanolamine modulates the rate of rat hepatocyte proliferation in vitro and in vivo. Proc Natl Acad Sci 94(14):7320–7325
33. Gamer AO, Rossbacher R, Kaufmann W, van Ravenzwaay B (2008) The inhalation toxicity of di- and triethanolamine upon repeated exposure. Food Chem Toxicol 46(6):2173–2183. https://doi.org/10.1016/j.fct.2008.02.020
34. Lee C-Y, Shiau R-J, Chou H-W, Hsieh Y-Z (2018) Combining aptamer-modified gold nanoparticles with barcode DNA sequence amplification for indirect analysis of ethanolamine. Sensors Actuators B Chem 254:189–196. https://doi.org/10.1016/j.snb.2017.07.073
35. Liang G, Man Y, Jin X, Pan L, Liu X (2016) Aptamer-based biosensor for label-free detection of ethanolamine by electrochemical impedance spectroscopy. Anal Chim Acta 936:222–228. https://doi.org/10.1016/j.aca.2016.06.056
36. Mahmoud M, Laufer S, Deigner HP (2019) An aptamer based thermofluorimetric assay for ethanolamine. Biochimie 158:233–237. https://doi.org/10.1016/j.biochi.2019.01.014
37. Green NM (1990) Avidin and streptavidin. Methods Enzymol 184:51–67
38. Schneider CA, Rasband WS, Eliceiri KW (2012) NIH image to ImageJ: 25 years of image analysis. Nat Methods 9(7):671–675
39. Schüling T, Eilers A, Scheper T, Walter J (2018) Aptamer-based lateral flow assays. AIMS Bioeng 5(2):78–102

Supplementary Information

Visual aptamer-based capillary assay for ethanolamine using magnetic particles and strand displacement

Mostafa Mahmoud[1,2], Stefan Laufer[2] and Hans-Peter Deigner[1,3*]

1-Furtwangen University, Institute of Precision Medicine, Jakob-Kienzle-Straße 17, 78054, Villingen-Schwenningen, Germany

2- Department of Pharmaceutical and Medicinal Chemistry, Institute of Pharmaceutical Sciences, Eberhard Karls Universität Tübingen, Auf der Morgenstelle 8, 72076

Tübingen, Germany

3- Fraunhofer Institute IZI, Leipzig, EXIM Department, Schillingallee 68, D-18057, Rostock, Germany

*Correspondence to deigner@hs-furtwangen.de

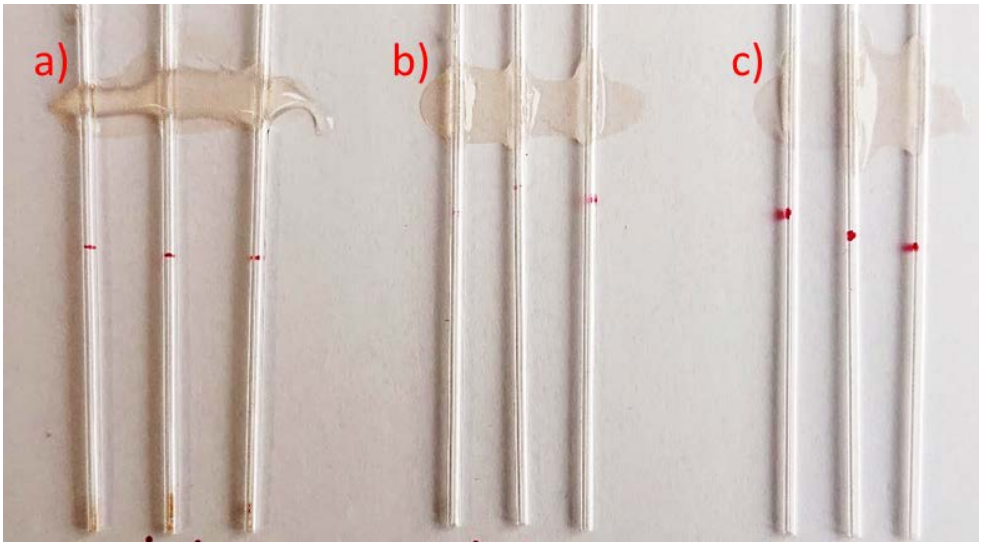

Figure S1 a) oligonucleotide-coated capillaries and oligonucleotide functionalized beads with no-complementarity, b) oligonucleotide-coated capillaries with streptavidin coated magnetic beads and c) non-coated capillaries and aptamer coated magnetic beads.

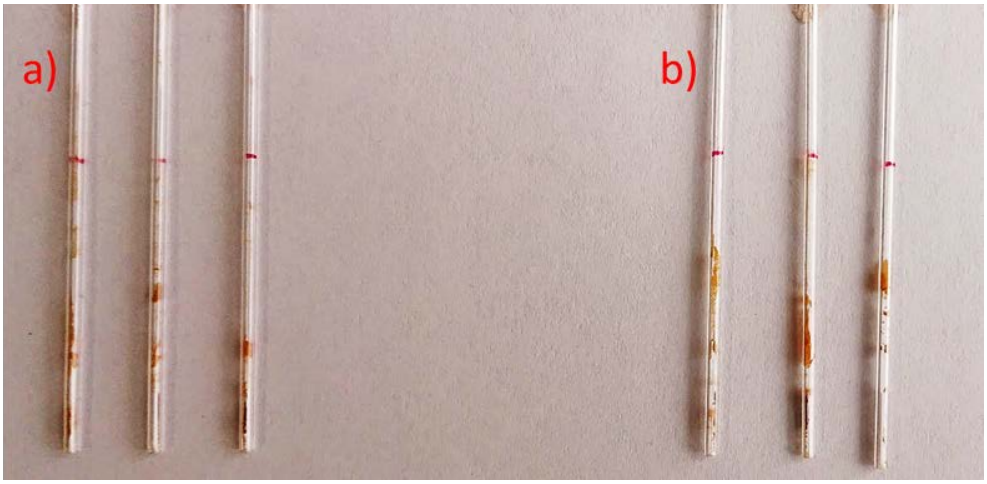

Figure S2 capillaries functionalized with a no-binding sequence as negative control after reaction with ethanolamine solution a) 100 nM and b) 200 nM. Both show no displacement of the magnetic particles and no magnetic spots can be seen above the fill line (magnet placement position).

Figure S3 capillaries challenged with 1µM phenylethylamine, 1µM propylamine and 1µM ethanol respectively. No visual response could be detected for lower concentrations.

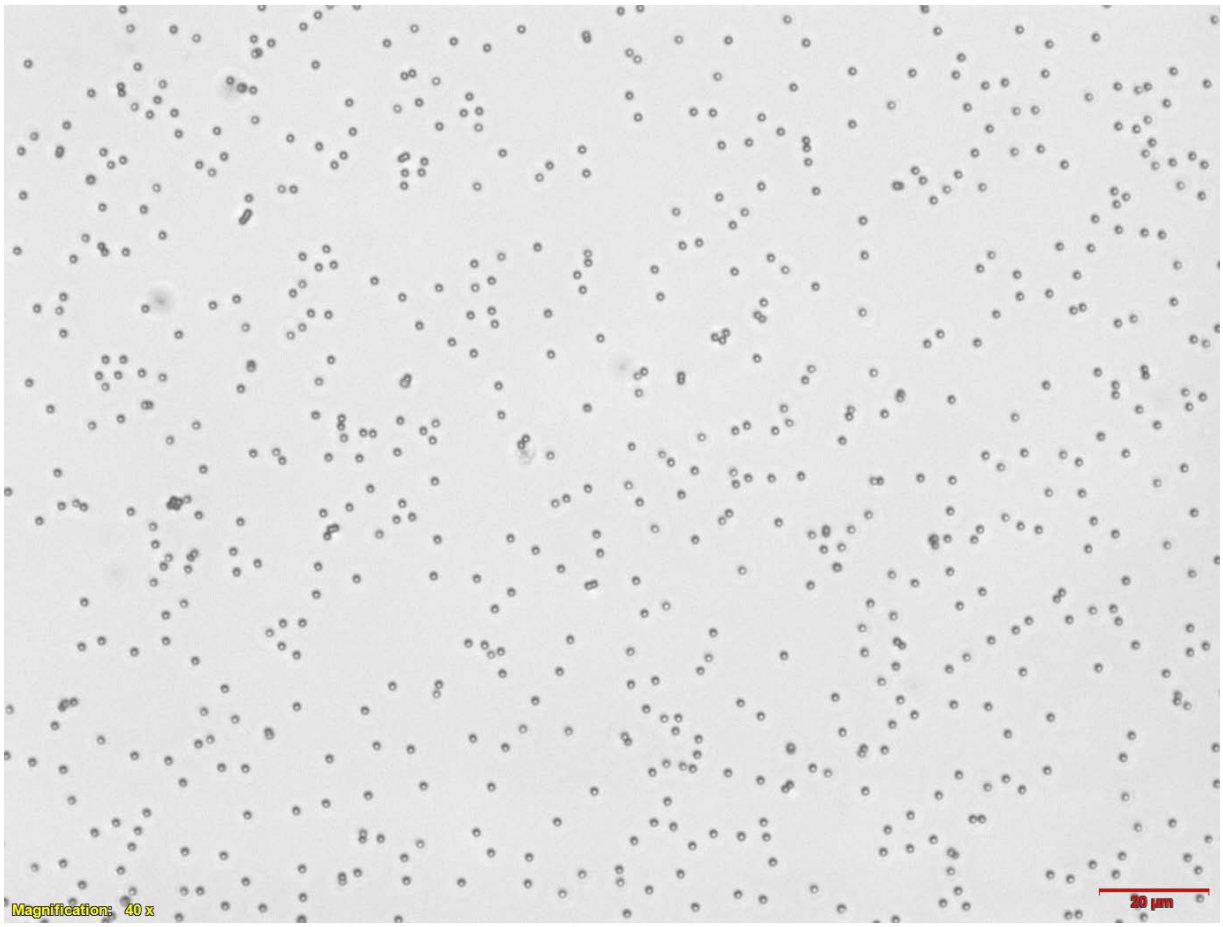

Figure S4 light microscopy image of the magnetic particles (Dynabeads 1 µm) with 40x magnification. The particles were coated with the ethanolamine aptamer and show no aggregates. Particle concentration 10 mg/ml.

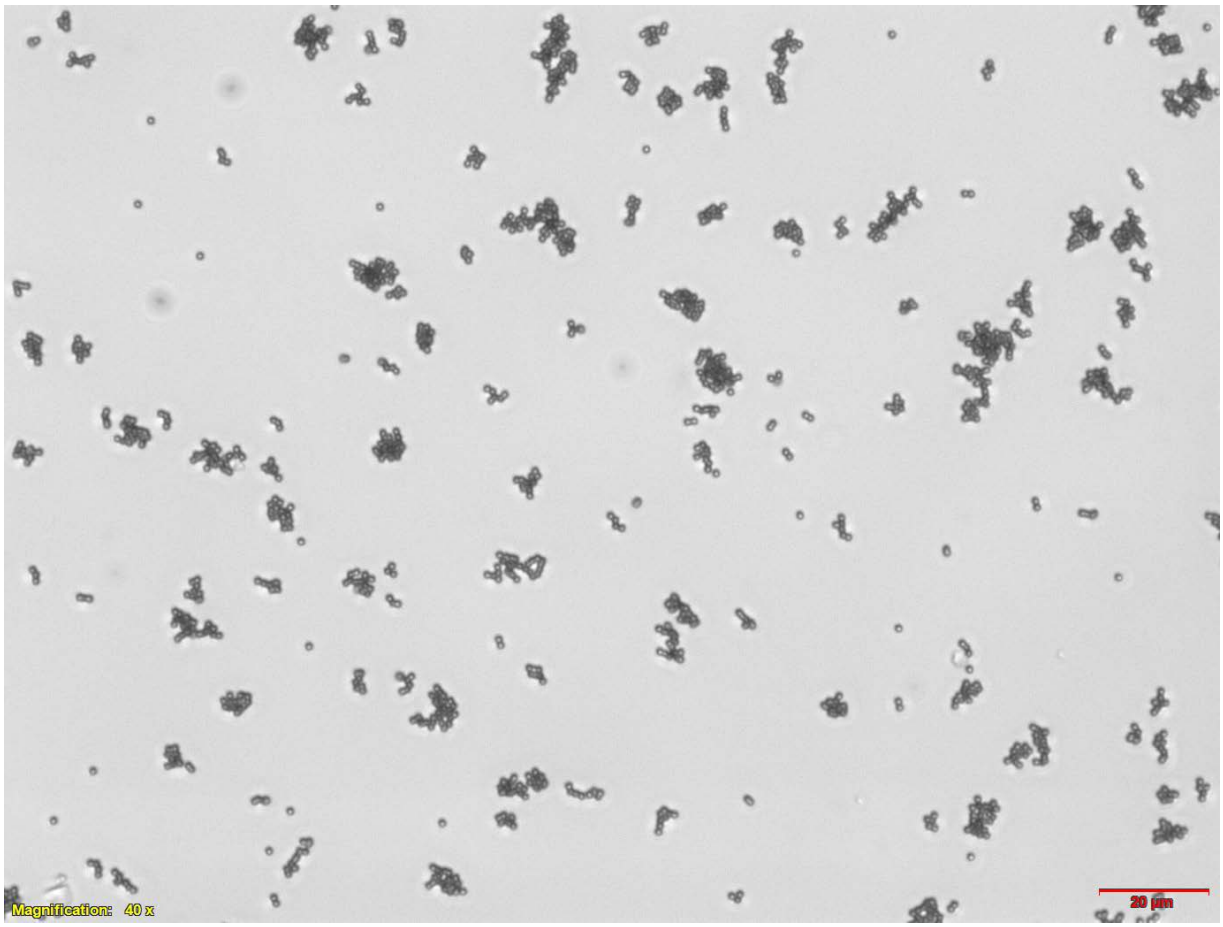

Figure S5 light microscopy image of the magnetic particles (Dynabeads 1 µm) with 40x magnification. Aptamer coated particles were reacted with particles coated with the short complementary strand. The hybridization resulted in formation of aggregates (chains) of particles.

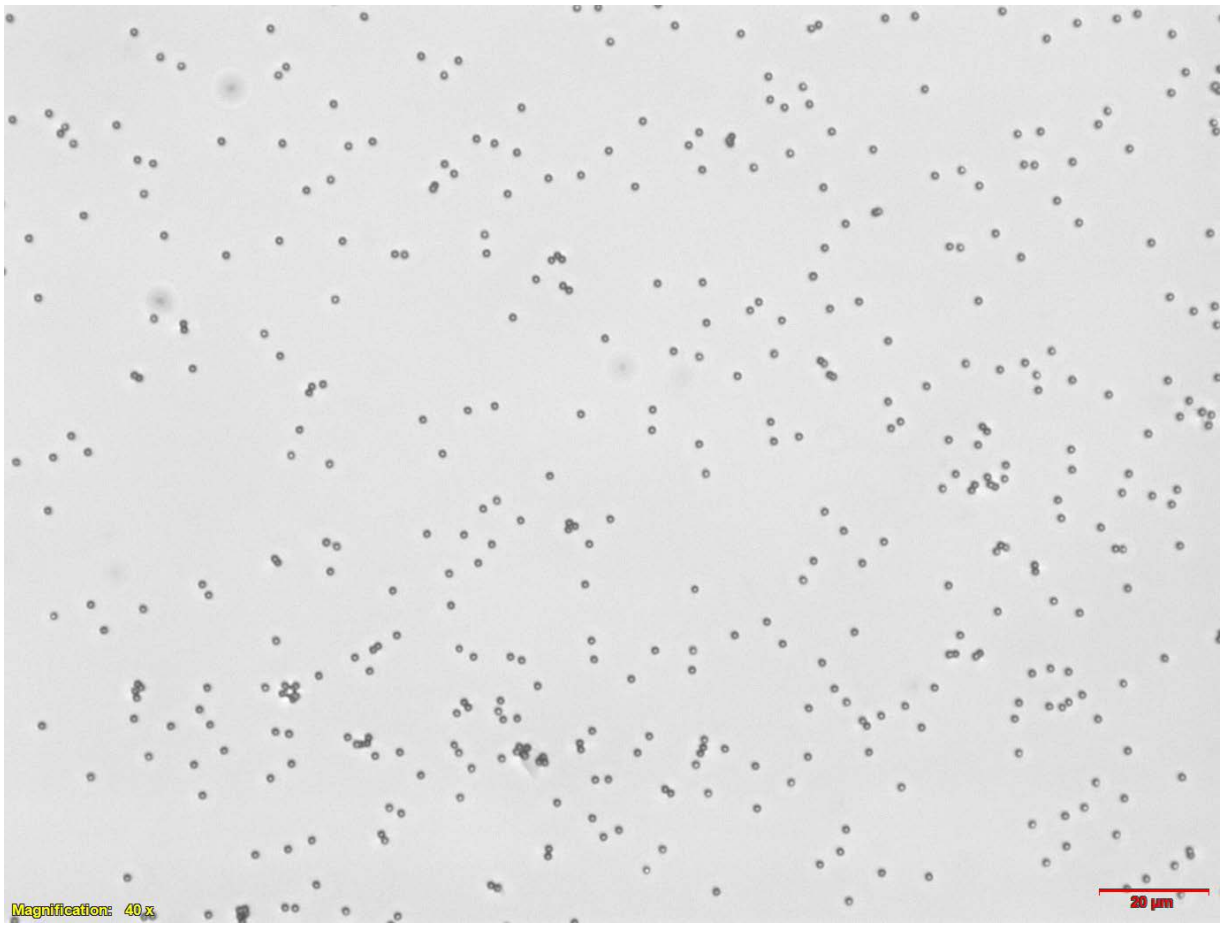

Figure S6 light microscopy image of the magnetic particles (Dynabeads 1 µm) with 40x magnification. The particles from image S5 were reacted with 200 nM ethanolamine for 5 minutes. The presence of the target led to the displacement of the particles (no aggregates).

Chapter 5

Combining aptamers and antibodies: lateral flow quantification for thrombin and interleukin-6 with smartphone readout

Status: In Press: Sensors and Actuators B: Chemical ISSN: 0925-4005
DOI: https://doi.org/10.1016/j.snb.2020.129246

Reprinted (adapted) with permission from Mahmoud M, Ruppert C, Rentschler S, Laufer S, Deigner H-P. Combining aptamers and antibodies: lateral flow quantification for thrombin and interleukin-6 with smartphone readout. Sensors and Actuators B: Chemical. 2020:129246.

Combining aptamers and antibodies: lateral flow quantification for thrombin and interleukin-6 with smartphone readout

Authors: Mostafa Mahmoud[1,2,3], Christoph Ruppert[1,2,3], Simone Rentschler[1,2,3], Stefan Laufer[3] and Hans-Peter Deigner[1,2,4,5*]

*Correspondence: dei@hs-furtwangen.de

Keywords: Duplex Lateral Flow Assay, Point-of-Care Diagnostics, Nanoparticles, Quantum Dots Image Processing, Immunoassay, Aptamer Assay, 3D-printing, Smartphone Imaging

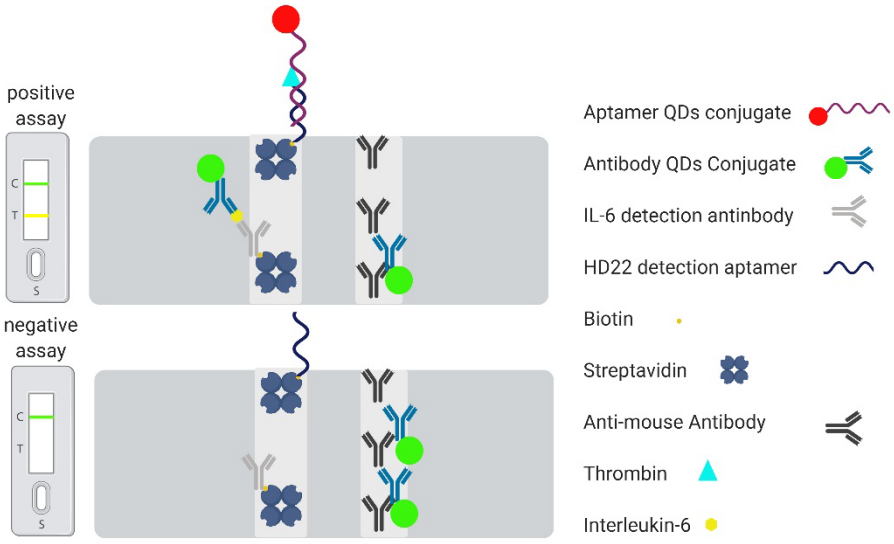

Graphical representation of the developed assay, showing positive and negative assay results

Abstract:

Modern strategies in precision medicine require diagnostic tools for fast assessment of biomarkers. A popular and well-established assay format for the rapid detection of disease markers directly at the point of care is the lateral flow assay, which enables medical staff to directly use body fluids such as blood or urine for diagnosis, without the need for a professional laboratory environment. Interleukin-6 and thrombin are clinically relevant biomarkers that are associated with infectious diseases, inflammation, and blood coagulation, and can provide valuable information on the status and treatment responses of patients with COVID-19. This work presents a novel method for the quantification of these biomarkers by using fluorescent green and red quantum dots as labels for interleukin-6 antibodies and thrombin binding aptamers, respectively. For readout, a 3D printed smartphone imager with a built in UV-LED light source is used. Through separation of RGB-channels, the acquired images can be processed to achieve a fully functional duplex lateral flow assay for simultaneous quantification of interleukin-6 and thrombin on the same test line (optical multiplexing). Furthermore, the assay performs well in complex samples (10% serum samples). In conclusion, this novel combination of antibody and aptamer-based detection in a single lateral flow assay reduces turnaround time, and the user-friendly smartphone imager facilitates availability, particularly in low resource settings.

1. Introduction

Fast, inexpensive, and readily available diagnostic tools for biomarker assessment are becoming increasingly important in precision medicine. Point-of-care (POC) tests are of particular interest, especially in disease epidemics, because they are designed to be used at

sites of patient care and to provide rapid results, thus enabling better clinical decision-making and improved clinical outcomes (1, 2). Lateral flow assays (LFAs) meet all the criteria necessary for application as POC tests (3). They have been applied in early detection of complex diseases, such as cancer (4, 5) and sepsis (6, 7), through high sensitivity and specificity multiplex quantification of various analytes.

If reliable quantitative results are necessary for analytes such as blood biomarkers, readout hardware, such as professional LFA readers, must be used. Optical strip readers can enable precise signal quantification, thus overcoming the drawback of operator dependent result interpretation, and can also improve the detectability and sensitivity of multiplex LFA sensors (8, 9). Because smartphones have become an ubiquitous part of everyday life, even in remote areas and low resource settings, smartphone-based readout of LFAs presents a major opportunity for use in POC tests (10, 11).

Numerous approaches exist for smartphone-based analysis of LFAs without additional hardware; some include using simple aids, such as a cardboard dark box, or 3D-printed accessories for applications in food analysis, drug monitoring or diagnostics (11–14). Recently, aptamers have been explored as replacements for antibodies in LFA (15, 16).

Aptamers are in vitro selected single strand oligonucleotides that bind various target molecules, e.g., proteins, small molecules, and toxins (15, 17–19). The thrombin binding aptamer (TBA) used in this work is a 15mer DNA aptamer identified in 1992 to bind thrombin exosite I (20). TBA has been studied extensively, and its binding structure has been characterized by NMR spectroscopy (21) and X-ray crystallography (22). According to these

studies, TBA binds α-thrombin in an antiparallel quadruplex structure but shows no detectable binding to γ-thrombin or to other serum proteins or enzymes (23).

Interleukin (IL) 6 and thrombin are both relevant in multiple diseases, such as chronic inflammation, autoimmunity, infectious diseases, cancer, neurodegenerative diseases, and sepsis (24–27). More recently, both molecules have been found to play important roles in severe coronavirus disease 2019 (COVID-19) and to serve as potential biomarkers (28).

COVID-19 can lead to a variety of complications, such as pneumonia, sepsis, respiratory arrest, and acute respiratory distress syndrome (ARDS). COVID-19 results in significant mortality, and ARDS is the main cause of death (29). Clinical data suggest that is one of the main mechanisms of ARDS is cytokine storm syndrome, which involves an uncontrolled systemic inflammatory response resulting from the extensive release of pro-inflammatory cytokines and chemokines (e.g., tumor necrosis factor, IL-6, and IL-1β) (29, 30) and correlates with COVID-19 severity (31). Blood levels of IL-6, a pro-inflammatory mediator, are lower in patients with mild disease but significantly elevated in critically ill patients (32). Even higher IL-6 levels are found in patients who die in the course of the disease (33). IL-6 levels therefore might be predictive of fatal outcomes, and initial determination of IL-6 might provide an opportunity to assess worsening clinical symptoms and COVID-19 progression (34, 35). IL-6 detection might even be used to identify patients eligible for a specific immunosuppressive treatment (36). Moreover, IL-6 stimulates coagulation cascades in response to SARS-CoV-2-induced inflammation by disrupting the production of tissue factor and ultimately thrombin production (37), thus contributing to coagulation abnormalities, coagulopathy, and thrombotic complications in patients with severe COVID-19 (38, 39). Early detection of patients with increased risk of coagulopathy by measuring thrombin might allow for timely therapeutic intervention and thus

decrease SARS-CoV-2 microthrombosis and the associated poor outcomes.

Quantification of IL-6 and thrombin levels (40) therefore may be highly useful in COVID-19 treatment and monitoring of therapy. For IL-6, the clinical range in healthy adults is 1.0–5.0 pg/mL, but levels rapidly increase in disease and can reach concentrations on the order of µg/ml in extreme conditions (e.g., septic shock) (24). Similarly, thrombin circulates at picomolar concentrations in the blood and regulates coagulation. However, at sites of injury, thrombin concentrations as high as several hundred nanomolar can be found. This process is regulated by natural thrombin inhibitors and is localized. Nevertheless, free thrombin levels of 5–20 nM indicate a high risk of thrombosis, and concentrations above 20 nM indicate thrombosis (41). We therefore set out to develop a straightforward and fast test for both parameters that requires minimal hardware for quantitative readout.

We present a duplex LFA system for detecting IL-6 and thrombin on the basis of red and green quantum dot (QD) labels and readout through a 3D printed smartphone reader with a built-in UV-LED light source. By splitting the colored pictures through RGB-channels, we achieved quantitative optical duplex detection on the same test line. Therefore, the system is suitable for multiparameter diagnostic applications while providing all benefits associated with POC testing.

2. Materials and Methods

2.1. Materials

Carboxyl modified QDs (Qdot 525 ITK, Qdot 605 ITK) were purchased from Thermo Fisher Scientific, (Waltham, USA). Two anti-human IL-6 antibodies (biotinylated goat polyclonal or mouse monoclonal) were purchased from Peprotech (Hamburg, Germany). An amine

modified thrombin binding aptamer (TBA: (5`-amine-TT TTT TTT TTT TTT TTT TTT GGT TGG TGT GGT TGG-3`)) and corresponding biotin labeled detection aptamer (HD22: 5`-biotin-AGT CCG TGG TAG GGC AGG TTG GGG TGA CT-3`) were purchased from Integrated DNA Technologies IDT (Leuven, Belgium). Buffers and reagents were purchased from Sigma Aldrich. All buffers and reagents were prepared with milliQ water (≥ 18 MΩ). Lateral flow test strips with a streptavidin test line and anti-mouse-antibody control line were provided by R-Biopharm (Darmstadt, Germany). A human IL-6 ELISA kit was purchased from PeproTech (Hamburg, Germany), and a human thrombin ELISA kit was purchased from Abcam (Cambridge, MA).

2.2. Synthesis of QD labeled antibodies and aptamers

Carboxyl QD conjugates (*Qdot ITK 525* for conjugation to anti-IL-6 antibody, *Qdot ITK 605* for conjugation to thrombin aptamer) were produced according to the following protocol:

Qdot ITK carboxyl stock solution (5 µl of 8 µM stock) was diluted in 50 µl MES (2-(N-morpholino)ethanesulfonic acid) buffer (50 mM, pH 6.4). Then 5 µL EDC (N-ethyl-N'-(3-dimethylaminopropyl)carbodiimide) (10 mg/mL in milliQ water) and 5 µL N-hydroxysulfosuccinimide (sulfo-NHS) (10 mg/L, in milliQ water) were added, and the mixture was incubated for 30 minutes under 500 rpm orbital mixing, at 22°C.

Then 80 µL antibody solution (monoclonal mouse anti-IL6, 0.5 mg/mL in phosphate buffered saline (PBS) pH 7.4) was added to activated *Qdot ITK 525* solution for QD-525-anti-IL-6-conjugate synthesis, or 80 µL TBA (100 nM, in milliQ water) was added to activated *Qdot ITK 605* solution for QD-605-TBA-conjugate synthesis. Both reaction mixes were adjusted to 200 µL with MES buffer (pH 6.4) and incubated for 90 minutes under 500 rpm, at 22°C. Then 150 µl HEPES (4-(2-hydroxyethyl)piperazine-1-ethanesulfonic acid) buffer (50 mM, 0.1%

Tween 20 (polyethylene glycol sorbitan monolaurate), and 10 mg/mL bovine serum albumin (BSA), pH 7.4) were added. The conjugates were then stored at 4°C overnight.

2.3. Characterization of the QDs

Agarose gel electrophoresis of QDs before and after conjugation to the IL-6 antibody and TBA was performed on a 1% (w/v) agarose gel in 1× Tris-acetate-EDTA buffer. Electrophoresis was performed at 10 V/cm for 20 minutes, and pictures were taken with a Gel iX20 Imager device (Intas, Göttingen, Germany). Fluorescence spectrum measurements were collected with a TECAN Infinite 200Pro plate reader from Tecan Group Ltd. (Männedorf, Switzerland). The prepared conjugates were diluted in ddH_2O to 100 µL. Afterward, the QDs were excited at 365 nm, and the fluorescence emission between 450 and 600 nm for QD525, or 550 and 700 nm for QD605, was recorded. Emission peaks were normalized to the peak maximum and plotted against the wavelength. DLS-spectra were acquired with a Zetasizer Nano ZS instrument (Malvern, Worcestershire UK).

2.4. Running buffer and assay component optimization

The buffer volume was 90 µL for single-plex experiments and 80 µL for duplex experiments. For all experiments, a volume of 10 µL of each QD conjugate (QD-525-anti-IL-6-conjugate or QD-605-TBA-conjugate) was used per lateral flow strip.

The following buffers were tested: LFA running buffer (50 mM bis-Tris, 8% Triton X-100 (t-octylphenoxypolyethoxyethanol), and 0.3% BSA, pH 7.5), aptamer binding buffer (20 mM Tris-HCl, 140 mM NaCl, and 2 mM $MgCl_2$, pH 7.5), and aptamer binding buffer with an additional 8% Triton X-100, a mix of 50% aptamer binding buffer and 50% LFA running buffer, and PBST (1× PBS with 0.1% Tween20). A 20 µL volume of buffer was replaced with the corresponding analyte (IL-6 250 nM, thrombin 866 nM). A 2.5 µL volume of the buffer was replaced with IL-

6 detection antibody (50 µg/ml) for the IL-6 experiments, and a 0.625 µL volume was replaced with HD22 (1 µM) for the thrombin experiments.

2.5. LFA assay procedure

In the single-plex experiments, 10 µL of either QD-525-anti-IL-6-conjugate or QD-605-TBA-conjugate was added to the prepared samples in aptamer binding buffer with 8% Triton X-100 and either 0.625 µL HD22 (1 µM) in thrombin assays or 2.5 µL IL-6 detection antibody (50 µg/ml) in IL-6 assays, in a 2 ml flat bottom reaction vessel. Similarly, in the duplex experiments, 10 µL of each QD conjugate was added to the prepared samples in aptamer binding buffer with 8% Triton X-100 containing 0.625 µL HD22 (1 µM) and 2.5 µL IL-6 detection antibody (50 µg/ml) in a 2 ml flat bottom reaction vessel. The final volume of the prepared reaction mixes was fixed at 100 µL. For serum experiments, 10 µL of buffer was replaced by human serum to achieve a content of 10% serum. Lateral flow strips were then placed in the prepared mixture. Samples were given 15 min to flow through the LFA strips, and were then allowed to dry for 5 minutes and imaged for further analysis.

2.6. Specificity experiments

To assess the specificity of the assay, we challenged the LFA strips with structurally similar molecules as controls. For the thrombin response, prothrombin at a final concentration of 173.2 nM; a mix of thrombin (86.6 nM) and antithrombin III (200 nM); and a mix of prothrombin (86.6 nM) with antithrombin III (100 nM) were used. For the IL-6 response, IL-2 (50 nM) and IL-8 (50 nM) were used. The thrombin/antithrombin III mixes were preincubated for 30 minutes at room temperature. Similarly to the protocol for the duplex experiments, 10 µL of each QD conjugate was added to the prepared samples in aptamer binding buffer with 8% Triton X-100 containing 0.625 µL HD22 (1 µM) and 2.5 µL of IL-6 detection antibody (50

µg/ml) in a 2 ml flat bottom reaction vessel. The final volume of the prepared reaction mixes was fixed at 100 µL.

2.7. ELISA experiments

The thrombin ELISA kit was used according to the manufacturer's protocol. Thrombin was diluted in 1× diluent to final amounts of 0, 0.00215, 0.0043, 0.0086, 0.0172, and 0.0258 pmol. For the recovery experiments, thrombin was diluted to the same concentrations in 1× diluent containing 10% serum. To account for variability, each concentration was assayed in quintuplicate, with 50 µl sample per well. The samples were incubated for 2 hours at room temperature. The biotinylated detection antibody was incubated for 1 hour, and this was followed by a 30 minute incubation step with streptavidin-peroxidase conjugate. After each step, the plates were washed five times with 200 µl 1× wash buffer per well; 15 minutes after the addition of the chromogen substrate, the stop solution was added. The absorbance was measured on a TECAN infinite 200Pro plate reader at a wavelength of 450 nm with 570 nm as the reference wavelength.

A Human IL-6 Standard ABTS ELISA kit was used according to the manufacturer's protocol. A Nunc-MaxiSorp™ flat bottom 96-well plate (Thermo Fisher) was coated with 100 µl capture antibody at a concentration of 0.5 µg/ml overnight at room temperature. Unbound sites were blocked with 300 µl blocking buffer (1x PBS and 1% BSA, pH 7.2) per well for 1 hour at room temperature. IL-6 was diluted in diluent (1x PBS, 0.05% Tween-20, and 0.1% BSA, pH 7.2) to final amounts of 0, 0.000625, 0.00125, 0.0025, 0.005, and 0.0075 pmol. For the recovery experiment, the IL-6 was diluted to the same concentrations in diluent containing 10% serum. To account for variability, each concentration was assayed in quintuplicate, with 100 µl sample per well. The samples were incubated for 2 hours at room temperature. The biotinylated

detection antibody (1 µg/ml) was incubated for 2 hours, and this was followed by a 30 minute incubation step with avidin-HRP conjugate. After each step, the plates were washed four times with 300 µl wash buffer (PBS and 0.05% Tween-20, pH 7.2) per well. A 100 µl volume of ABTS solution was added per well, and the absorbance was measured after 30 min at a wavelength of 405 nm, with 650 nm as the reference wavelength.

2.8. Smartphone imager: 3D-printed LFA reader for Huawei P30 Pro

Pictures of the LFA test strips were taken with a *Huawei P30 Pro* smartphone by using a 3D-printed dark box (Figure 1). The developed smartphone imager was composed of four 3D-printed parts (bottom part, top part (consisting of a lid and exchangeable smartphone adapter), and sample plate for seven LFA strips) and was equipped with a 365 nm UV-LED light source consisting of a UV-LED, ∅ 50 mm aluminum heatsink, 350 mA power supply, and power supply cable with a switch for connection to the European standard 220 V power grid. The *Huawei P30 Pro* camera provided 40 MP resolution. Pictures were taken without zoom and with the flash disabled, under standard settings. The 3D-models for download and the technical specifications of the electronic components are provided in the Electronic Supplementary Material. All 3D-printed parts were produced with an *Ultimaker 3* printer with black and red PLA filament at 0.2 mm layer height resolution. As a reference readout system, a BioImager (ChemStudio Plus, Analytic Jena) equipped with suitable emission bandpass filters was used.

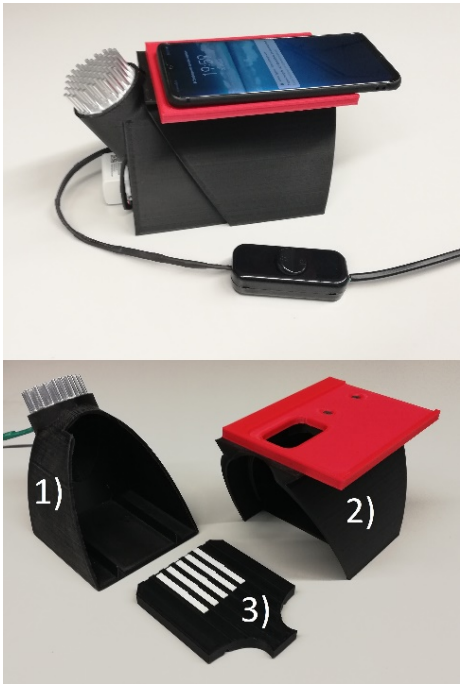

Figure 1: Smartphone imager consisting of 1) a bottom part equipped with a UV-LED light source, 2) a top part comprising a darkbox lid equipped with an exchangeable adapter for a Huawei P30 Pro smartphone, and 3) a sample plate for up to seven LFA strips (5 mm width).

2.9. Data processing: color separation

Images captured with the BioImager (*ChemStudio Plus*, Analytik Jena) and the smartphone imager were analyzed in ImageJ. With the BioImager, images were captured with the corresponding emission filters (565–625 nm bandpass, Omega Optical nr. 595BP60/50 for red particles; 514–557 nm bandpass, Omega Optical nr. 535BP60/50 for green particles). This process resulted in separate images for each analyte. The images were quantified with the gel analyzer tool, and the signal was plotted against the concentration. In the case of the smartphone dark box, no physical emission filters were used. The smartphone images were first split into RGB channels and then analyzed with the gel analyzer tool.

Data analysis (plotting, fitting with linear and non-linear regression analysis, and statistical significance analysis) was performed in GraphPad Prism version 8.02 for Windows, La Jolla California USA, www.graphpad.com.

3. Results and discussion

3.1. QD conjugate characterization

Fluorescence emission spectra, agarose gel electrophoresis, and dynamic light scattering were used to verify the successful conjugation of the IL-6 antibody and TBA to the QDs. The emission spectra showed a shift of approximately 2 nm for the IL-6 QD conjugates and 1 nm for the TBA QD conjugates (Figure S2). This behavior is in agreement with reports in previous publications, reviewed in (42). Because most modern QDs are synthesized to avoid any significant changes to their optical properties after bioconjugation, agarose gel electrophoresis was used to further study the conjugates and confirm successful conjugation. A band shift was observed (Figure S2) after conjugation for both QD conjugates. DLS spectra (Figure S2) further confirmed the successful conjugation of the antibodies and aptamers (diameters: QD525-unconjugated, 11.7 nm; QD525-anti IL-6, 15.7 nm; QD605-unconjugated, 21.0 nm; and QD605-TBA, 28.2 nm).

3.2. Running buffer optimization

The binding of aptamers as well as antibodies is highly dependent on the buffer's salt concentration. Different buffers were tested in a single-plex format with either the QD-605-TBA-conjugate for thrombin detection or the QD-525-anti-IL-6-conjugate for IL-6 detection, to identify the optimal multiplex running buffer.

For the QD-605-TBA-conjugates, as shown in Figure S2, no signal was detected with the LFA running buffer, owing to a lack of monovalent and divalent cations in the buffer. The aptamer binding buffer showed a high signal, albeit with a very high background because of the lack of surfactants and the passive adsorption of the QD conjugates on the lateral flow membrane. The highest binding was obtained with the aptamer binding buffer containing 8% Triton X-

100; this result was attributable to the aptamer's dependence on the salt concentration for proper folding and subsequent binding, and the blocking of non-specific adsorption by the surfactant. A mix of 50% LFA buffer and 50% aptamer binding buffer showed a deterioration in binding, owing to the decrease in salt concentration, whereas PBST showed suboptimal binding, thus indicating the aptamer's dependency on cations.

In contrast, the QD-525-anti-IL-6 conjugates showed optimal binding with the LFA running buffer. The aptamer binding buffer led to aggregation of the conjugates, and no signal was detected. The aptamer binding buffer with 8% Triton X-100 as well as the 50% aptamer binding buffer-50% LFA running buffer showed comparable signals and slightly inhibited binding. PBST had a lower signal than both buffers.

The data clearly indicated that a trade-off was necessary, because no buffer conditions were simultaneously optimal for both the antibody and the aptamer conjugates. The aptamer running buffer with Triton X-100 was chosen for further experiments. This buffer showed the highest signal for the thrombin binding conjugates and acceptable performance for the IL-6 conjugates.

3.3. Optimization of the amounts of HD22 and IL-6 detection antibody

Different amounts of the detection aptamer and the IL-6 detection antibody were tested in a single-plex format. In the case of the detection aptamer (Figure S3), increasing amounts led to inhibition of the test line signal, because the free HD22 saturated the test line and inhibited the binding of the QDs. Decreasing the amount led to a constant signal, thus indicating that all the HD22 was bound to the QD-TBA-thrombin complex. However, there was no significant difference in the signals obtained with different IL-6 detection antibody concentrations (Figure

S4). Therefore, volumes of 2.5 µL detection antibody and 0.625 µL HD22 per strip were used for developing the assay.

3.4. Single-plex and setup testing

To test the optimized assay conditions, we challenged the lateral flow strips with different concentrations of the analyte in a single-plex format. Then images were captured with the smartphone setup (RGB photos) and the BioImager with the corresponding filters (grayscale photos). To validate the designed smartphone box imaging setup, we compared the signals with the BioImager results. For IL-6 (Figure S5), the data showed a concentration dependent signal for both setups; however, the smartphone signals were slightly higher than the imager signals. In contrast, for thrombin (Figure S6), the results with the two setups agreed well; nevertheless, the smartphone showed a relatively higher signal attributable to the sizes of the camera sensors in both setups. The smartphone setup thus was comparable to the BioImager and therefore could be used for quantification of the QD-labeled aptamers and antibodies.

3.5. Duplex LFA IL-6/thrombin

Under the optimized assay conditions, the lateral flow strips were simultaneously challenged with increasing concentrations of thrombin and IL-6 (1:1 ratio). After a buffer running time of 15 minutes, the strips were allowed to dry for 5 minutes, and images were captured with the smartphone setup; the images then were processed (RGB splitting) and analyzed in ImageJ (Figure S8). As seen in Figures 2 and 3, a concentration dependent response from both the red and green channels was detected. For IL6, the data showed a linear response with a limit of detection (limit of detection = blank mean value + $3*SD_{blank}$) of 100 pM. In contrast, thrombin showed a typical binding curve with exponential behavior, a limit of detection of 3 nM, and a K_D value of 146 ± 21 nM, which is comparable to previously published K_D values in the

nanomolar range (97.6 ± 2.2 nM (43) and 102.6 ± 5.1 nM (44)). In addition, the limits of detection and quantification for thrombin were comparable to those of published aptamer LFA methods (2.5 nM (45) and 0.85 nM (46)).

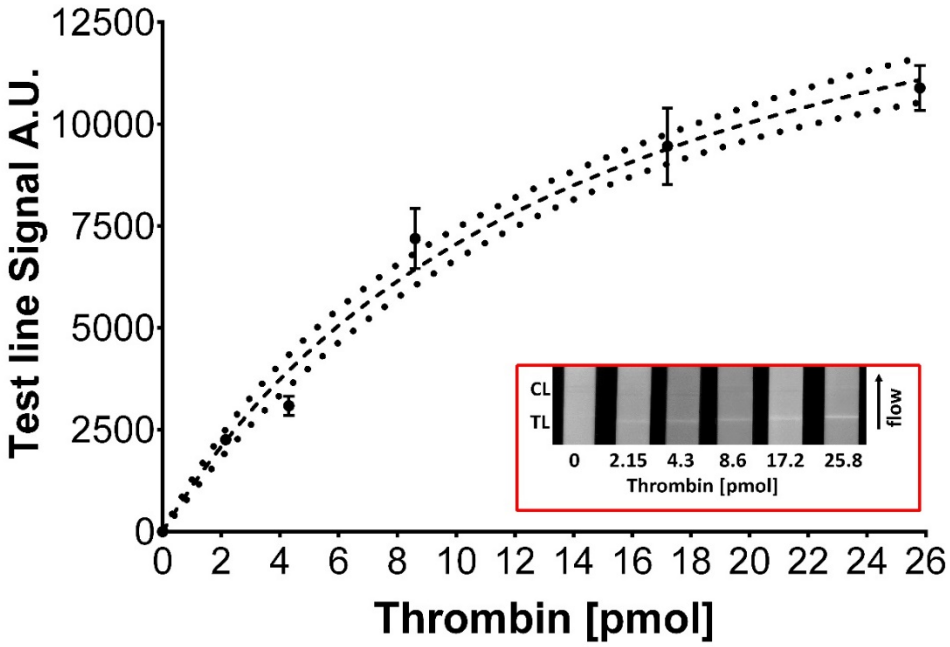

Figure 2 Plot of test line signal intensity (A.U.) against the amount of thrombin (pmol) in the sample (100 µL). The test line intensity was measured in ImageJ software (gel analyzer tool). The points show the mean values, and the error bars represent the standard deviation n=5. The line represents the best fit with the one site total binding equation Y=Bmax*X/(Kd+X) + NS*X + background, adjusted r^2= 0.9948. The dashed lines represent the 95% CI of the best fitting lines. The inset shows a monochromatic image of the LFA strips' red channel after digital RGB splitting in ImageJ (CL: control line, TL: test line).

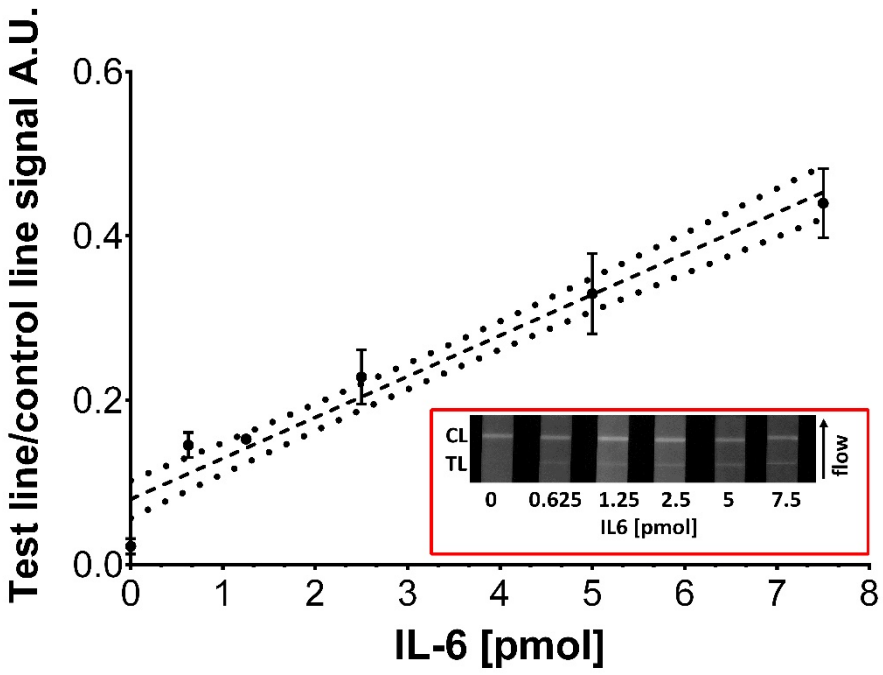

Figure 3 Plot of test line signal intensity normalized to that of the control line (A.U.) versus the IL-6 amount (pmol) in the sample (100 µL). The test line and control line intensity values were measured in ImageJ software (gel analyzer tool). The points show the mean values, and the error bars represent the standard deviation n=5. The line represents the best fit with the equation Y = 0.05X + 0.0784 r^2= 0.9520. The dashed lines represent the 95% CI of the best fitting lines. The inset shows a monochromatic image of the LFA strips' green channel after digital RGB splitting in ImageJ (CL: control line, TL: test line).

3.6. Serum experiments and recovery

To test the matrix effect in the assay, we challenged the lateral flow strips with 10% serum content in samples containing IL-6 and thrombin in increasing concentrations. The recovery rates and coefficients of variation are shown in Table 1. The recovery rates for IL-6 and thrombin were 86–130% and 80–120% (Figures S9 and S10), with a CV % average of 9.8 ± 3.4 and 14.2 ± 3.1, respectively.

Table 1: Percentage recovery for IL-6 (pmol) and thrombin (pmol) and the coefficients of variation n=5.

IL6 (pmol)/thrombin (pmol)	Recovery %	CV %
0.625/2.15	86.64/126	13.41/17.84
1.25/ 4.3	108.5/105.33	10.25/15.98
2.5/8.6	96.55/86.71	4.17/13.39
5/17.2	135.76/80.45	11.66/9.56

3.7. Specificity of the response of the LFA

The specificity of thrombin binding aptamers has been extensively studied (41). TTBA has been found to cross react with prothrombin, and binding to thrombin has been found to be inhibited by antithrombin III. In contrast, HD22 is more selective toward free thrombin and shows no cross reactivity to prothrombin. Because both aptamers were used in the LFA, the specificity of the response was tested. For prothrombin as well as thrombin/antithrombin III and prothrombin/antithrombin III, no test line was detected at concentrations of 173.2 nM (17.2 pmol), 86.6 nM (8.6 pmol)/200 nM (20 pmol), and 86.6 nM (8.6 pmol)/100 nM (10 pmol), respectively (Figure S11). These results were consistent with previously published results (41), in which the use of both aptamers in a sandwich assay increased the selectivity for free thrombin. Additionally, when we challenged the LFA strips with IL-2 and IL-8 at a concentration of 50 nM, we observed a clear control line but no detectable test lines (Figure S12). This result was expected because the monoclonal antibodies used are highly specific for IL-6.

3.8. Comparison with published assays and ELISA

Various approaches to design a POC assay for IL-6 and thrombin have been described in the literature (Table 2). Nevertheless, no duplex assay for both analytes has been described. For IL-6 and thrombin, the most sensitive approaches are based on ELISA with detection limits reaching low pg/ml and ng/ml concentrations, respectively. However, most of these assays are time intensive, including incubation, washing, and detection steps requiring up to 5 hours. In contrast, lateral flow approaches provide faster results with lower sensitivity. Nevertheless, these approaches can be used to detect and quantify abnormal concentrations and disease conditions. In comparison to the published methods, this method can detect both analytes simultaneously in 20 minutes through smartphone-based quantification.

Table 2: Comparison of assays reported for the quantification of IL-6 and thrombin.

Analyte/assay format	**LOD**	**Reference**
IL-6/LFA	0.38 ng/mL	(47)
IL-6/LFA	15 pM (0.31 ng/ml)	(6)
IL6- electrochemiluminescence immunoassay	2.63 pg/mL	(48)
IL-6/LFA	100 pM (2.1 ng/ml)	This work
Thrombin/microfluidic aptasensor	8.21 nM	(49)
Thrombin/LFA	0.85 nM	(46)
Thrombin/LFA	1.5 nM	(50)
Thrombin/electrochemiluminescence aptasensor	10 nM	(51)
Thrombin/LFA	3 nM	This work

To further compare the LFA method to well established assays, we used ELISA as a reference method for both analytes. The assay was performed in single-plex format, because no duplex ELISA kit is available for both analytes. The results (Figure S13 and S14) showed high agreement between the ELISA and the LFA methods ($r = 0.996$ and $P = 0.004$ for thrombin; $r = 0.992$ and $P = 0.0077$ for IL-6).

4. Conclusion

This work presents a simple, cost efficient LFA combined with an affordable smartphone detection system for determination of thrombin and IL-6. Although IL-6 quantification displayed a higher limit of detection, owing to the buffer components and the affinity of the antibodies, the assay performed well in complex media (10% serum). Therefore, this assay could be applied to analyze real samples. The simplicity and efficiency, combined with smartphone quantification, make this assay ideal for POC application in low resource settings. A novel combination of aptamers and antibodies with QD labels allows for smartphone-based

quantification. The 3D printed dark box could be modified to fit other smartphones for the simultaneous quantification of IL-6 and thrombin.

Acknowledgements

Partial support provided by Bundesministerium für Bildung und Forschung (FlowArray project 13FH121PX8, and by the MultiFlow project 03FH046PX4) is gratefully acknowledged.

HPD is grateful to Prof. Friedhelm Beyersdorf and Bartosz Rylski, Freiburg, for facilitating this work.

We thank Mrs. Ayesha Talib from MPI Potsdam for support with DLS measurements.

Authors´ contributions

MM: conceptualization, experiments, and manuscript writing

CR: experiments and manuscript writing

SR: experiments and manuscript writing

SL and HPD: conceptual design and contribution to manuscript writing

Availability of data and materials

Charts and tables referred to in the text as well as files used for the 3D printing are available in the Electronic Supplementary Material (ESM).

Ethics approval and consent to participate

Not applicable.

Consent for publication

Not applicable.

Competing interests

The authors declare no conflicts of interest.

Author details

[1] Furtwangen University, Medical and Life Sciences Faculty, Jakob-Kienzle Str. 17, D-78054 Villingen Schwenningen, Germany. [2] Institute of Precision Medicine, Jakob-Kienzle Str. 17, D-78054 Villingen-Schwenningen, Germany. [3] University of Tuebingen, Pharmaceutical Institute, Department of Pharmaceutical Chemistry, Auf der Morgenstelle 8, D-72076 Tuebingen, Germany. [4] Fraunhofer Institute IZI, Leipzig, EXIM Department, Schillingallee 68, D-18057 Rostock, Germany. [5] University of Tuebingen, Faculty of Science, Auf der Morgenstelle 8, D-72076 Tuebingen, Germany.

References

1. Price CP. Clinical review Point of care testing. 2001:1285-8.
2. Sun AC, Hall DA. Point-of-Care Smartphone-based Electrochemical Biosensing. 2019:2-16.
3. Borse V, Srivastava R. Fluorescence lateral flow immunoassay based point-of-care nanodiagnostics for orthopedic implant-associated infection. Sensors & Actuators: B Chemical. 2018.
4. Stobiecka M, Ratajczak K, Jakiela S. Toward early cancer detection: Focus on biosensing systems and biosensors for an anti-apoptotic protein survivin and survivin mRNA. Biosensors and Bioelectronics. 2019;137:58-71.
5. Ratajczak K, Stobiecka M. High-performance modified cellulose paper-based biosensors for medical diagnostics and early cancer screening: A concise review. Carbohydrate Polymers. 2020;229:115463.
6. Ruppert C, Kaiser L, Jacob LJ, Laufer S, Kohl M, Deigner H-P. Duplex Shiny app quantification of the sepsis biomarkers C-reactive protein and interleukin-6 in a fast quantum dot labeled lateral flow assay. Journal of Nanobiotechnology. 2020;18(1):130.
7. Tsai T-T, Huang T-H, Ho NY-J, Chen Y-P, Chen C-A, Chen C-F. Development of a multiplex and sensitive lateral flow immunoassay for the diagnosis of periprosthetic joint infection. Scientific Reports. 2019;9(1):15679.
8. Kim H, Chung D-R, Kang M. A new point-of-care test for diagnosis of infectious diseases based on multiplex lateral flow immunoassay. Analyst. 2019.
9. Drancourt M, Michel-lepage A, Boyer S. The Point-of-Care Laboratory in Clinical Microbiology. 2016;29(3):429-47.
10. Hanafiah KM, Id NA, Bustami Y. Development of Multiplexed Infectious Disease Lateral Flow Assays : Challenges and Opportunities. 2017:1-9.
11. Rajendran VK, Bakthavathsalam P, Mohammed B, Ali J. Smartphone based bacterial detection using biofunctionalized fluorescent nanoparticles. 2014:1815-21.

12. Lee S, Kim G, Moon J. Development of a Smartphone-Based Reading System for Lateral Flow Immunoassay. 2014;14(11):8453-7.

13. Yu L, Shi Z, Fang C, Zhang Y, Liu Y, Li C. Disposable lateral flow-through strip for smartphone-camera to quantitatively detect alkaline phosphatase activity in milk. Biosensors and Bioelectronics. 2015;69:307-15.

14. Ruppert C, Phogat N, Laufer S, Kohl M, Deigner H-P. A smartphone readout system for gold nanoparticle-based lateral flow assays: application to monitoring of digoxigenin. Microchimica Acta. 2019;186(2):119.

15. Chen A, Yang S. Replacing antibodies with aptamers in lateral flow immunoassay. Biosensors & bioelectronics. 2015;71:230-42.

16. Schüling T, Eilers A, Scheper T, Walter J. Aptamer-based lateral flow assays. AIMS BIOENGINEERING. 2018;5(2):78-102.

17. Radom F, Jurek PM, Mazurek MP, Otlewski J, Jeleń F. Aptamers: Molecules of great potential. Biotechnology Advances. 2013;31(8):1260-74.

18. Toh SY, Citartan M, Gopinath SCB, Tang T-H. Aptamers as a replacement for antibodies in enzyme-linked immunosorbent assay. Biosensors and Bioelectronics. 2015;64(0):392-403.

19. Tombelli S, Minunni M, Mascini M. Analytical applications of aptamers. Biosensors & bioelectronics. 2005;20(12):2424-34.

20. Nagatoishi S, Tanaka Y, Tsumoto K. Circular dichroism spectra demonstrate formation of the thrombin-binding DNA aptamer G-quadruplex under stabilizing-cation-deficient conditions. Biochemical and biophysical research communications. 2007;352(3):812-7.

21. Wang KY, McCurdy S, Shea RG, Swaminathan S, Bolton PH. A DNA aptamer which binds to and inhibits thrombin exhibits a new structural motif for DNA. Biochemistry. 1993;32(8):1899-904.

22. Padmanabhan K, Padmanabhan KP, Ferrara JD, Sadler JE, Tulinsky A. The structure of alpha-thrombin inhibited by a 15-mer single-stranded DNA aptamer. The Journal of biological chemistry. 1993;268(24):17651-4.

23. Anna A, Carme F, Maria T, Ramon E. Thrombin Binding Aptamer, More than a Simple Aptamer: Chemically Modified Derivatives and Biomedical Applications. Current Pharmaceutical Design. 2012;18(14):2036-47.

24. Hunter CA, Jones SA. IL-6 as a keystone cytokine in health and disease. Nature Immunology. 2015;16(5):448-57.

25. Johnson DE, O'Keefe RA, Grandis JR. Targeting the IL-6/JAK/STAT3 signalling axis in cancer. Nature Reviews Clinical Oncology. 2018;15(4):234-48.

26. Saibeni S, Saladino V, Chantarangkul V, Villa F, Bruno S, Vecchi M, et al. Increased thrombin generation in inflammatory bowel diseases. Thrombosis Research. 2010;125(3):278-82.

27. Chapman J. Thrombin in inflammatory brain diseases. Autoimmunity Reviews. 2006;5(8):528-31.

28. Colafrancesco S, Scrivo R, Barbati C, Conti F, Priori R. Targeting the Immune System for Pulmonary Inflammation and Cardiovascular Complications in COVID-19 Patients. Frontiers in Immunology. 2020;11(1439).

29. Li X, Geng M, Peng Y, Meng L, Lu S. Molecular immune pathogenesis and diagnosis of COVID-19. Journal of Pharmaceutical Analysis. 2020;10(2):102-8.

30. Jose RJ, Manuel A. COVID-19 cytokine storm: the interplay between inflammation and coagulation. The Lancet Respiratory Medicine. 2020;8(6):e46-e7.

31. Mehta P, McAuley DF, Brown M, Sanchez E, Tattersall RS, Manson JJ. COVID-19: consider cytokine storm syndromes and immunosuppression. The Lancet. 2020;395(10229):1033-4.

32. Liu F, Li L, Xu M, Wu J, Luo D, Zhu Y, et al. Prognostic value of interleukin-6, C-reactive protein, and procalcitonin in patients with COVID-19. Journal of Clinical Virology. 2020;127(January):104370-.

33. Zhu J, Pang J, Ji P, Zhong Z, Li H, Li B, et al. Elevated interleukin-6 is associated with severity of COVID-19: a meta-analysis. Journal of Medical Virology. 2020;2019:0-2.

34. Ruan Q, Yang K, Wang W, Jiang L, Song J. Clinical predictors of mortality due to COVID-19 based on an analysis of data of 150 patients from Wuhan, China. Intensive Care Medicine. 2020;46(5):846-8.

35. Ulhaq ZS, Soraya GV. Interleukin-6 as a potential biomarker of COVID-19 progression. Médecine et Maladies Infectieuses. 2020;50(4):382-3.

36. Sarzi-Puttini P, Giorgi V, Sirotti S, Marotto D, Ardizzone S, Rizzardini G, et al. COVID-19, cytokines and immunosuppression: what can we learn from severe acute respiratory syndrome? Clinical and experimental rheumatology. 2020;38(2):337-42.

37. Abbasifard M, Khorramdelazad H. The bio-mission of interleukin-6 in the pathogenesis of COVID-19: A brief look at potential therapeutic tactics. Life Sciences. 2020;257(January):118097-.

38. Connors JM, Levy JH. COVID-19 and its implications for thrombosis and anticoagulation. Blood. 2020;135(23):2033-40.

39. Zhou F, Yu T, Du R, Fan G, Liu Y, Liu Z, et al. Clinical course and risk factors for mortality of adult inpatients with COVID-19 in Wuhan, China: a retrospective cohort study. The Lancet. 2020;395(10229):1054-62.

40. Russell SM, Alba-Patiño A, Barón E, Borges M, Gonzalez-Freire M, de la Rica R. Biosensors for Managing the COVID-19 Cytokine Storm: Challenges Ahead. ACS Sensors. 2020;5(6):1506-13.

41. Trapaidze A, Hérault JP, Herbert JM, Bancaud A, Gué AM. Investigation of the selectivity of thrombin-binding aptamers for thrombin titration in murine plasma. Biosensors & bioelectronics. 2016;78:58-66.

42. Foubert A, Beloglazova NV, Rajkovic A, Sas B, Madder A, Goryacheva IY, et al. Bioconjugation of quantum dots: Review & impact on future application. TrAC Trends in Analytical Chemistry. 2016;83:31-48.

43. Derszniak K, Przyborowski K, Matyjaszczyk K, Moorlag M, de Laat B, Nowakowska M, et al. Comparison of Effects of Anti-thrombin Aptamers HD1 and HD22 on Aggregation of Human Platelets, Thrombin Generation, Fibrin Formation, and Thrombus Formation Under Flow Conditions. Frontiers in Pharmacology. 2019;10(68).

44. Pasternak A, Hernandez FJ, Rasmussen LM, Vester B, Wengel J. Improved thrombin binding aptamer by incorporation of a single unlocked nucleic acid monomer. Nucleic acids research. 2011;39(3):1155-64.

45. Xu H, Mao X, Zeng Q, Wang S, Kawde AN, Liu G. Aptamer-functionalized gold nanoparticles as probes in a dry-reagent strip biosensor for protein analysis. Anal Chem. 2009;81(2):669-75.

46. Gao Y, Zhu Z, Xi X, Cao T, Wen W, Zhang X, et al. An aptamer-based hook-effect-recognizable three-line lateral flow biosensor for rapid detection of thrombin. Biosensors and Bioelectronics. 2019;133:177-82.

47. de Souza Sene I, Costa V, Brás DC, de Oliveira Farias EA, Nunes GE, Bechtold IH. A Point of Care Lateral Flow Assay for Rapid and Colorimetric Detection of Interleukin 6 and Perspectives in Bedside Diagnostics. J Clin Med Res. 2020;2(2):1-16.

48. Prieto B, Miguel D, Costa M, Coto D, Álvarez FV. New quantitative electrochemiluminescence method (ECLIA) for interleukin-6 (IL-6) measurement. Clinical Chemistry and Laboratory Medicine (CCLM). 2010;48(6):835.

49. Yu N, Wu J. Rapid and reagentless detection of thrombin in clinic samples via microfluidic aptasensors with multiple target-binding sites. Biosensors and Bioelectronics. 2019;146:111726.

50. Liu G, Gurung AS, Qiu W. Lateral Flow Aptasensor for Simultaneous Detection of Platelet-Derived Growth Factor-BB (PDGF-BB) and Thrombin. Molecules (Basel, Switzerland). 2019;24(4):756.

51. Fang L, Lü Z, Wei H, Wang E. A electrochemiluminescence aptasensor for detection of thrombin incorporating the capture aptamer labeled with gold nanoparticles immobilized onto the thio-silanized ITO electrode. Analytica Chimica Acta. 2008;628(1):80-6.

Electronic Supporting Material

Combining aptamers and antibodies: lateral flow quantification for thrombin and interleukin-6 with smartphone readout

Authors: Mostafa Mahmoud[1,2,3], Christoph Ruppert[1,2,3], Simone Rentschler[1,2,3], Stefan Laufer[3] and Hans-Peter Deigner[1,2,4,5*]

*Correspondence: dei@hs-furtwangen.de

3D-models: all 3D-printed parts where produced with an Ultimaker 3, 3D-printer at 0.2mm layer height resolution in black and red PLA.

3D-models are available in the ESM

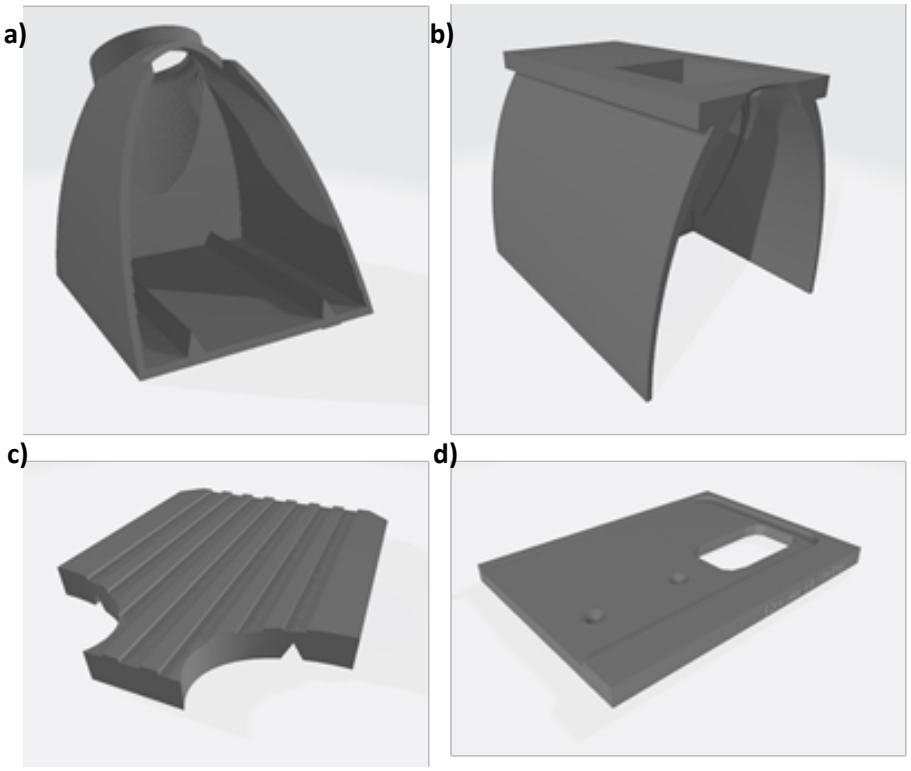

Figure S1: 3D-printed parts for smartphone reader a) bottom part (105 x 133 x 117 mm), holder for UV-LED and electronics, b) Lid (110 x 140 x 112 mm), c) sample plate for up to 7 LFA-strips (90 x 110 x 10 mm), d) Adapter for Huawei P30 Pro (97 x 133 x 8 mm)

Electronic components (LED light source):

UV-LED: model: NCSU276A UV SMD-LED on 10x10mm circuit board (Nichia, Japan)
P=780mW, λ=365nm center wavelength

Power supply: model: SLP033SS (Eaglerise Electric, China)
Input: 100-240V AC (50/60 Hz, 0.08A)
Output: I=350mA, 0.5-10V DC

Heatsink: model: ICK S R 50 x 20 (Fischer Elektronik, Germany)

∅=50mm, h=20mm

All components where purchased from LUMITRONIX LED-Technik (www.leds.de, Germany). The LED-module was attached to the center of the heatsink with double sided heat conducting adhesive tape attached to the darkbox with heat resistant glue and wired according to manufacturer´s recommendation.

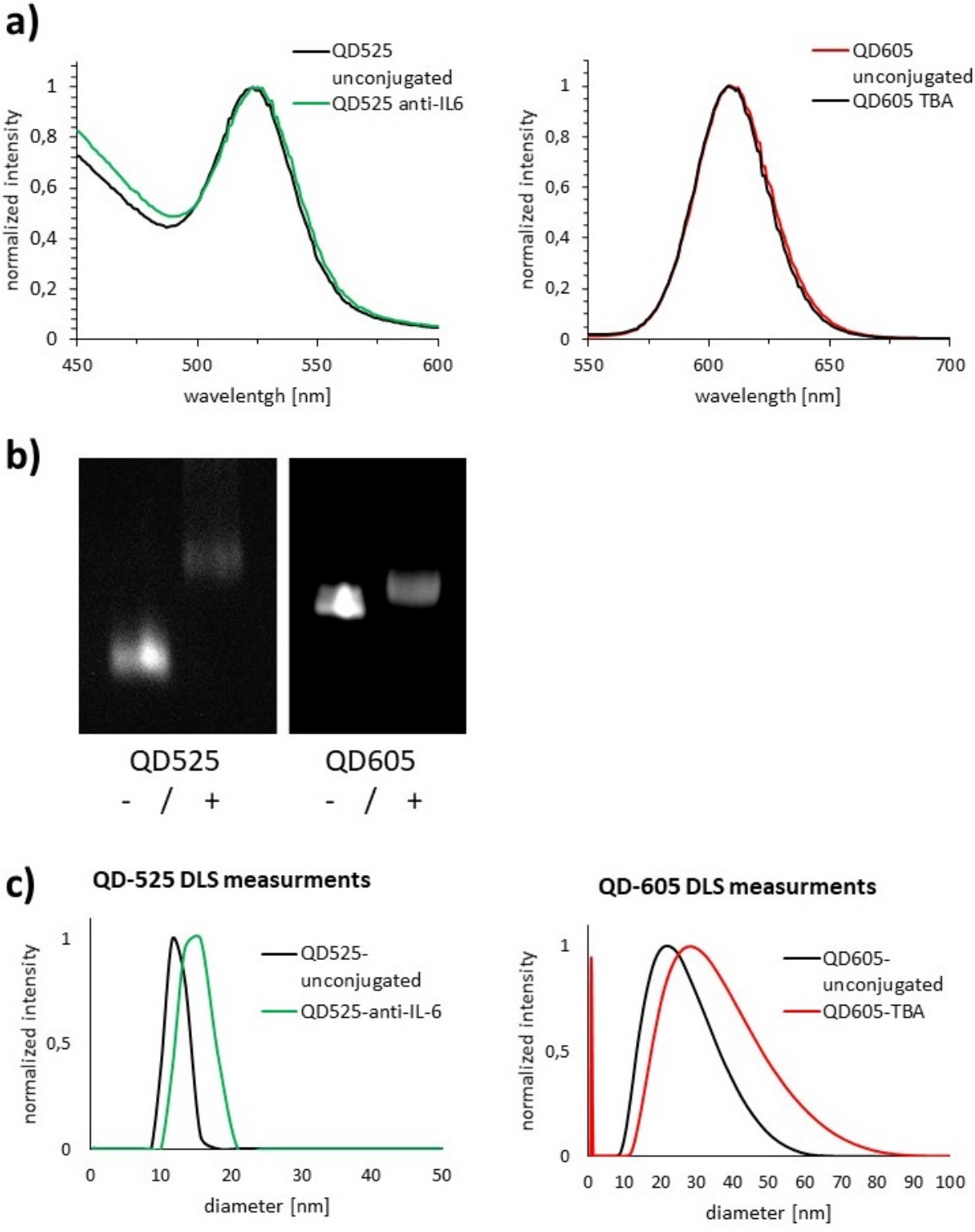

Figure S2 Characterization of the prepared Quantum Dot conjugates. (a) Fluorescence emission spectra of QD525 and QD605 (b) Agarose gel electrophoresis of Quantum Dots prior (-) and after (+) conjugation to antibodies IL-6 (QD525) or thrombin binding aptamer (TBA) (QD605). (c) Dynamic light scattering of Quantum Dots and corresponding antibody and aptamer conjugates. Diameters; QD525- unconjugated: 11.7 nm, QD525-anti IL-6: 15.7 nm, QD605-unconjugated: 21.0 nm, QD605-TBA: 28.2 nm (DLS-spectra acquired with Zetasizer Nano ZS; Malvern Worcestershire UK)

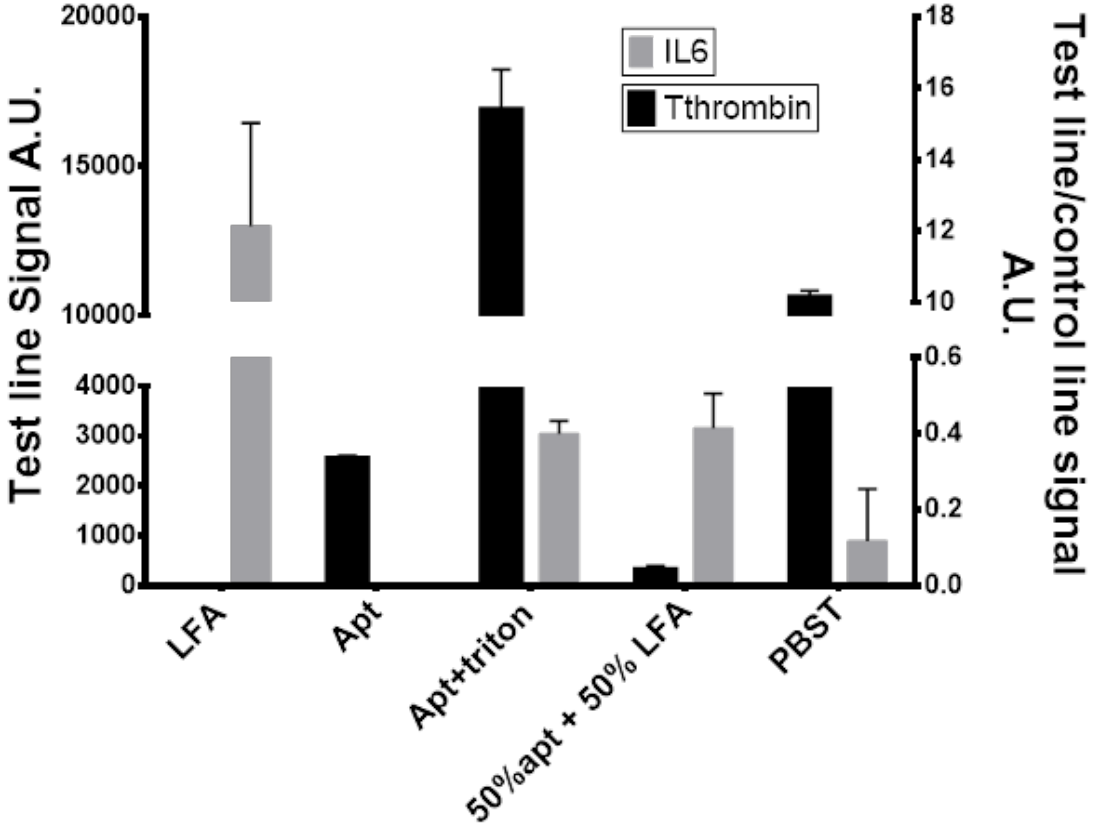

Figure S3 Plot comparing test line signal intensity (A.U.) of thrombin QDs (left y-axis), normalized signal intensity (test line / control line) of IL-6 QDs in different buffers. The intensity of the lines was measured using ImageJ software (gel analyzer tool). The points show the mean value and the error bars represent the standard deviation n=5.

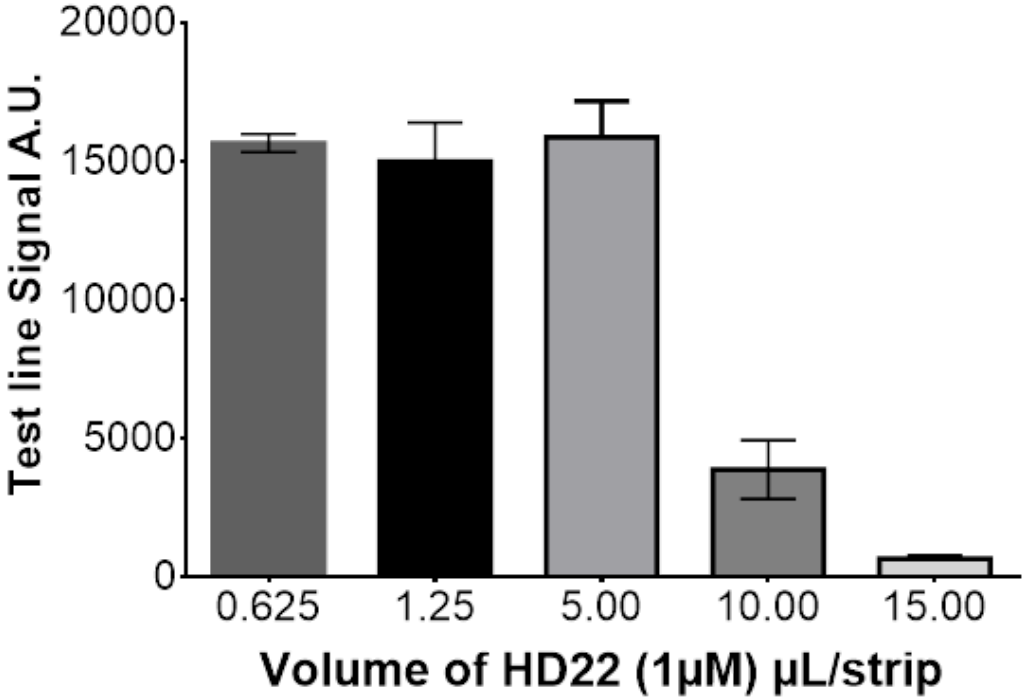

Figure S4 Plot of test line signal intensity (A.U.) for different amounts of HD22 detection aptamer (volume in µL from a 1 µM stock solution). The test line intensity was measured using ImageJ software (gel analyzer tool). The points show the mean value and the error bars represent the standard deviation n=2.

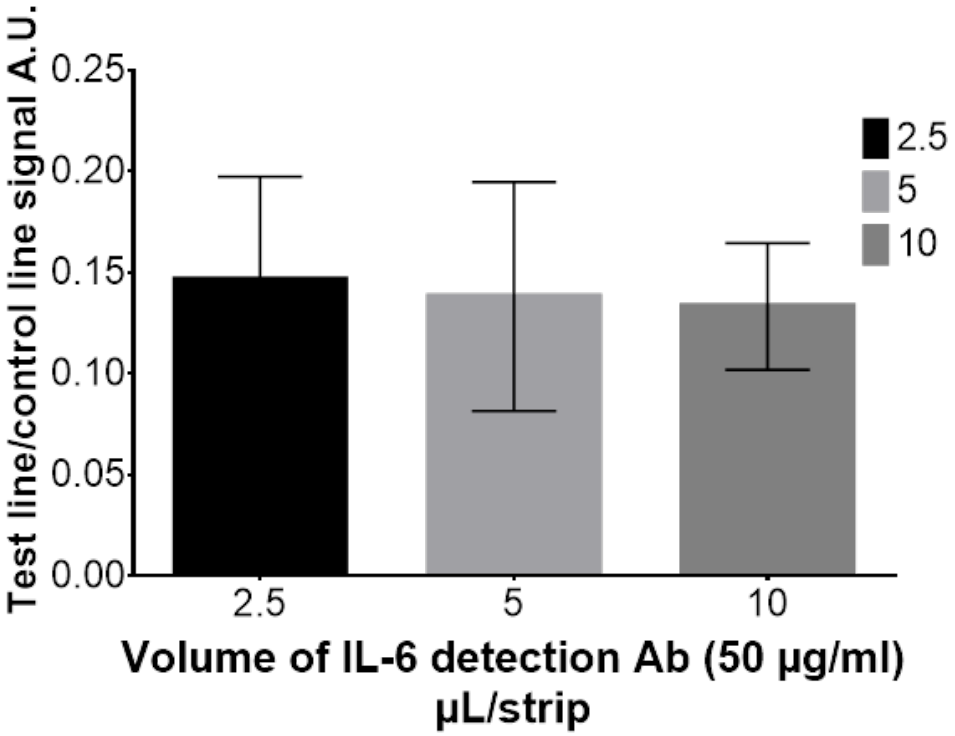

Figure S5 Plot of normalized signal intensity (A.U.) for different amounts of IL-6 detection antibody (volume in µL from a 50 µg/ml stock solution). The signal intensity was measured using ImageJ software (gel analyzer tool) then normalized to the control line signal. The points show the mean value and the error bars represent the standard deviation n=2.

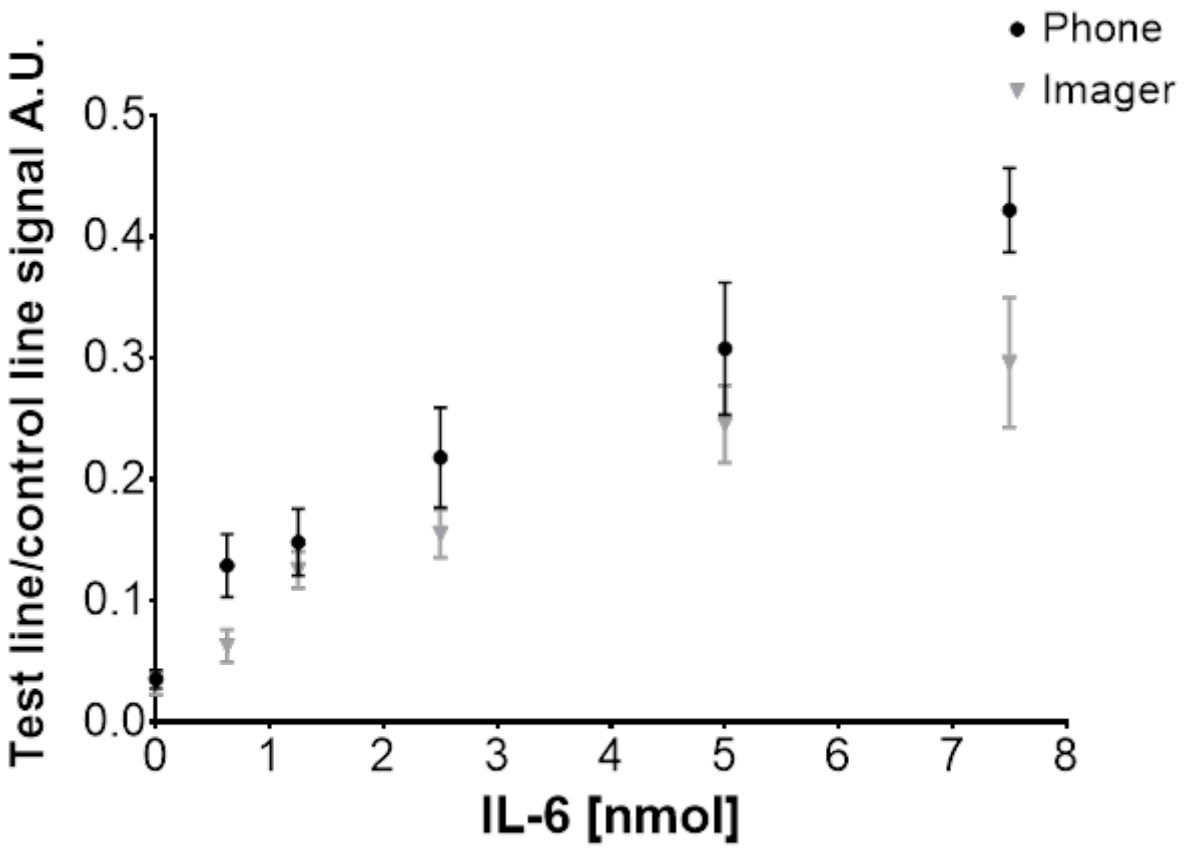

Figure S6 Plot comparing normalized signal intensity (test line/control line A.U.) of images captured using the BioImager and the smartphone setup for the green QDs conjugates. The test line intensity was measured using ImageJ software (gel analyzer tool). The points show the mean value and the error bars represent the standard deviation n=5.

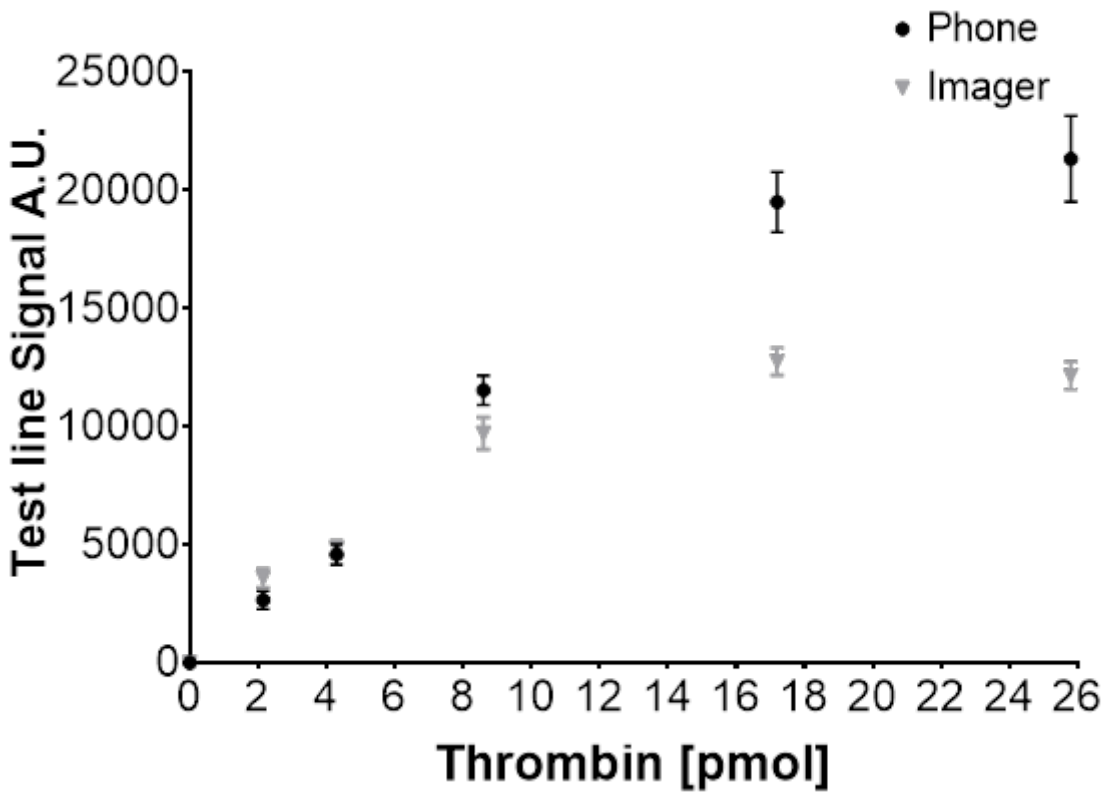

Figure S7 Plot comparing test line signal intensity (A.U.) of images captured using the BioImager and the smartphone setup for the red QDs conjugates. The test line intensity was measured using ImageJ software (gel analyzer tool). The points show the mean value and the error bars represent the standard deviation n=5.

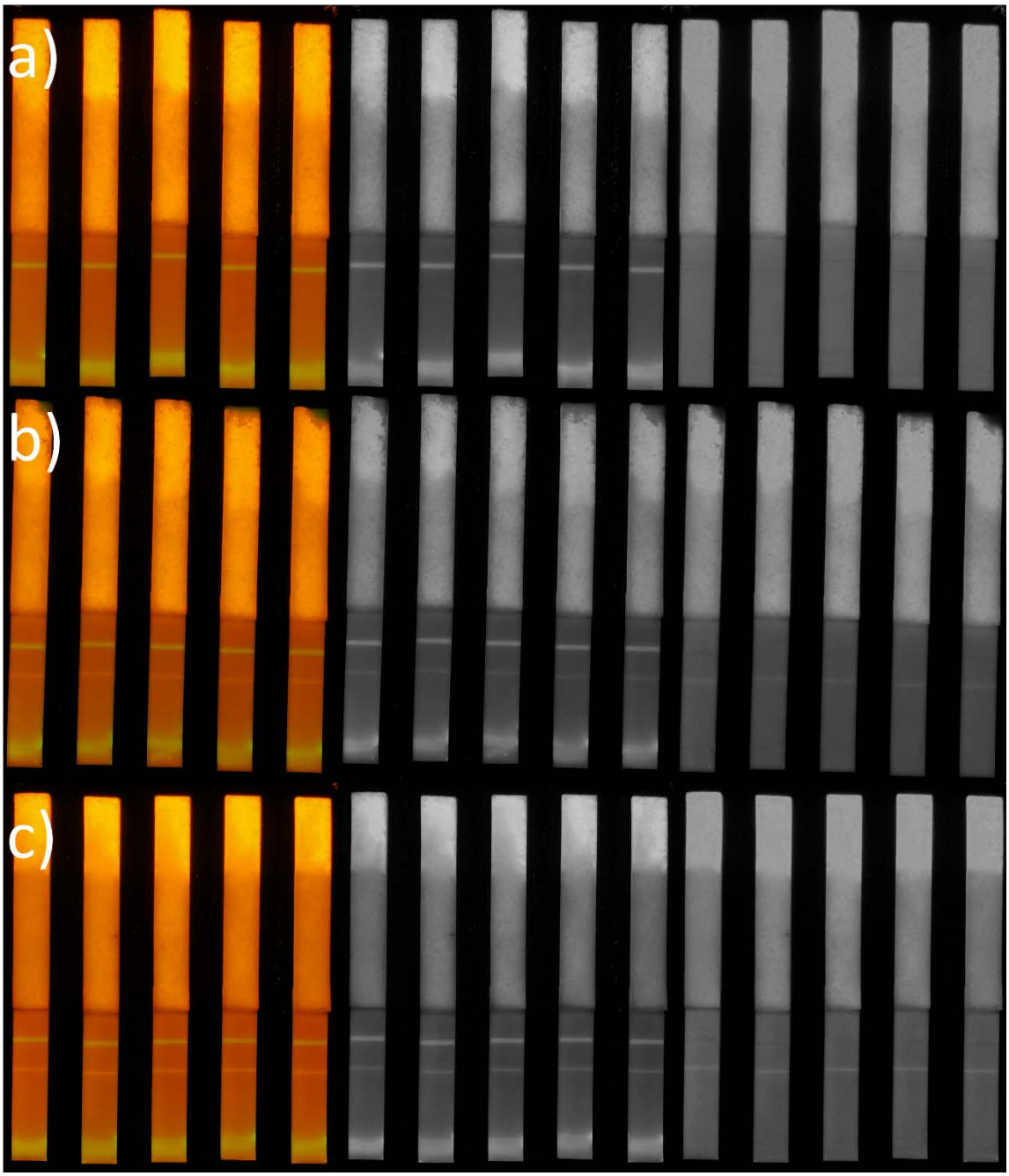

Figure S8 a representative image of the lateral flow strips captured using the smartphone setup (colour image with blue channel subtracted) and after splitting of the channels using imagej to green and red respectively a) negative control (no analyte), b) 2.15 pmol thrombin and 0.625 pmol IL-6, and c) 17.2 pmol thrombin and 5 pmol IL-6.

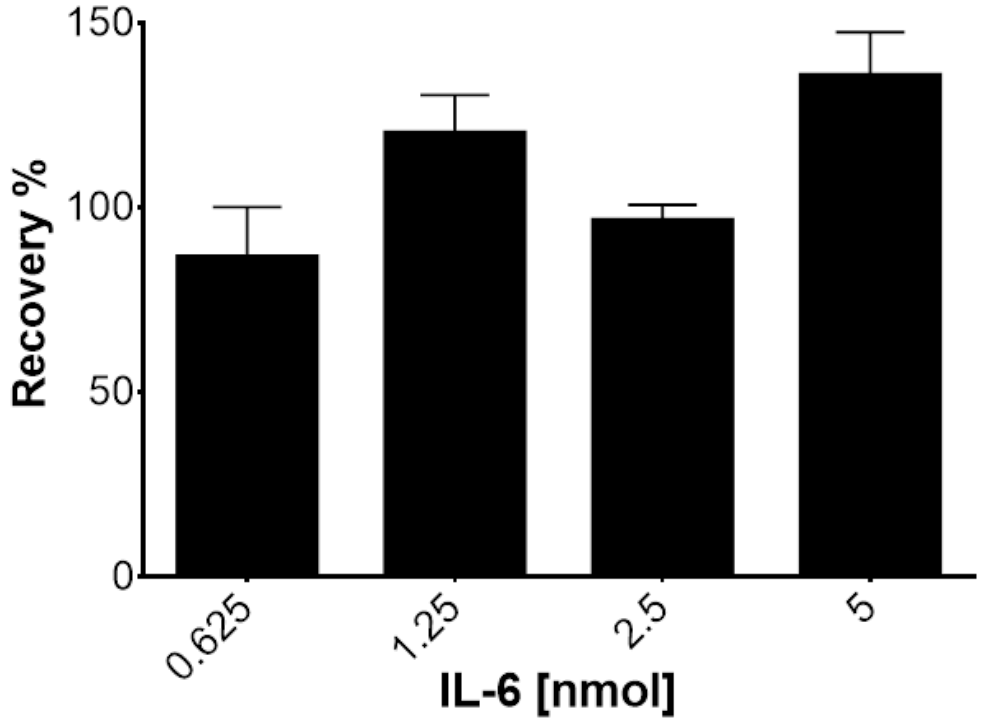

Figure S9 Recovery for 10% serum samples spiked with IL-6 (nmol). The points show the mean value and the error bars represent the standard deviation n=5.

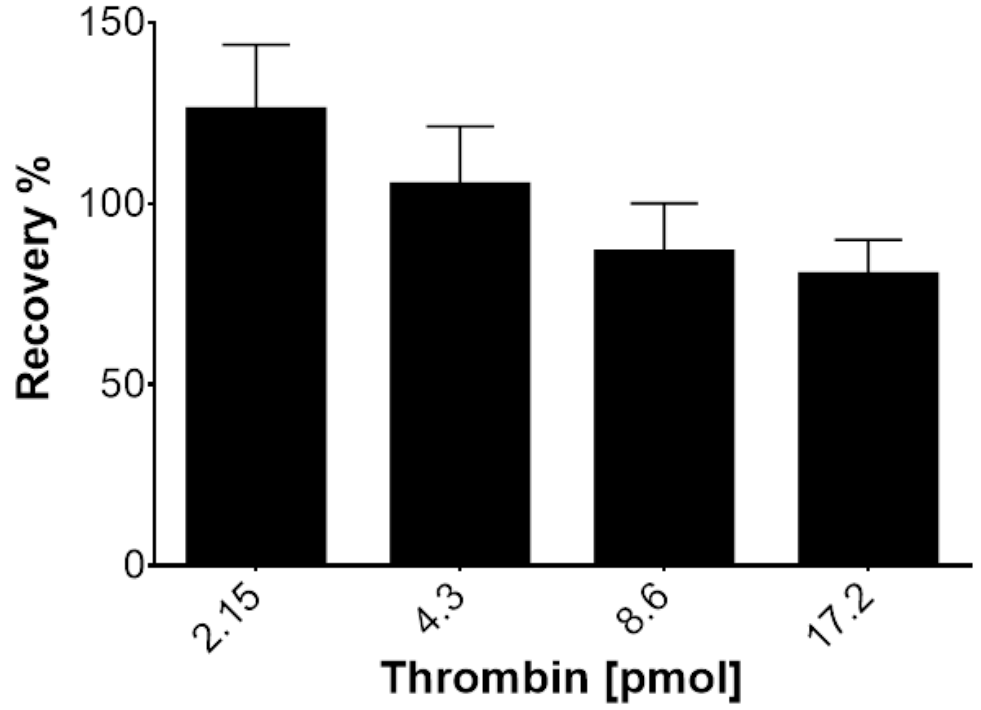

Figure S10 Recovery % for 10% serum samples spiked with thrombin (pmol). The points show the mean value and the error bars represent the standard deviation n=5.

Figure S11 a representative image of the lateral flow strips captured using the smartphone setup (colour image with blue channel subtracted) from left to right, prothrombin thrombin/antithrombin III and prothrombin/antithrombin III. No test line signal could be detected.

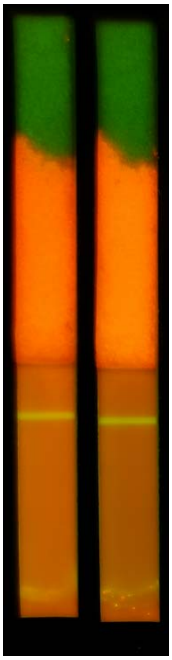

Figure S12 a representative image of the lateral flow strips captured using the smartphone setup (colour image with blue channel subtracted) from left to right, prothrombin thrombin/antithrombin III and prothrombin/antithrombin III. No test line signal could be detected.

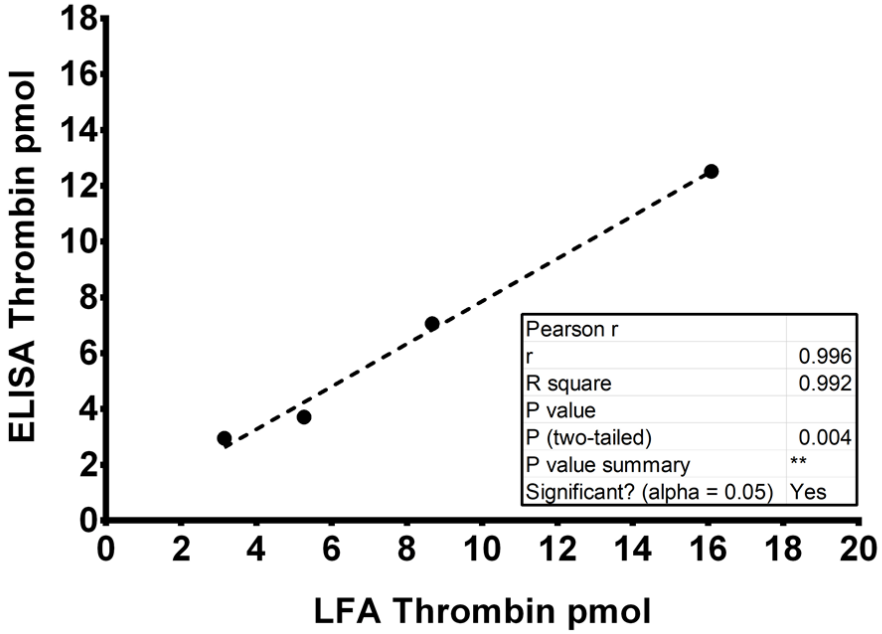

Figure S13 Comparison of thrombin in 10% serum measured with the LFA method and the ELISA kit.

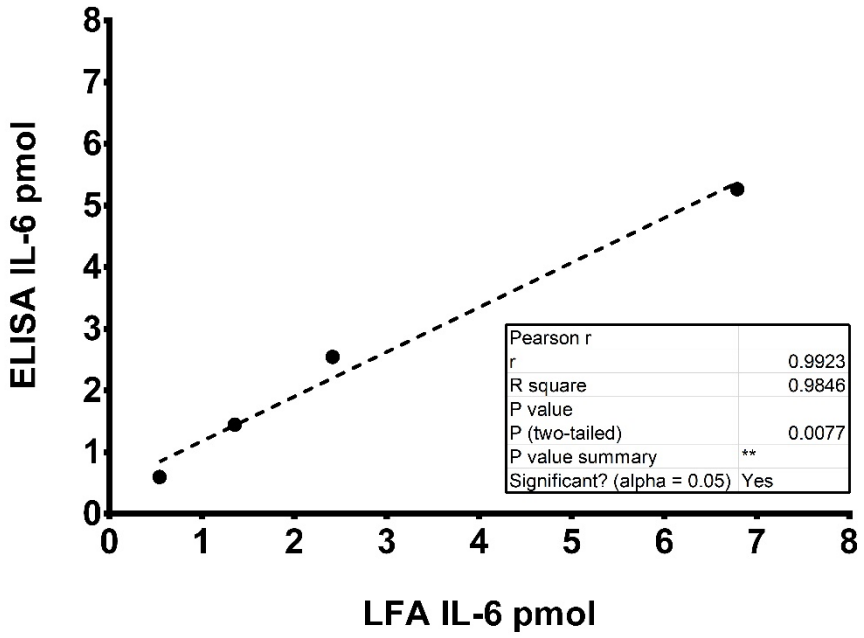

Figure S14 Comparison of IL-6 in 10% serum measured with the LFA method and the ELISA kit.

Conclusions

The Ultimate goal of point of care assay design is a platform combining simplicity, sensitivity, high-throughput and multiplexing capabilities. However, this aim remains quite challenging and a compromise on one or other parameter has to be made. This is usually due to immunoassay format and readout limitations. Through this research, I designed novel point of care platforms to address these bottlenecks with specific focus on small molecules. On the high-throughput front, combining aptamers with qPCR instrument to measure the melting temperatures allows for analyzing up to 96 samples in a matter of minutes. In contrast to mass spectrometry, the technique is simple, has low sample requirement and is less complex. Moreover, the availability of qPCR in clinic settings as opposed to mass spectrometry makes the transfer to point of care straightforward. While multiplexing is theoretically possible through using different aptamers, it has yet to be experimentally confirmed. On the other hand, the capillary-magnetic particles platform offers simplicity combined with high sensitivity and directly proportional analyte dependent signal. The assay simplicity, low cost and visual detection makes it an optimal option for small molecules quantification as a point of care platform. Compared to other visual detection point of care, the use of magnetic particles and plastic capillaries allows spatial separation as well as the inclusion of washing steps if needed. Nonetheless, multiplexing using this platform is limited to a combination of different capillaries in a cassette or a device. Building on this, I developed an LFA for IL-6 and thrombin using quantum dots with different emission spectra. This enabled the simultaneous detection of two analytes on the same test line. Additionally, it was combined with a smartphone 3D printed readout setup. The use of universal lateral flow with streptavidin and mouse antibody allows the simple transfer of the setup to other targets.

The results of this work lay the groundwork for alternative non conventional point of care assays. It presents different platforms based on state of the art components. While this is sufficient as a proof of concept, the transfer to routine diagnostics requires in depth validation studies. On the other hand, it offers fast and simple platforms for other non-clinical applications e.g. environmental monitoring.

In summary, aptamers can be incorporated in traditional and non-traditional assay formats. They provide alternatives specifically for challenging molecules to antibodies e.g. small molecules and toxins. Nevertheless, further research and full characterization of aptamers binding structures is still needed. Additionally, a focus on gaps where antibodies fail to provide solutions, might bring aptamers to their full potential.

References

[1] P. Fechner, O. Bleher, M. Ewald, K. Freudenberger, D. Furin, U. Hilbig, F. Kolarov, K. Krieg, L. Leidner, G. Markovic, G. Proll, F. Proll, S. Rau, J. Riedt, B. Schwarz, P. Weber, and J. Widmaier, "Size does matter! label-free detection of small molecule-protein interaction," *Anal Bioanal Chem*, vol. 406, no. 17, pp. 4033–51, 2014.

[2] R. Vanholder, R. De Smet, P. Vogeleere, C. Hsu, and S. Ringoir, *The Uraemic Syndrome*, book section 1, pp. 1–33. Springer Netherlands, 1996.

[3] G. E. Ward, K. L. Carey, and N. J. Westwood, "Using small molecules to study big questions in cellular microbiology," *Cell Microbiol*, vol. 4, no. 8, pp. 471–82, 2002.

[4] I. S. Dunn, *Searching for molecular solutions: empirical discovery and its future*. John Wiley & Sons, 2010.

[5] T. Golper, M. Marx, C. Shuler, and W. Bennett, *Drug Dosage in Dialysis Patients*, book section 30, pp. 750–820. Springer Netherlands, 1996.

[6] P. D. Leeson and B. Springthorpe, "The influence of drug-like concepts on decision-making in medicinal chemistry," *Nat Rev Drug Discov*, vol. 6, no. 11, pp. 881–890, 2007.

[7] J. Piehler, A. Brecht, and G. Gauglitz, "Affinity detection of low molecular weight analytes," *Analytical Chemistry*, vol. 68, no. 1, pp. 139–143, 1996.

[8] P. Yager, G. J. Domingo, and J. Gerdes, "Point-of-care diagnostics for global health," *Annual Review of Biomedical Engineering*, vol. 10, no. 1, pp. 107–144, 2008.

[9] M. Schito, T. F. Peter, S. Cavanaugh, A. S. Piatek, G. J. Young, H. Alexander, W. Coggin, G. J. Domingo, D. Ellenberger, E. Ermantraut, I. V. Jani, A. Katamba,

K. M. Palamountain, S. Essajee, and D. W. Dowdy, "Opportunities and Challenges for Cost-Efficient Implementation of New Point-of-Care Diagnostics for HIV and Tuberculosis," *The Journal of Infectious Diseases*, vol. 205, no. suppl_2, pp. S169–S180, 2012.

[10] C. P. Price, "Point of care testing," *Bmj*, vol. 322, no. 7297, pp. 1285–1288, 2001.

[11] V. Gubala, L. F. Harris, A. J. Ricco, M. X. Tan, and D. E. Williams, "Point of care diagnostics: status and future," *Analytical chemistry*, vol. 84, no. 2, pp. 487–515, 2012.

[12] N. P. Pai, C. Vadnais, C. Denkinger, N. Engel, and M. Pai, "Point-of-care testing for infectious diseases: diversity, complexity, and barriers in low-and middle-income countries," *PLoS Med*, vol. 9, no. 9, p. e1001306, 2012.

[13] P. Yager, G. J. Domingo, and J. Gerdes, "Point-of-care diagnostics for global health," *Annual review of biomedical engineering*, vol. 10, 2008.

[14] R. Peeling and D. Mabey, "Point-of-care tests for diagnosing infections in the developing world," *Clinical microbiology and infection*, vol. 16, no. 8, pp. 1062–1069, 2010.

[15] P. K. Drain, E. P. Hyle, F. Noubary, K. A. Freedberg, D. Wilson, W. R. Bishai, W. Rodriguez, and I. V. Bassett, "Diagnostic point-of-care tests in resource-limited settings," *The Lancet Infectious Diseases*, vol. 14, no. 3, pp. 239–249, 2014.

[16] G. A. Posthuma-Trumpie, J. Korf, and A. van Amerongen, "Lateral flow (immuno) assay: its strengths, weaknesses, opportunities and threats. a literature survey," *Analytical and bioanalytical chemistry*, vol. 393, no. 2, pp. 569–582, 2009.

[17] K. M. Koczula and A. Gallotta, "Lateral flow assays," *Essays in biochemistry*, vol. 60, no. 1, pp. 111–120, 2016.

[18] M. Sajid, A.-N. Kawde, and M. Daud, "Designs, formats and applications of lateral flow assay: A literature review," *Journal of Saudi Chemical Society*, vol. 19, no. 6, pp. 689–705, 2015.

[19] B. Ngom, Y. Guo, X. Wang, and D. Bi, "Development and application of lateral flow test strip technology for detection of infectious agents and chemical contaminants: a review," *Analytical and bioanalytical chemistry*, vol. 397, no. 3, pp. 1113–1135, 2010.

[20] J.-O. Lee, H.-M. So, E.-K. Jeon, H. Chang, K. Won, and Y. H. Kim, "Aptamers as molecular recognition elements for electrical nanobiosensors," *Analytical and bioanalytical chemistry*, vol. 390, no. 4, pp. 1023–1032, 2008.

[21] C. Tuerk and L. Gold, "Systematic evolution of ligands by exponential enrichment: Nra ligands to bacteriophage t4 dna polymerase," *Science*, vol. 249, no. 4968, pp. 505–10, 1990.

[22] A. D. Ellington and J. W. Szostak, "In vitro selection of nra molecules that bind specific ligands," *Nature*, vol. 346, no. 6287, pp. 818–22, 1990.

[23] F. Radom, P. M. Jurek, M. P. Mazurek, J. Otlewski, and F. Jeleń, "Aptamers: Molecules of great potential," *Biotechnology Advances*, vol. 31, no. 8, pp. 1260–1274, 2013.

[24] S. Y. Toh, M. Citartan, S. C. B. Gopinath, and T.-H. Tang, "Aptamers as a replacement for antibodies in enzyme-linked immunosorbent assay," *Biosensors and Bioelectronics*, vol. 64, no. 0, pp. 392–403, 2015.

[25] S. Tombelli, M. Minunni, and M. Mascini, "Analytical applications of aptamers," *Biosens Bioelectron*, vol. 20, no. 12, pp. 2424–34, 2005.

[26] Y. Xu, X. Yang, and E. Wang, "Review: Aptamers in microfluidic chips," *Anal Chim Acta*, vol. 683, no. 1, pp. 12–20, 2010.

[27] Y. Zhang, B. S. Lai, and M. Juhas, "Recent advances in aptamer discovery and applications," *Molecules (Basel, Switzerland)*, vol. 24, no. 5, p. 941, 2019.

[28] J. Zhou and J. Rossi, "Aptamers as targeted therapeutics: current potential and challenges," *Nat Rev Drug Discov*, vol. 16, no. 3, pp. 181–202, 2017.

[29] D. Patel and S. N. Witt, "Ethanolamine and phosphatidylethanolamine: Partners in health and disease," *Oxidative Medicine and Cellular Longevity*, vol. 2017, p. 18, 2017.

[30] D. S. Wishart, D. Tzur, C. Knox, R. Eisner, A. C. Guo, N. Young, D. Cheng, K. Jewell, D. Arndt, S. Sawhney, C. Fung, L. Nikolai, M. Lewis, M. A. Coutouly, I. Forsythe, P. Tang, S. Shrivastava, K. Jeroncic, P. Stothard, G. Amegbey, D. Block, D. D. Hau, J. Wagner, J. Miniaci, M. Clements, M. Gebremedhin, N. Guo, Y. Zhang, G. E. Duggan, G. D. Macinnis, A. M. Weljie, R. Dowlatabadi, F. Bamforth, D. Clive, R. Greiner, L. Li, T. Marrie, B. D. Sykes, H. J. Vogel, and L. Querengesser, "Hmdb: the human metabolome database," *Nucleic Acids Res*, vol. 35, no. Database issue, pp. D521–6, 2007.

[31] D. Matas, A. Juknat, M. Pietr, Y. Klin, and Z. Vogel, "Anandamide protects from low serum-induced apoptosis via its degradation to ethanolamine," *J Biol Chem*, vol. 282, no. 11, pp. 7885–92, 2007.

[32] H. Sasaki, H. Kume, A. Nemoto, S. Narisawa, and N. Takahashi, "Ethanolamine modulates the rate of rat hepatocyte proliferation in vitro and in vivo," *Proceedings of the National Academy of Sciences*, vol. 94, no. 14, pp. 7320–7325, 1997.

[33] R. F. Kelly, K. T. Lamont, S. Somers, D. Hacking, L. Lacerda, P. Thomas, L. H. Opie, and S. Lecour, "Ethanolamine is a novel stat-3 dependent cardioprotective agent," *Basic Research in Cardiology*, vol. 105, no. 6, pp. 763–770, 2010.

[34] A. A. Farooqui, S. I. Rapoport, and L. A. Horrocks, "Membrane phospholipid alterations in alzheimer's disease: Deficiency of ethanolamine plasmalogens," *Neurochemical Research*, vol. 22, no. 4, pp. 523–527, 1997.

[35] J. S. Modica-Napolitano and P. F. Renshaw, "Ethanolamine and phosphoethanolamine inhibit mitochondrial function in vitro: implications for mitochondrial dysfunction hypothesis in depression and bipolar disorder," *Biological Psychiatry*, vol. 55, no. 3, pp. 273–277, 2004.

[36] S. Wang, S. Zhang, L.-C. Liou, Q. Ren, Z. Zhang, G. A. Caldwell, K. A. Caldwell, and S. N. Witt, "Phosphatidylethanolamine deficiency disrupts α-synuclein homeostasis in yeast and worm models of parkinson disease," *Proceedings of the National Academy of Sciences*, vol. 111, no. 38, pp. E3976–E3985, 2014.

[37] A. O. Gamer, R. Rossbacher, W. Kaufmann, and B. van Ravenzwaay, "The in-

halation toxicity of di- and triethanolamine upon repeated exposure," *Food and Chemical Toxicology*, vol. 46, no. 6, pp. 2173–2183, 2008.

[38] C.-Y. Lee, R.-J. Shiau, H.-W. Chou, and Y.-Z. Hsieh, "Combining aptamer-modified gold nanoparticles with barcode dna sequence amplification for indirect analysis of ethanolamine," *Sensors and Actuators B: Chemical*, vol. 254, pp. 189–196, 2018.

[39] D. Mann, C. Reinemann, R. Stoltenburg, and B. Strehlitz, "In vitro selection of dna aptamers binding ethanolamine," *Biochem Biophys Res Commun*, vol. 338, no. 4, pp. 1928–34, 2005.

[40] A. Heilkenbrinker, C. Reinemann, R. Stoltenburg, J.-G. Walter, A. Jochums, F. Stahl, S. Zimmermann, B. Strehlitz, and T. Scheper, "Identification of the target binding site of ethanolamine-binding aptamers and its exploitation for ethanolamine detection," *Analytical Chemistry*, vol. 87, no. 1, pp. 677–685, 2015.

[41] X. Cheng, X. Liu, T. Bing, R. Zhao, S. Xiong, and D. Shangguan, "Specific dna g-quadruplexes bind to ethanolamines," *Biopolymers*, vol. 91, no. 10, pp. 874–883, 2009.

[42] C. Reinemann, R. Stoltenburg, and B. Strehlitz, "Investigations on the specificity of dna aptamers binding to ethanolamine," *Analytical Chemistry*, vol. 81, no. 10, pp. 3973–3978, 2009.

[43] G. Liang, Y. Man, X. Jin, L. Pan, and X. Liu, "Aptamer-based biosensor for label-free detection of ethanolamine by electrochemical impedance spectroscopy," *Analytica Chimica Acta*, vol. 936, pp. 222–228, 2016.

[44] M. Mahmoud, S. Laufer, and H.-P. Deigner, "Visual aptamer-based capillary assay for ethanolamine using magnetic particles and strand displacement," *Microchimica Acta*, vol. 186, no. 11, p. 690, 2019.

[45] J. A. HUNTINGTON, "Molecular recognition mechanisms of thrombin," *Journal of Thrombosis and Haemostasis*, vol. 3, no. 8, pp. 1861–1872, 2005.

[46] J. Crawley, S. Zanardelli, C. Chion, and D. Lane, "The central role of thrombin in hemostasis," *Journal of thrombosis and haemostasis*, vol. 5, pp. 95–101, 2007.

[47] E. Di Cera, "Thrombin as procoagulant and anticoagulant," *J Thromb Haemost*, vol. 5 Suppl 1, pp. 196–202, 2007.

[48] A. M. Wendelboe and G. E. Raskob, "Global burden of thrombosis: Epidemiologic aspects," *Circ Res*, vol. 118, no. 9, pp. 1340–7, 2016.

[49] K. Wakui, T. Yoshitomi, A. Yamaguchi, M. Tsuchida, S. Saito, M. Shibukawa, H. Furusho, and K. Yoshimoto, "Rapidly neutralizable and highly anticoagulant thrombin-binding dna aptamer discovered by mace selex," *Molecular Therapy - Nucleic Acids*, vol. 16, pp. 348–359, 2019.

[50] T. Amato, A. Virgilio, L. Pirone, V. Vellecco, M. Bucci, E. Pedone, V. Esposito, and A. Galeone, "Investigating the properties of tba variants with twin thrombin binding domains," *Scientific Reports*, vol. 9, no. 1, p. 9184, 2019.

[51] B. Deng, Y. Lin, C. Wang, F. Li, Z. Wang, H. Zhang, X.-F. Li, and X. C. Le, "Aptamer binding assays for proteins: The thrombin example—a review," *Analytica Chimica Acta*, vol. 837, pp. 1–15, 2014.

[52] L. Schrodinger, "The pymol molecular graphics system, version 1.8." 2015.

[53] H. M. Berman, J. Westbrook, Z. Feng, G. Gilliland, T. N. Bhat, H. Weissig, I. N. Shindyalov, and P. E. Bourne, "The protein data bank," *Nucleic Acids Research*, vol. 28, no. 1, pp. 235–242, 2000.

[54] I. Russo Krauss, A. Merlino, A. Randazzo, E. Novellino, L. Mazzarella, and F. Sica, "High-resolution structures of two complexes between thrombin and thrombin-binding aptamer shed light on the role of cations in the aptamer inhibitory activity," *Nucleic Acids Research*, vol. 40, no. 16, pp. 8119–8128, 2012.

[55] I. Russo Krauss, A. Pica, A. Merlino, L. Mazzarella, and F. Sica, "Duplex–quadruplex motifs in a peculiar structural organization cooperatively contribute to thrombin binding of a DNA aptamer," *Acta Crystallographica Section D*, vol. 69, pp. 2403–2411, Dec 2013.

[56] L. C. Bock, L. C. Griffin, J. A. Latham, E. H. Vermaas, and J. J. Toole, "Selection of single-stranded dna molecules that bind and inhibit human thrombin," *Nature*, vol. 355, no. 6360, pp. 564–566, 1992.

[57] R. F. Macaya, P. Schultze, F. W. Smith, J. A. Roe, and J. Feigon, "Thrombin-binding dna aptamer forms a unimolecular quadruplex structure in solution," *Proc Natl Acad Sci U S A*, vol. 90, no. 8, pp. 3745–9, 1993.

[58] P. Schultze, R. F. Macaya, and J. Feigon, "Three-dimensional solution structure of the thrombin-binding dna aptamer d(ggttggtgtggttgg)," *J Mol Biol*, vol. 235, no. 5, pp. 1532–47, 1994.

[59] K. Y. Wang, S. McCurdy, R. G. Shea, S. Swaminathan, and P. H. Bolton, "A dna aptamer which binds to and inhibits thrombin exhibits a new structural motif for dna," *Biochemistry*, vol. 32, no. 8, pp. 1899–904, 1993.

[60] K. Y. Wang, S. H. Krawczyk, N. Bischofberger, S. Swaminathan, and P. H. Bolton, "The tertiary structure of a dna aptamer which binds to and inhibits thrombin determines activity," *Biochemistry*, vol. 32, no. 42, pp. 11285–11292, 1993.

[61] J. A. Kelly, J. Feigon, and T. O. Yeates, "Reconciliation of the x-ray and nmr structures of the thrombin-binding aptamer d(ggttggtgtggttgg)," *J Mol Biol*, vol. 256, no. 3, pp. 417–22, 1996.

[62] K. Padmanabhan, K. P. Padmanabhan, J. D. Ferrara, J. E. Sadler, and A. Tulinsky, "The structure of alpha-thrombin inhibited by a 15-mer single-stranded dna aptamer," *J Biol Chem*, vol. 268, no. 24, pp. 17651–4, 1993.

[63] K. Padmanabhan and A. Tulinsky, "An ambiguous structure of a dna 15-mer thrombin complex," *Acta Crystallogr D Biol Crystallogr*, vol. 52, no. Pt 2, pp. 272–82, 1996.

[64] J. A. Huntington, "Molecular recognition mechanisms of thrombin," *Journal of Thrombosis and Haemostasis*, vol. 3, no. 8, pp. 1861–1872, 2005.

[65] J. Liu, Z. Cao, and Y. Lu, "Functional nucleic acid sensors," *Chemical Reviews*, vol. 109, no. 5, pp. 1948–1998, 2009.

[66] J. Wang, Z. Cao, Y. Jiang, C. Zhou, X. Fang, and W. Tan, "Molecular signaling aptamers for real-time fluorescence analysis of protein," *IUBMB Life*, vol. 57, no. 3, pp. 123–8, 2005.

Appendix

1. International patent application: WO2019229066A1

”Detection of target molecules by determining the melting temperature of a recognition molecule” Status: pending

2. European patent application: EP3597775A1

”Method for the detection and quantification of small molecules and fluidic platform for performing the same” Status: pending

(12) INTERNATIONAL APPLICATION PUBLISHED UNDER THE PATENT COOPERATION TREATY (PCT)

(19) World Intellectual Property Organization
International Bureau

(43) International Publication Date
05 December 2019 (05.12.2019)

WIPO | PCT

(10) International Publication Number
WO 2019/229066 A1

(51) International Patent Classification:
C12Q 1/6818 (2018.01) *C12N 15/115* (2010.01)

(21) International Application Number:
PCT/EP2019/063828

(22) International Filing Date:
28 May 2019 (28.05.2019)

(25) Filing Language: English

(26) Publication Language: English

(30) Priority Data:
18175561.2 01 June 2018 (01.06.2018) EP

(71) Applicant: **INFANDX AG** [DE/DE]; Balthasarstralte 18, 50670 Kolıl (DE).

(72) Inventors: **MAHMOUD, Mostafa Mohamed Safwat Ahmed;** Villinger Straße 14, 78054 Villingen-Schwenningen (DE). **DEIGNER, Hans-Peter;** Martin-Luther-Str.23, 68623 Lampertheim (DE).

(74) Agent: **WINTER BRANDL FÜRNISS HÜBNER RÖSS KAISER POLTE - PARTNERSCHAFT MBB;** Alois-Steinecker-Str. 22, 85354 Freising (DE).

(81) Designated States *(unless otherwise indicated, for every kind of national protection available)*: AE, AG, AL, AM, AO, AT, AU, AZ, BA, BB, BG, BH, BN, BR, BW, BY, BZ, CA, CH, CL, CN, CO, CR, CU, CZ, DE, DJ, DK, DM, DO, DZ, EC, EE, EG, ES, FI, GB, GD, GE, GH, GM, GT, HN, HR, HU, ID, IL, IN, IR, IS, JO, JP, KE, KG, KH, KN, KP, KR, KW, KZ, LA, LC, LK, LR, LS, LU, LY, MA, MD, ME, MG, MK, MN, MW, MX, MY, MZ, NA, NG, NI, NO, NZ, OM, PA, PE, PG, PH, PL, PT, QA, RO, RS, RU, RW, SA, SC, SD, SE, SG, SK, SL, SM, ST, SV, SY, TH, TJ, TM, TN, TR, TT, TZ, UA, UG, US, UZ, VC, VN, ZA, ZM, ZW.

(84) Designated States *(unless otherwise indicated, for every kind of regional protection available)*: ARIPO (BW, GH, GM, KE, LR, LS, MW, MZ, NA, RW, SD, SL, ST, SZ, TZ, UG, ZM, ZW), Eurasian (AM, AZ, BY, KG, KZ, RU, TJ, TM), European (AL, AT, BE, BG, CH, CY, CZ, DE, DK, EE, ES, FI, FR, GB, GR, HR, HU, IE, IS, IT, LT, LU, LV, MC, MK, MT, NL, NO, PL, PT, RO, RS, SE, SI, SK, SM,

(54) **Title:** DETECTION OF TARGET MOLECULES BY DETERMINING THE MELTING TEMPERATURE OF A RECOGNITION MOLECULE

Figure 2

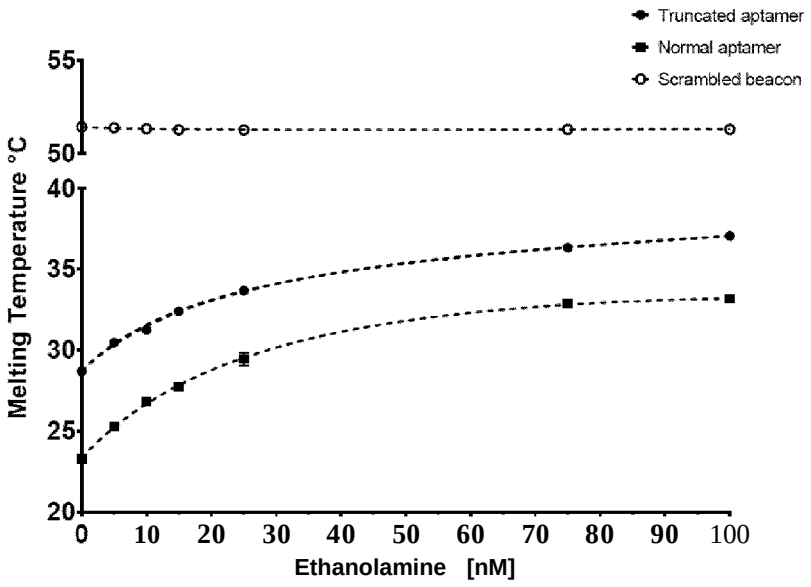

(57) Abstract: The present invention relates to a method of detection of at least one target molecule comprising determining the melting temperature change upon binding to at least one recognition molecule, an aptamer and its use in said method, a use of said method for determination of thermodynamic properties of binding between a recognition molecule and a target molecule, a use of said method for the identification of recognition molecules recognizing a known target, and the use of calorimetry for the detection of a target molecule in a liquid sample

[Continued on next page]

WO 2019/229066 A1

TR), OAPI (BF, BJ, CF, CG, Cl, CM, GA, GN, GQ, GW, KM, ML, MR, NE, SN, TD, TG).

Published:

— *with international search report (Art. 21(3))*
— *with sequence listing part of description (Rule 5.2(a))*

Detection of target molecules by determining the melting temperature of a recognition molecule

Technical field

The present invention relates to a method of detection of at least one target molecule comprising determining the melting temperature change upon binding to at least one recognition molecule, an aptamer and its use in said method, a use of said method for determination of thermodynamic properties of binding between a recognition molecule and a target molecule, a use of said method for the identification of recognition molecules recognizing a known target, and the use of calorimetry for the detection of a target molecule in a liquid sample.

Background of the Invention

The reliable detection and quantification of small molecules, such as metabolites and signalling molecules found endogenously in living organisms or toxins as well as contaminants found in the environment, independent of HPLC and mass spectrometry remains a challenge.

The use of HPLC systems requires expensive equipment and well-trained personnel. On the other hand, biosensors or assays based on antibodies specific for small molecules lack the high throughput and suffer from drawbacks usually associated with the assay format e.g. lack of immunogenicity, the need for labelling in competitive formats or the requirement for two binding epitopes for sandwich formats, as these are hardly compatible with small molecule targets.

In contrast, aptamer-based biosensors can address these drawbacks. They are advantageous over antibodies in terms of cost, stability, reversibility of denaturation, sensitivity, and specificity. Methods based on aptamers for protein detection and quantification vary a lot and offer a variety of approaches such as fluorescence sensors, electrochemical sensors, aptamer arrays and aptamer-gold nanoparticles sensors.

However, due to difference in mass and size, most aptamer-based biosensors for small molecules mentioned in the literature require a complex setup and a sophisticated

detection method to achieve the high throughput performance. Moreover, they usually require immobilization of aptamers and/or washing and incubation steps.

Aptamers are RNA/DNA sequences capable of binding to target molecules specifically and with high affinity. They were first introduced in 1990 through an in-vitro selection process known as systemic evolution of ligands by exponential enrichment (SELEX). Various aptamers against small molecules have been reported in the literature (McKeague, M. & DeRosa, M.C. Challenges and Opportunities for Small Molecule Aptamer Development. *Journal of Nucleic Acids* **2012,** 20 (201 2).).

The uniqueness of aptamers relates to conformational changes associated with binding. Aptamers adopt different conformational structures based on internal base pairings e.g. stem loops, G-quadruplexes and pseudoknots. These structures are either stabilized or destroyed upon target binding. In fact, this feature of nucleic acids has been used to design molecular beacons to signal the presence of specific target nucleic acid sequence.

Based on this concept, Hamaguchi et al. (Hamaguchi, N., Ellington, A. & Stanton, M. Aptamer beacons for the direct detection of proteins. *Anal Biochem* **294,** 126-1 3 1 (2001).) developed an aptamer beacon where target induced conformational change enabled detection and quantification of thrombin using a fluorophore on one end of the loop and a quencher on the other. This homogeneous assay format does not require immobilization of the biorecognition molecules on solid support thus evading the dependence on the relatively slow diffusion kinetics faced by common bioassays, but driving the bioreaction by its fast binding kinetics.

One of the major drawbacks faced by solid phase assays and biosensors lies in the dependence on mass transport rather than the fast assay kinetics. Differential scanning fluorimetry has been used to identify low-molecular-weight ligands that bind and stabilize purified proteins and the governing thermodynamics have been studied extensively. It has been recently shown that quantifying proteins using thermofluorimetric analysis is possible (Hu, J., Kim, J. & Easley, C.J. Quantifying Aptamer-Protein Binding via Thermofluorimetric Analysis. *Analytical methods:*

advancing methods and applications **7,** 7358-7362 (201 5); Kim, J. et al. Protein quantification using controlled DNA melting transitions in bivalent probe assemblies. *Anal Chem* **87,** 9576-9579 (201 5).).

This method, however, depends on a DNA intercalating dye as a reporter molecule e.g. SYBR green. SYBR green has associated drawbacks and limitations which include the shift of melting temperature of the DNA depending on the dye concentration and preferential binding to DNA fragments with higher GC content.

SYBR green is also known to compete with target binding leading to imprecise estimation of the melting temperature. This competition of SYBR green and similar intercalating dyes, has been applied to quantify target binding through fluorescence signal change upon target binding. Moreover, quantification was through the fluorescence signal and peak height and not related to the determination of a melting temperature shift. A similar principle was applied for the quantification of cyclic adenosine monophosphate with an antibody-oligonucleotide construct.

Accordingly, it remains a problem to reliably detect and quantify small molecules, such as metabolites and signalling molecules as well as contaminants found in the environment, independent of the use of HPLC and mass spectrometry.

Therefore, a novel method is required for easy, quick and reproducible determination of the presence of small target molecules and their quantity down to very low concentrations.

It is thus an object of the present invention to provide a novel method for detection of at least one target molecule.

It is a further object of the present invention to provide a novel aptamer molecule which could be used in said method, and its use therein.

It is another object of the present invention to provide a use of this method for determination of thermodynamic binding properties as well as for the identification of recognition molecules able to recognize a known target.

Ultimately, it is another object of the present invention to provide a use of calorimetry for the detection of a target molecule in a liquid sample.

Summary of the Invention

These objects have been solved by the aspects of the present invention as specified hereinafter.

According to the first aspect of the present invention, a method of detection of at least one target molecule is provided comprising contacting a liquid sample with at least one recognition molecule, wherein the at least one recognition molecule is able to specifically bind to the at least one target molecule, wherein specific binding of the at least one recognition molecule to the at least one target molecule induces a change in the melting temperature of the recognition molecule, and determining the melting temperature of the at least one recognition molecule after contacting with the liquid sample, and comparing the melting temperature of the at least one recognition molecule which has been determined in the step of determining the melting temperature with a standardized curve to identify the presence of the at least one target molecule in the liquid sample.

According to a preferred embodiment of the first aspect of the invention, the melting temperature of the at least one recognition molecule is determined by monitoring the temperature melting curve of the liquid sample.

According to another preferred embodiment of the first aspect of the invention, the detection of the at least one target molecule is a quantitative detection or quantification of the concentration of the at least one target molecule in the sample.

According to another preferred embodiment of the first aspect of the invention, the method for detection of at least one target molecule is based on calorimetry, preferably

wherein detection of fluorescence and/or UV absorbance does not form part of the method.

According to yet another preferred embodiment of the first aspect of the invention, a standardized calibration curve for the relation between melting temperatures and concentration of the at least one target molecule is prepared prior to contacting the liquid sample with at least one recognition molecule according to the method of the first aspect of the invention.

According to a preferred embodiment of the first aspect of the invention, the change in the melting temperature of the at least one recognition molecule is detected by measuring a melting profile of the liquid sample, preferably by using a calorimetry device, more preferably by using a quantitative PCR (qPCR) machine.

According to a preferred embodiment of the first aspect of the invention, one recognition molecule specifically binding to one target molecule is present in the liquid sample.

According to another preferred embodiment of the first aspect of the invention, two or more different recognition molecules are contacted with the liquid sample, wherein each of the two or more different recognition molecules is able to specifically bind to a different target molecule and/or wherein each of the two or more recognition molecules has a different temperature melting curve influenced by binding to its respective target molecule.

According to one preferred embodiment of the first aspect of the invention, the recognition molecule(s) is/are selected from the group comprising aptamers, spiegelmers, RNA, DNA, modified nucleic acids, affimers, or the like, preferably wherein the recognition molecule(s) is/are (an) aptamer(s), more preferably wherein the recognition molecule(s) is/are (an) aptamer beacon(s).

According to a preferred embodiment of the first aspect of the invention, the recognition molecule(s) is/are immobilized.

According to another preferred embodiment of the first aspect of the invention, the at least one target molecule is selected from the group comprising small molecules, pharmaceuticals, ions, proteins, peptides, receptors, pollutants, drugs, cells or parts of cells, bacteria, viruses, or the like, preferably wherein the at least one target molecule does not consist of RNA or DNA.

According to yet another preferred embodiment of the first aspect of the invention, a pair of fluorophore and quencher are provided on one or more of the at least one recognition molecules provided in the liquid sample and wherein the pair of fluorophore and quencher provided on one or more of the at least one recognition molecule are brought into spatial proximity upon binding to the target molecule, preferably wherein a pair of fluorophore and quencher are provided on each of the at least one recognition molecules.

According to a preferred embodiment of the first aspect of the invention, a pair of Forster resonance energy transfer (FRET) donor and FRET acceptor molecules are provided on one or more of the at least one recognition molecules provided in the liquid sample and wherein the pair of FRET donor and FRET acceptor molecules provided on one or more of the at least one recognition molecule are brought into spatial proximity upon binding to the target molecule, preferably wherein a pair of FRET donor and FRET acceptor molecules are provided on each of the at least one recognition molecules.

According to one preferred embodiment of the first aspect of the invention, at least one recognition molecule is in the form of an aptamer beacon, and at least one different recognition molecule is not in the form of an aptamer beacon, and these recognition molecules can compete for binding to the target molecule.

According to one more preferred embodiment of the first aspect of the invention, the at least one recognition molecules in the form of an aptamer beacon is labelled, preferably fluorescently labelled, more preferably by a pair of fluorophore and quencher and/or by a pair of FRET donor and FRET acceptor molecules, as defined hereinabove.

According to an even more preferred embodiment of the first aspect of the invention, the at least one recognition molecule in the form of an aptamer beacon has a shorter sequence than the at least one different recognition molecule not in the form of an aptamer beacon.

According to another preferred embodiment of the first aspect of the invention, the method further involves determination of temperature-dependent Circular Dichroism (CD) spectra and comparison with standardized CD spectra and/or defined points of a standardized CD curve.

According to yet another preferred embodiment of the first aspect of the invention, the method further involves determination of UV absorbance and/or a fluorescent signal and comparison with a standardized UV absorbance or fluorescence curve.

According to a more preferred embodiment of the first aspect of the invention, a standardized calibration curve for the relation between the CD spectra and/or the UV absorbance and/or the fluorescent signal and concentration of the target molecule is prepared prior to contacting the liquid sample with at least one recognition molecule according to the method of the first aspect of the invention.

According to an even more preferred embodiment of the first aspect of the invention, the step of comparing the melting temperature of the method of the first aspect of the invention includes comparing the CD spectra and/or the UV absorbance and/or the fluorescent signal determined in the step of determining the melting temperature of the method of the first aspect of the invention with standardized CD spectra or a standardized UV absorbance or fluorescence curve to identify the presence of the at least one target molecule in a sample.

According to the second aspect of the present invention, an aptamer of SEQ ID No. 1 (ATT CAA TTT GAG GCG GGT GGG TGG GTT GAA T ; 31 nucleotide ethanolamine aptamer) is provided.

According to the third aspect of the present invention, a use of the aptamer according to the second aspect of the present invention in the method according to the first aspect of the invention is provided.

According to the fourth aspect of the present invention, a use of the method according to the first aspect of the invention for determination of thermodynamic properties of binding of a recognition molecule to a target molecule is provided.

According to the fifth aspect of the present invention, a use of the method according to the first aspect of the invention for the identification of recognition molecules recognizing a known target is provided.

According to the sixth aspect of the present invention, a use of calorimetry for the detection of a target molecule in a liquid sample by using a recognition molecule able to specifically bind to the target molecule is provided, wherein the recognition molecule bound to the target molecule has a different temperature melting curve in comparison to the recognition molecule alone.

Description of Figures

Figure 1 shows the melting temperature in °C plotted against the concentration of ampicillin.

Figure 2 shows the melting temperature in °C plotted against the concentration of ethanolamine.

Figure 3 shows the melting temperature of the 42 nt ethanolamine-binding aptamer of SEQ ID No. 2 in °C for the negative control in buffer and upon addition of 1µM phenylethylamine.

Figure 4 shows raw signal data from the qPCR machine for temperature in °C plotted against fluorescence intensity in case of ampicillin and the ampicillin-binding aptamer of SEQ ID No. 3.

Figure 5 shows a first derivative graph of the signal measured over temperature in case of ampicillin and the ampicillin-binding aptamer of SEQ ID No. 3.

Figure 6 shows raw signal data from the qPCR machine for temperature in °C plotted against fluorescence intensity in case of ethanolamine and the 31 nt ethanolamine-binding aptamer of SEQ ID No. 1.

Figure 7 shows a first derivative graph of the signal measured over temperature in case of ethanolamine and the 31 nt ethanolamine-binding aptamer of SEQ ID No. 1.

Figure 8 shows raw signal data from the qPCR machine for temperature in °C plotted against fluorescence intensity in case of ampicillin and the scrampled ampicillin-control sequence of SEQ ID No. 4.

Figure 9 shows a first derivative graph of the signal measured over temperature in case of ampicillin and the scrampled ampicillin-control sequence of SEQ ID No. 4.

Figure 10 shows raw signal data from the qPCR machine for temperature in °C plotted against fluorescence intensity in case of ethanolamine and the scrambled ethanolamine-control sequence of SEQ ID No. 5.

Figure 11 shows a first derivative graph of the signal measured over temperature in case of ethanolamine and the scrambled ethanolamine-control sequence of SEQ ID No. 5.

Figure 12 shows a) the melting profile of different concentrations of the 42 nt ethanolamine-binding aptamer of SEQ ID No. 2 using 10X SYBR green, b) the melting profile of different concentration of the 31 nt ethanolamine-binding aptamer of SEQ ID No. 1 using 10X SYBR green, c) the melting profile of different concentrations of the 42 nt ethanolamine-binding aptamer beacon of SEQ ID No. 2, and d) the melting profile of different concentrations of the 31 nt ethanolamine-binding aptamer beacon of SEQ ID No. 1.

Detailed Description of the Invention

The present inventors have identified and provide herein a simple method for the detection and quantification of small target molecules based on the shift of the melting temperature of recognition molecules, such as e.g. aptamer beacons. In case of aptamer beacons, the presence of the target molecule leads to either stabilization or destruction of the beacon structure leading to a shift in the melting temperature.

The method can be carried out using any qPCR machine or other machine capable of capturing a melting profile and yields fast results within minutes of analysis time. In comparison to a common FRET experiment, it is simpler, faster and more reproducible. Moreover, the use of the melting profile for the determination of the presence and/or quantity of the target molecule shifts the focus on the melting temperature rather than on a change in fluorescence signal alone.

This minimizes the potential influence of fluorescent background and fluctuations in signal due to non-optimal folding of the recognition molecules such as aptamers or structure switching related with uncontrolled temperatures as opposed to controlled temperature curves inside a device such as a PCR machine. The present invention is considered the first report on using melting temperature shift of recognition molecules such as aptamer beacons to quantify small target molecules.

Applying a temperature gradient significantly accelerates the establishment of partial equilibria, thus reducing assay times. Further, as signals (changes in melting points of e.g. aptamer beacons) are detected along a temperature shift, signals are obtained within any temperature of the gradient and do not require an exactly matching temperature. Since the principle is based on changes of thermodynamics of the whole system it can be much more sensitive than methods applying establishment of static (e.g. strand-displacement based) equilibration.

In addition, a preferred embodiment of the method of the present invention using e.g. a fluorophore-quencher structure in a beacon format is superior to a method applying DNA-intercalating or double-strand DNA-binding dyes such as SYBR-green

since thermodynamics in such a system is way too complex to provide clear and separated melting-shift signals by optical readouts.

The inventors' findings pave the way for establishing assays for small molecules in combination with PCR machines or any similar device capable of capturing the melting profile. In general, quantification is performed by measuring a standard curve recording concentration-dependent optical signals across a suitable temperature range to identify melting temperatures at given conditions; measure unknown concentrations of the target by recording the melting temperature(s) alone, and processing the measured melting temperature by an algorithm providing a best fit function for assigning melting temperatures to target molecule concentrations.

An indirect format for target molecule determination is also provided. According to a preferred embodiment of the present invention, this format has an unlabelled binding aptamer and an aptamer beacon competing for the binding region. Through capturing the melting temperature of such a probe, the target molecule could be determined and quantified. Similarly, the method according to the present invention could also give insights on the binding thermodynamics and mechanisms using different probes.

The method of the present invention also has great multiplexing potential. Since aptamers for different targets are of different length, they are expected to have different melting temperatures. In a common binding buffer, different aptamers could bind to their targets at the same time and provide information about their differential melting temperature shifts.

An onsite point of care diagnostic kit is provided making full use of the concept of the method presented here. Based on the advances made in PCR on chip technology, a simple miniaturization of the assay should be possible to achieve and could form the core of said kit.

The challenges and bottlenecks faced by miniaturized PCR assays, e.g. the need for non-metallic heating elements not to interfere with the enzymes for the PCR reaction, would not apply here since the assay is based on profiling the melting

temperature and no polymerase reaction is involved. The applications for such a kit would include but not limited to clinical diagnostics, environmental testing, contamination for food and water and testing for drugs of abuse.

The present invention provides a method of detection of at least one target molecule comprising the steps of contacting a liquid sample with at least one recognition molecule, wherein the at least one recognition molecule is able to specifically bind to the at least one target molecule, wherein specific binding of the at least one recognition molecule to the at least one target molecule induces a change in the melting temperature of the recognition molecule, and determining the melting temperature of the at least one recognition molecule after contacting with the liquid sample, and comparing the melting temperature of the at least one recognition molecule which has been determined in the step of determining the melting temperature with a standardized curve to identify the presence of the at least one target molecule in the liquid sample.

According to a preferred embodiment of the present invention, the melting temperature is determined by monitoring the temperature melting curve of the sample to be tested. Such monitoring may be done by any device capable of monitoring and obtaining a temperature melting curve of a sample. Devices which are suitable for said purpose are known to persons skilled in the art and may preferably be selected from PCR machines, preferably from PCR machines capable of performing quantitative PCR (qPCR).

In the present invention, a method of detection may preferably be a method of detecting the presence of at least one target molecule in a sample, more preferably of the presence of a target molecule in a concentration above a given cut-off concentration in a sample. Such cut-off concentration depends on the target molecule, the available corresponding recognition molecules and the cut-off concentration which is specific for the distinct combination of target molecule and recognition molecule. Such cut-off concentration can easily be determined by the skilled person by using routine procedures.

According to another preferred embodiment, a method of detection is a method of quantitative detection or quantification of the concentration of the at least one target molecule in the sample. Quantitative detection or quantification of the concentration may preferably be used interchangeably herein. Quantitative detection of at least one target molecule may preferably mean the determination of at least one target molecule concentration in a sample, more preferably wherein said concentration is at least at or above the cut-off concentration mentioned herein.

Preferably, the term “at least one target molecule” may mean one or more target molecules, more preferably two or more, even more preferably three or more target molecules, further preferably four or more target molecules, further preferably five or more target molecules. According to a particularly preferred embodiment, this term may mean one or two target molecules, more preferably one target molecule. Similarly preferably, the term “at least one recognition molecule” may mean one or more recognition molecules, more preferably two or more, even more preferably three or more recognition molecules. According to a particularly preferred embodiment, this term may mean one or two recognition molecules, more preferably one recognition molecule.

The potential for multiplexing the method of the present invention by providing more than one target molecule and more than one recognition molecule is not particularly limited as long as the recognition molecules used concomitantly have different melting temperatures and/or melting temperature shifts upon binding to their target molecule. According to a preferred embodiment, at least one recognition molecule specifically binding to one target molecule is present in the sample. According to another preferred embodiment, at least one recognition molecule specifically binding to a target molecule is present in the sample for each target molecule present in the sample, more preferably one recognition molecule specifically binding to a target molecule is present in the sample for each target molecule present in the sample. Thus, according to a preferred embodiment, the sample comprises one or more pairs of recognition molecules specifically binding to target molecules.

Specific binding in the context of the present invention may preferably mean any kind of interaction between the target molecule and the recognition molecule which is

able to shift the melting temperature or induce a change in the melting temperature of the recognition molecule.

Interestingly, the method of the present invention allows a limit of detection (LOD) of a target molecule which is lower than the K_D of the binding of the recognition molecule to the target molecule. For more information on this phenomenon, reference is made to the publication of Heilkenbrinker A. et al., Anal Chem. 2015 Jan 6;87(1):677-85. doi: 10.1021/ac5034819. Epub 2014 Dec 10.

Determination of the melting temperature of the recognition molecule/s alone as well as the melting temperature of the recognition molecule/s after contacting with a sample potentially containing target molecule/s may preferably be determined by using calorimetry. One preferred way of determining melting temperatures is described in the publication "Determination of DNA and RNA Melting Point on UV-VIS Photometer SPECORD ® PLUS" from Alexandra Kastner of analytikjena (Lit_UV-01_11_e | 02/2011 | AK).

One prerequisite for the method of the present invention is the availability of a standardized melting temperature curve which correlates melting temperatures of a sample with the concentration in a sample of the target molecule to which the recognition molecule specifically binds. Preferably, such a standardized curve is prepared prior to carrying out the method of the present invention. The preparation of this standardized curve does not require undue experimentation and is well within the skills of an expert in the art. Within the context of the present invention, a standardized curve may be referred to as a calibration curve and *vice versa.*

Preferably, the melting temperature of the at least one recognition molecule is determined by monitoring the temperature melting curve of the liquid sample which is contacted with the recognition molecule, preferably wherein the liquid sample contains the target molecule. More preferably, the change in the melting temperature is detected by measuring a melting profile of the liquid sample, preferably by using a calorimetry device, more preferably by using a device capable of performing quantitative PCR (qPCR).

According to a preferred embodiment of the method of the present invention, the method is not based on detection of fluorescence and/or UV absorbance. According to another preferred embodiment of the method of the present invention, the method does not comprise measurements based on microscale thermophoresis, more preferably the method does not comprise measurements of the mobility of molecules in temperature gradients, even more preferably the method does not comprise measurements of the mobility of molecules, particularly preferably the method is not based on thermophoresis. An overview of this technology is published in Jerabek-Willemsen M et al. *Assay and Drug Development Technologies.* 201 1;9(4):342-353.

According to another preferred embodiment of the present invention, a pair of fluorophore and quencher are provided on one or more of the at least one recognition molecules provided in the liquid sample and wherein the pair of fluorophore and quencher provided on one or more of the at least one recognition molecule are brought into spatial proximity upon binding to the target molecule, preferably wherein a pair of fluorophore and quencher are provided on each of the at least one recognition molecules, more preferably wherein different pairs of fluorophore and quencher are provided on each of the at least one recognition molecules in cases where more than one recognition molecule is used.

According to another preferred embodiment of the present invention, a pair of Forster resonance energy transfer (FRET) donor and FRET acceptor molecules are provided on one or more of the at least one recognition molecules provided in the liquid sample and wherein the pair of FRET donor and FRET acceptor molecules provided on one or more of the at least one recognition molecule are brought into spatial proximity upon binding to the target molecule, preferably wherein a pair of FRET donor and FRET acceptor molecules are provided on each of the at least one recognition molecules, more preferably wherein different pairs of FRET donor and FRET acceptor molecules are provided on each of the at least one recognition molecules in cases where more than one recognition molecule is used.

According to a preferred embodiment, the pairs of fluorophore and quencher or FRET donor and FRET acceptor molecules as mentioned above may be replaced by any pair of molecules which either generate a fluorescent signal when brought in close proximity which is lost again when proximity is no longer given or, alternatively, extinguish a fluorescent signal when brought in close proximity which is regenerated when proximity is lost.

According to a preferred embodiment, the recognition molecule/s is selected from the group comprising aptamers, spiegelmers, RNA, DNA, modified nucleic acids, affimers, or the like, preferably wherein the recognition molecule(s) is/are (an) aptamer(s), more preferably wherein the recognition molecule(s) is/are (an) aptamer beacon(s).

Aptamers as recognition molecules which are able to bind to small target molecules are well-known in the art. Preferred aptamers as recognition molecules can be taken from Pfeiffer F and Mayer G (2016) Selection and Biosensor Application of Aptamers for Small Molecules. Front. Chem. 4:25. doi: 10.3389/fchem. 201 6.00025, more preferably from Table 1 of this publication.

Preferably, the at least one target molecule is selected from the group comprising small molecules, pharmaceuticals, ions, proteins, peptides, receptors, pollutants, drugs, cells or parts of cells, bacteria, viruses, or the like, more preferably wherein the at least one target molecule does not consist of RNA or DNA. Also, target molecules suitable as target molecules in the method of the present invention may preferably be taken from the aforementioned publication of Pfeiffer F and Mayer G, more preferably from Table 1 thereof.

Flowever, in the present invention, the recognition molecules are not particularly limited as long as they are able to specifically bind to a target molecule and wherein this binding induces a change in the melting temperature of the recognition molecule. Also, the target molecules are not specifically limited as long as they are able to specifically bind to a recognition molecule and wherein this binding induces a change in the melting

temperature of the recognition molecule. Preferably, the recognition molecule/s are immobilized.

According to another preferred embodiment, at least one recognition molecule used in the method of the present invention is in the form of an aptamer beacon, and at least one different recognition molecule is not in the form of an aptamer beacon, and wherein these recognition molecules can compete for binding to the target molecule.

Further preferably, the at least one recognition molecules in the form of an aptamer beacon is labelled, preferably fluorescently labelled, more preferably by a pair of fluorophore and quencher and/or by a pair of FRET donor and FRET acceptor molecules, or any other fluorescent label which differs in the generation of a fluorescent signal between close proximity and larger distance as explained above.

More preferably, the at least one recognition molecule in the form of an aptamer beacon has a shorter sequence than the at least one different recognition molecule not in the form of an aptamer beacon.

According to a preferred embodiment, the method of the present invention further involves determination of temperature-dependent Circular Dichroism (CD) spectra and comparison with standardized CD spectra and/or defined points of a standardized CD curve. According to another preferred embodiment, the method of the present invention further involves determination of UV absorbance and/or a fluorescent signal and comparison with a standardized UV absorbance or fluorescence curve.

According to a more preferred embodiment, a calibration curve for the relation between the CD spectra and/or the UV absorbance and/or the fluorescent signal and concentration of the target molecule is prepared prior to carrying out the method of the present invention. According to an even more preferred embodiment, step c) of the method of the invention includes comparing the CD spectra and/or the UV absorbance and/or the fluorescent signal determined in step b) with standardized CD spectra or a standardized UV absorbance or fluorescence curve to identify the presence and/or the concentration of the at least one target molecule in a sample.

According to one preferred embodiment of the present invention, melting curves of aptamer beacons provided with pairs of molecules either generating a fluorescent signal when in proximity or quenching a pre-existing fluorescent signal when brought in proximity may be generated in a PCR machine, more preferably in a PCR machine able to perform qPCR.

According to a particularly preferred embodiment, melting curves are generated in a Roche LightCycler, more preferably in accordance with the determination of fluorescence melting curves as described in Darby, AJ et al. (2002). High throughput measurement of duplex, triplex and quadruplex melting curves using molecular beacons and a LightCycler. Nucleic acids research. 30. e39. 10.1 093/nar/30.9.e39.

According to one aspect of the present invention, an aptamer having the sequence of SEQ ID No. 1 is claimed. This aptamer has been found by the inventors to exhibit improved folding and binding to ethanolamine in comparison to sequences disclosed in the prior art. Thus, the present invention also provides the use of the aptamer having the sequence of SEQ ID No. 1 to bind to ethanolamine. According to another aspect of the present invention, the use of the aptamer having the sequence of SEQ ID No. 1 in the method of the present invention is provided.

According to another aspect of the present invention, the method of the present invention is used for determination of thermodynamic properties of binding of a recognition molecule to a target molecule. According to yet another aspect of the present invention, the method of the present invention is used for the identification of recognition molecules recognizing a known target. To this end, target molecules may be provided in a sample and recognition molecules contacted therewith to cause a potential shift in melting temperature curves of the recognition molecule/s. In case that a shift is observed, this can be considered as an indication that the recognition molecule recognizes the target molecule.

According to one aspect of the present invention, the use of calorimetry is provided for the detection of a target molecule in a liquid sample by using a recognition

molecule able to specifically bind to the target molecule, wherein the recognition molecule bound to the target molecule has a different temperature melting curve in comparison to the recognition molecule alone.

All embodiments of the present invention as described herein are deemed to be combinable in any combination, unless the skilled person considers such a combination to not make any technical sense.

Examples

Aptamer beacons (with 5' Fluorescein and 3' DABCYL) were synthesized and purified by Integrated DNA Technologies (Coralville, IA). Ampicillin, ethanolamine, phenylethylamine and SYBR® Green I (10,000x in DMSO) were purchased from Sigma-Aldrich (Darmstadt, Germany).

The following are the sequences of the aptamers used, all of which had 5' Fluorescein and 3' DABCYL and with no labels for use with SYBR green.

31 nt Ethanolamine binding aptamer (SEQ ID No. 1):
ATTCAATTTGAGGCGGGTGGGTGGGTTGAAT

42 nt Ethanolamine binding aptamer (SEQ ID No. 2):
ATACCAGCTT ATT CAATTT GAG GCG GGT GGGTGGGTT GAATA

Ampicillin binding aptamer (SEQ ID No. 3):
CACGGCATGGTGGGCGTCGTG

Scrambled sequence used as ampicillin negative (SEQ ID No. 4):
ATT CAATTT CTCCCGTT GAAT

Scrambled sequence used as ethanolamine negative (SEQ ID No. 5):
CACGGCATGGTTCCATACTTAAGGGCGTCGTG

To account for signal variation and scattering of the data, the on-plate redundancy was at least 4 identical wells per parameter. Additionally, each experiment was repeated at least 4 times to assess both reproducibility and inter-assay variation.

The concentration of the aptamer beacon was fixed at 0.5 μM in all experiments except for the experiments with SYBR green (10x) and the corresponding melting analysis using aptamer beacons at the same concentrations (0.5, 1, 2 and 4 μM).

The beacons were pipetted in a 96 wells PCR plate at a volume of 20 pL in ampicillin binding buffer[25] consisting of (20 mM Tris, 100 mM NaCl, 0.02% TWEEN® 20, and 100 mM $MgCl_2$ at pH 7.6) or ethanolamine binding buffer consisting of (20 mM TRIS, 100 mM NaCl, 5 mM KCl, 2 mM $MgCl_2$, 1 mM $CaCl_2$, 0.02% Tween® 20 at pH 7.6).

The analyte concentration in case of ampicillin was varied from (0.5 to 32 pM) and were added in a volume of 2 pL per well. In case of ethanolamine and phenylethylamine, the analyte was varied from (5 to 100 nM).

The PCR machine (LightCycler® 480, Roche) was set to heat first till 99 °C followed by holding for 5 minutes to ensure the complete denaturing of any DNA base pairings. Then, the fluorescence was measured from 95 °C to 20 °C with the SYBR Green filter (465 nm excitation and 510 nm emission). As for the ampicillin, we found that heating to 99 °C can possibly lead to its degradation. Therefore, the PCR was set to heat only to 70 °C when detecting ampicillin.

Data analysis (plotting and fitting using one site binding equation) was performed using GraphPad Prism version 7.00 for Windows, GraphPad Software, La Jolla California USA, www.graphpad.com and JMP®, Version *<13. 1>,* First Derivative with 2nd order smoothing (4 neighbors). SAS Institute Inc., Cary, NC, 1989-2007. The raw data obtained from the PCR (Figures 4, 6, 8 and 10) was used to generate first derivative graphs for each individual experiment (Figures 5, 7, 9 and 11).

These first derivatives were fitted using a Gaussian distribution with the following equation Y=Amplitude*exp(-0.5*((X-Mean)/SD) ^2. The resulting Tm (defined as the Mean in the equation) was then plotted against the concentration (Fig. 1 and 2) to produce the standardized curves/calibration curves.

Example 1:

As proof of concept and feasibility of the approach presented herein, the ampicillin aptamer beacon (AMP4) of SEQ ID No. 3 was chosen. The secondary structure was predicted using mfold http://www.bioinfo.rpi.edu/applications/mfold to show a conserved region in the loop and a base pairing in the stem which is thought to play an important role in the binding (Song, K.-M., Jeong, E., Jeon, W., Cho, M. & Ban, C. Aptasensor for ampicillin using gold nanoparticle based dual fluorescence-colorimetric methods. *Analytical and Bioanalytical Chemistry* **402,** 2153-2161 (2012).).

Therefore, the presence of the target in the sample will lead to a destabilization of the stem loop structure in case of the ampicillin-binding aptamer beacon decreasing the energy needed to break the stem loop structure and hence decrease the melting temperature.

PCR plates containing the aptamer solution at 0.5 μM concentration per well and a volume of 20 μl were prepared. Then, 2 μl of ampicillin solution (0.5 pM to 32 pM) were pipetted in the wells in such a manner that there are 12 replicates per plate. The plates were then transferred to a lightcycler 480 for acquisition of the melting profile.

As shown in Figure 1, the presence of ampicillin decreased the melting temperature in comparison to the negative control (only buffer with no ampicillin). The method allowed the detection of concentrations as low as 1.5 ± 0.38 pM with an estimated K_d value of 0.621 ± 0.33 pM. The limit of detection was defined as (blank mean value + 3*SDbiank). As we expected the aptamer-ampicillin binding event leads to destabilization of the stem loop structure and thus to decrease in the energy needed to melt the aptamer beacon.

In case of ampicillin, it is well documented that the compound is highly unstable in high temperatures which leads to its hydrolysis (Mitchell, S.M., Ullman, J.L., Teel, A.L. & Watts, R.J. pH and temperature effects on the hydrolysis of three β-lactam antibiotics: ampicillin, cefalotin and cefoxitin. *Sci Total Environ* **466-467,** 547-555 (2014).; Hou, J.P. & Poole, J.W. Kinetics and Mechanism of Degradation of Ampicillin in Solution. *Journal of Pharmaceutical Sciences* **58,** 447-454 (1969).).

The hydrolysis reaction follows a pseudo first-order kinetics with respect to the initial concentration of ampicillin. This leads to the observed fast saturation within the calibration curve. This is, therefore, not due to the saturation of the aptamer beacons but rather due to the exponential degradation of the substrate. The counterproductive effects of the ampicillin degradation, however, restrict the quantification using thermofluorimetric analysis. Nevertheless, we could still detect amounts as low as 1.5 pM through setting the maximum temperature to 70°C.

Example 2:

As another example, ethanolamine-binding aptamers were used to further demonstrate the generalizability of the approach and show the case of stabilizing the folded beacon structure. It was previously shown that the ethanolamine aptamer G rich consensus region adopts a G-quartet structure and that this sequence is responsible for the binding.

Thus, we chose a 42 nucleotides sequence ethanolamine-binding aptamer (SEQ ID No. 2; labelled as “normal aptamer” in Figure 2) which is a truncated version of the original full-length 96 nucleotides aptamer (Mann, D., Reinemann, C., Stoltenburg, R. & Strehlitz, B. In vitro selection of DNA aptamers binding ethanolamine. *Biochemical and biophysical research communications* **338,** 1928-1934 (2005).).

This aptamer was further modified by adding a fluorophore (fluorescein) on the 5' end and a quencher (DABCYL) on the 3' end. The folding structure was predicted using mfold and did not show a perfect stem loop folding. Therefore, we decided to modify the sequence by truncating it further to 31 nucleotides (SEQ ID No. 1; labelled as “truncated aptamer” in Figure 2) to improve the folding. Moreover, this allowed us to check the effect of small modifications on the binding parameters.

Our results showed that even a modified structure was still capable of binding to the target. Further, the structural conformation only needs to provide a proximity between the fluorophore and the quencher to work and this may be provided by other means than stem loop *e.g.* by short complementary strands.

As seen in Figure 2, the addition of ethanolamine shifted the melting temperature through stabilizing the folded beacon structure. The limit of detection (LOD= blank mean value + 3*SDbiank) for the 42nt aptamer version was 2.2 ± 0.378 nM and the 31nt truncated version was 1.5 ± 0.615 nM. The estimated Kd value was 26.6 ± 4.4 nM and 28.8 ± 3.4 respectively.

We could show that even small modifications in the structure of the aptamer do not affect the binding (provided that the binding sequence is still present). The approach shows promising results that could be potentially transferred to other aptamers for small molecules.

Example 3:

The response of the assay using the 42 nt ethanolamine-binding aptamer of SEQ ID No. 2 to the structurally similar molecule phenylethylamine has further been studied.

It has previously been shown that phenylethylamine binds the full-length 96nt aptamer (see above) by affinity elution test at about 50% of the ethanolamine binding (Reinemann, C., Stoltenburg, R. & Strehlitz, B. Investigations on the Specificity of DNA Aptamers Binding to Ethanolamine. *Analytical chemistry* **81**, 3973-3978 (2009).).

Our results (Fig. 3), indicate, that using an increased concentration of 1 µM phenylethylamine, the 42 nucleotides aptamer of SEQ ID No. 2 showed a significant change in comparison to the control (Figure 3). Flowever, other aptamers with a specificity towards phenylethylamine are likely to successfully detect and quantify much lower concentrations of phenylethylamine.

Example 4:

In this example, SYBR green was tested as a candidate intercalating dye (Figure 12 a and b), however, the melting profile could not be captured for the aptamer concentrations used (0.5, 1, 2 and 4 µM and 10X SYBR green). The beacons, however, showed well-defined melting peaks (Figure 12 c and d).

Claims

1. Method of detection of at least one target molecule comprising:

a) Contacting a liquid sample with at least one recognition molecule, wherein the at least one recognition molecule is able to specifically bind to the at least one target molecule, wherein specific binding of the at least one recognition molecule to the at least one target molecule induces a change in the melting temperature of the recognition molecule, and

b) Determining the melting temperature of the at least one recognition molecule after contacting with the liquid sample, and

c) Comparing the melting temperature of the at least one recognition molecule which has been determined in step b) with a standardized calibration curve to identify the presence of the at least one target molecule in the liquid sample.

2. Method of claim 1, wherein the melting temperature of the at least one recognition molecule is determined by monitoring the temperature melting curve of the liquid sample, more preferably wherein the detection of the at least one target molecule is a quantitative detection or quantification of the concentration of the at least one target molecule in the sample.

3. Method of claim 1 or 2, wherein the method for detection of at least one target molecule is based on calorimetry, preferably wherein detection of fluorescence and/or UV absorbance does not form part of the method.

4. Method of any of claims 1 to 3, wherein the change in the melting temperature of the at least one recognition molecule is detected by measuring a melting profile of the liquid sample, preferably by using a calorimetry device, more preferably by using a quantitative PCR (qPCR) machine.

5. Method of any of claims 1 to 4, wherein the recognition molecule(s) is/are selected from the group comprising aptamers, spiegelmers, RNA, DNA,

modified nucleic acids, affimers, or the like, preferably wherein the recognition molecule(s) is/are (an) aptamer(s), more preferably wherein the recognition molecule(s) is/are (an) aptamer beacon(s), even more preferably wherein the recognition molecule(s) is/are immobilized.

6. Method of any of claims 1 to 5, wherein the at least one target molecule is selected from the group comprising small molecules, pharmaceuticals, ions, proteins, peptides, receptors, pollutants, drugs, cells or parts of cells, bacteria, viruses, or the like, preferably wherein the at least one target molecule does not consist of RNA or DNA.

7. Method of any of claims 1 to 6, wherein a pair of fluorophore and quencher are provided on one or more of the at least one recognition molecules provided in the liquid sample and wherein the pair of fluorophore and quencher provided on one or more of the at least one recognition molecule are brought into spatial proximity upon binding to the target molecule, preferably wherein a pair of fluorophore and quencher are provided on each of the at least one recognition molecules, alternatively wherein a pair of Forster resonance energy transfer (FRET) donor and FRET acceptor molecules are provided on one or more of the at least one recognition molecules provided in the liquid sample and wherein the pair of FRET donor and FRET acceptor molecules provided on one or more of the at least one recognition molecule are brought into spatial proximity upon binding to the target molecule, preferably wherein a pair of FRET donor and FRET acceptor molecules are provided on each of the at least one recognition molecules.

8. Method of any of claims 1 to 7, wherein at least one recognition molecule is in the form of an aptamer beacon, and wherein at least one different recognition molecule is not in the form of an aptamer beacon, and wherein these recognition molecules can compete for binding to the target molecule, preferably wherein the at least one recognition molecules in the form of an aptamer beacon is labelled, more preferably fluorescently labelled, even more preferably by a pair

of fluorophore and quencher and/or by a pair of FRET donor and FRET acceptor molecules, as defined in claim 7.

9. Method of claim 8, wherein the at least one recognition molecule in the form of an aptamer beacon has a shorter sequence than the at least one different recognition molecule not in the form of an aptamer beacon.

10. Method of any of claims 1 to 9, wherein the method further involves determination of temperature-dependent Circular Dichroism (CD) spectra and comparison with standardized CD spectra and/or defined points of a standardized CD curve, alternatively wherein the method further involves determination of UV absorbance and/or a fluorescent signal and comparison with a standardized UV absorbance or fluorescence curve.

11. Method of claim 10, wherein a calibration curve for the relation between the CD spectra and/or the UV absorbance and/or the fluorescent signal and concentration of the target molecule is prepared prior to step a), preferably wherein step c) includes comparing the CD spectra and/or the UV absorbance and/or the fluorescent signal determined in step b) with standardized CD spectra or a standardized UV absorbance or fluorescence curve to identify the presence of the at least one target molecule in a sample.

12. Aptamer having the sequence of SEQ ID No. 1.

13. Use of the aptamer of claim 12 in the method of any of claims 1 to 11.

14. Use of the method of any of claims 1 to 11 for determination of thermodynamic properties of binding of a recognition molecule to a target molecule.

15. Use of the method of any of claims 1 to 11 for the identification of recognition molecules recognizing a known target.

16. Use of calorimetry for the detection of a target molecule in a liquid sample by using a recognition molecule able to specifically bind to the target molecule, wherein the recognition molecule bound to the target molecule has a different temperature melting curve in comparison to the recognition molecule alone.

Figures

Figure 1

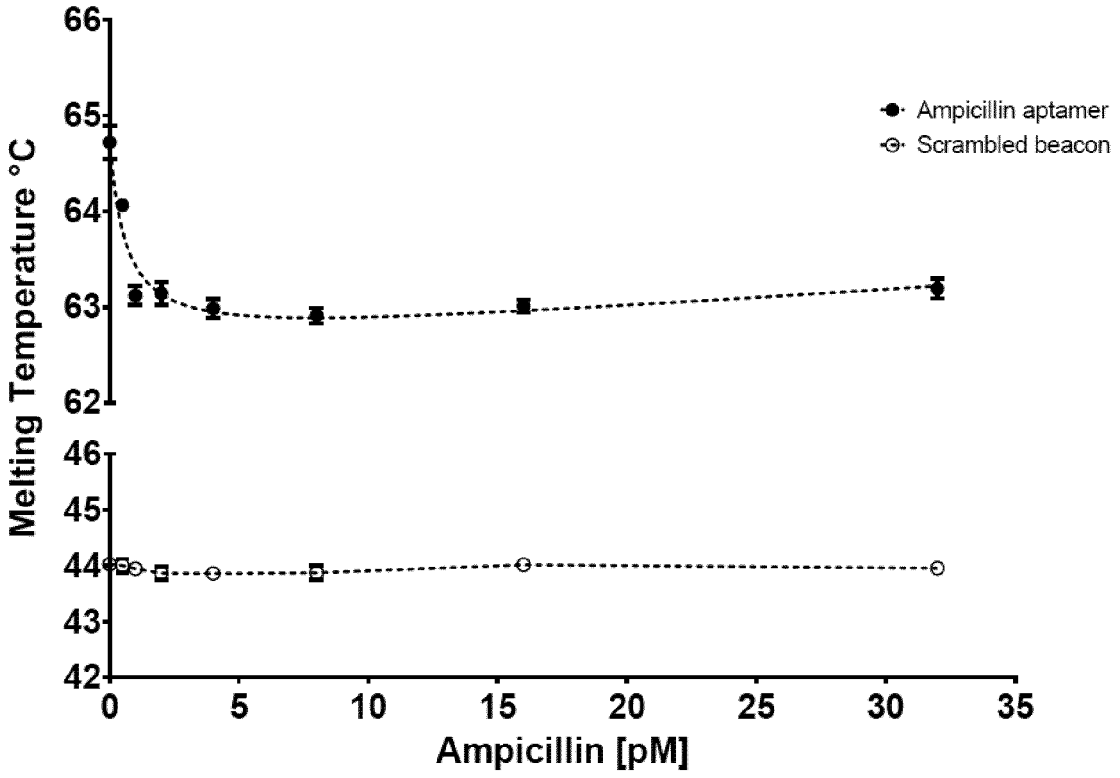

Figure 2

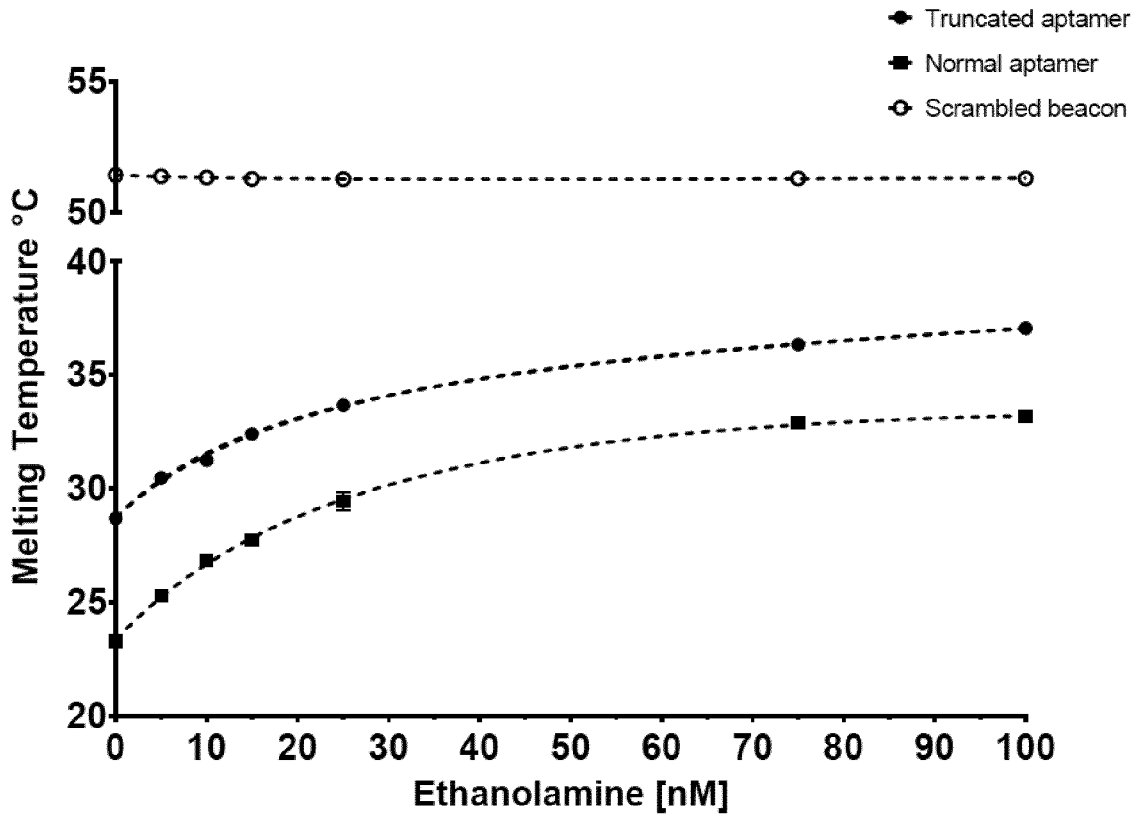
Truncated aptamer
Normal aptamer
Scrambled beacon
Melting Temperature °C
55
50
40
35
30
25
20
0
10
20
30
40
50
60
70
80
90
100
Ethanolamine [nM]

Figure 3

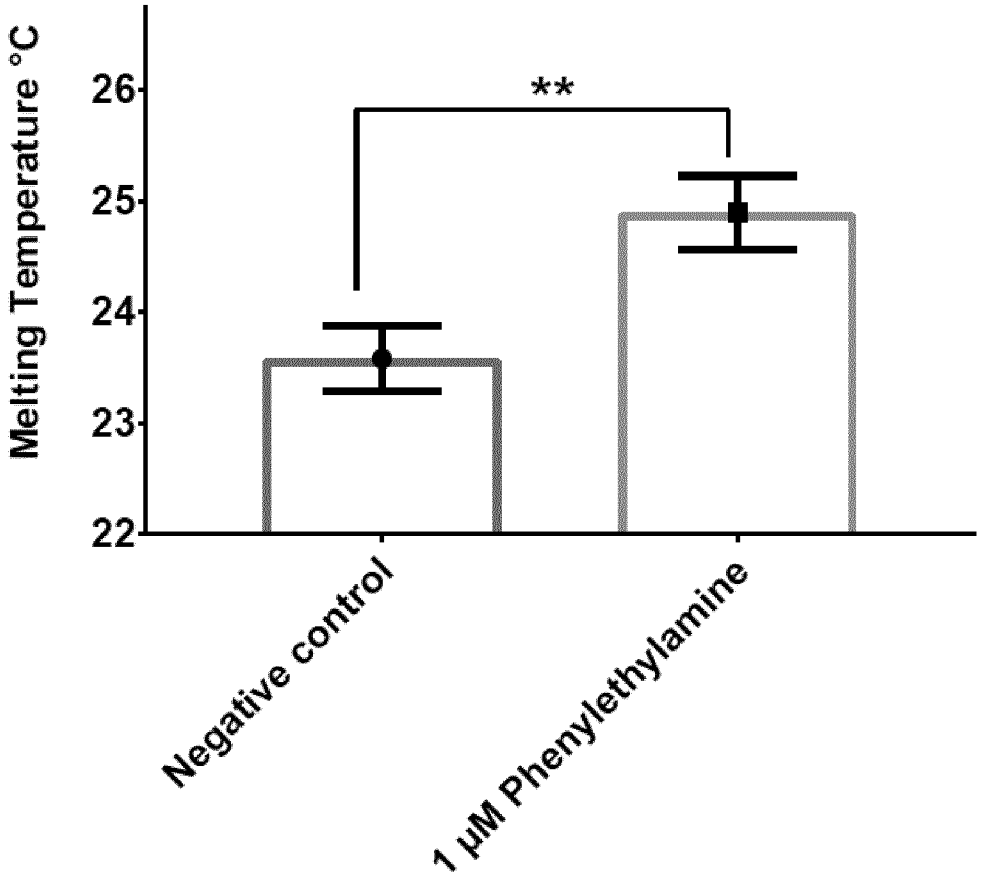
Melting Temperature °C
26
25
24
23
22
**
Negative control
1 µM Phenylethylamine

Figure 4

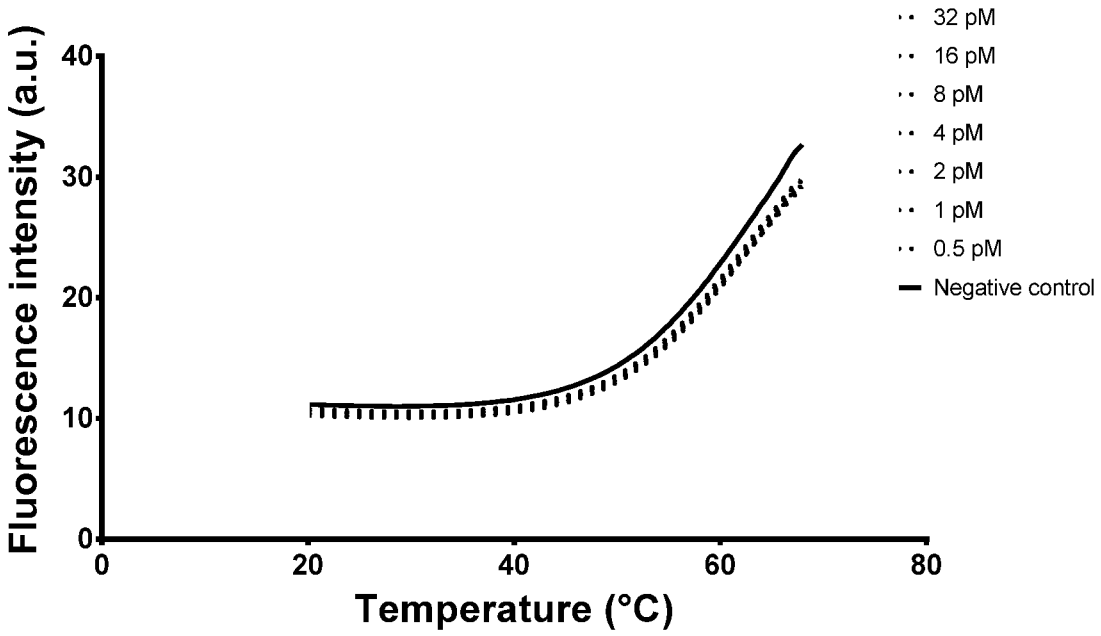
Fluorescence intensity (a.u.)
0
10
20
30
40
0
20
40
60
80
Temperature (°C)
32 pM
16 pM
8 pM
4 pM
2 pM
1 pM
0.5 pM
Negative control

Figure 5

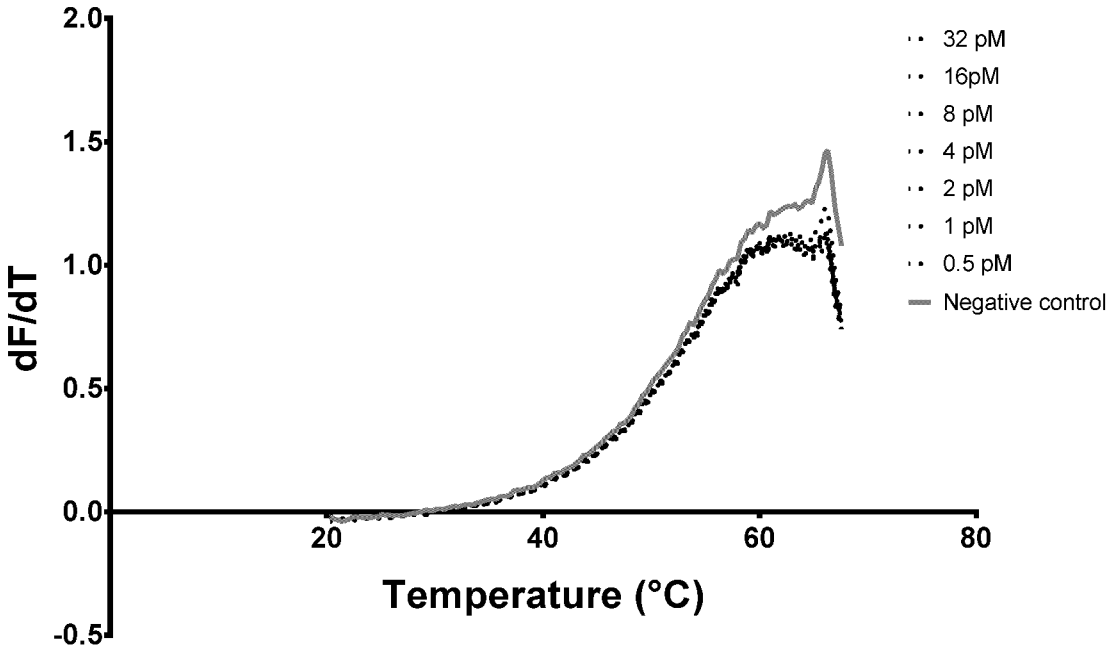
2.0
1.5
1.0
0.5
0.0
-0.5
dF/dT
20
40
60
80
Temperature (°C)
32 pM
16pM
8 pM
4 pM
2 pM
1 pM
0.5 pM
Negative control

Figure 6

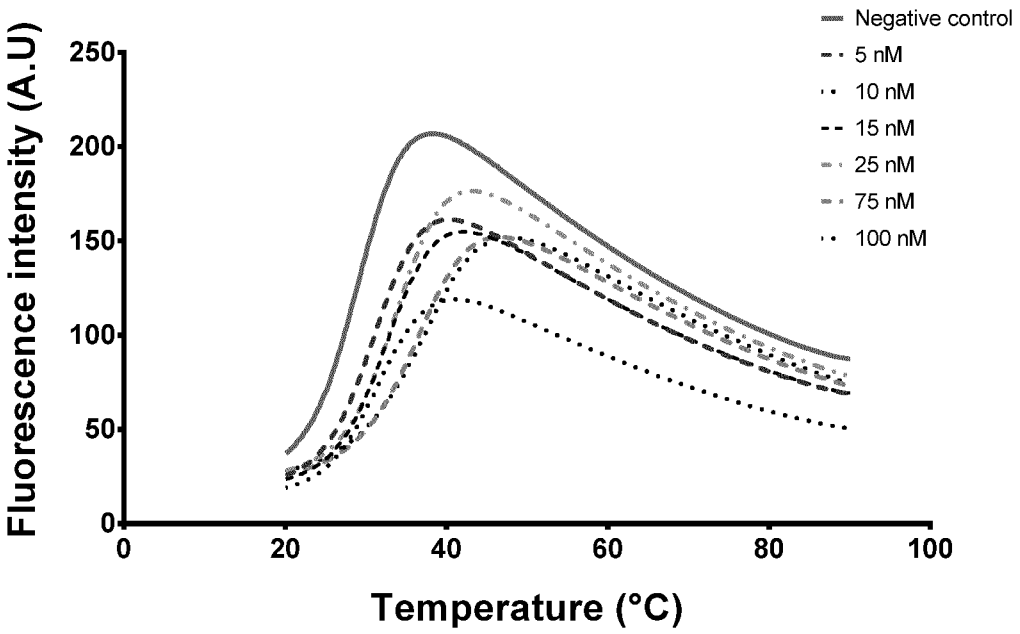
Negative control
5 nM
10 nM
15 nM
25 nM
75 nM
100 nM
Fluorescence intensity (A.U)
250
200
150
100
50
0
0
20
40
60
80
100
Temperature (°C)

Figure 7

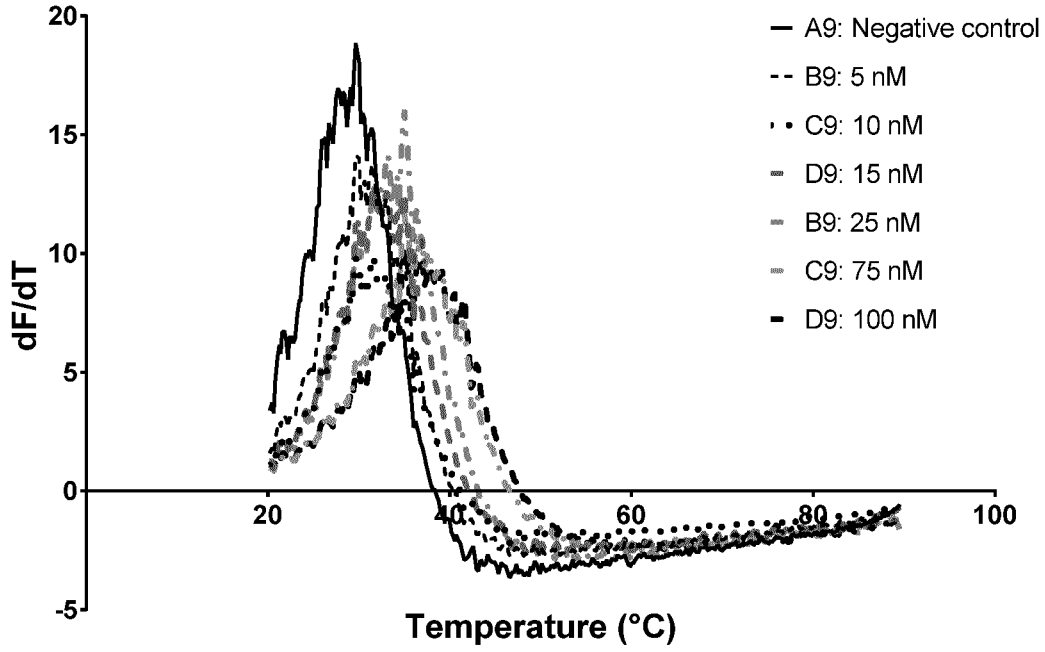
20
15
10
5
0
-5
dF/dT
20
40
60
80
100
Temperature (°C)
A9: Negative control
B9: 5 nM
C9: 10 nM
D9: 15 nM
B9: 25 nM
C9: 75 nM
D9: 100 nM

Figure 8

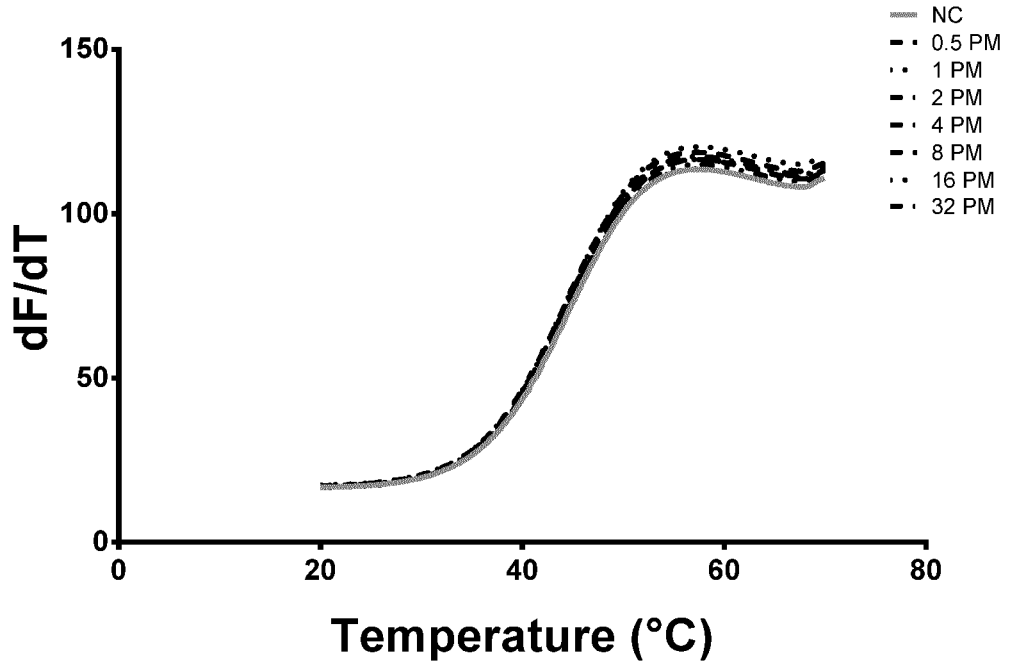
NC
0.5 PM
1 PM
2 PM
4 PM
8 PM
16 PM
32 PM
150
100
50
0
dF/dT
0
20
40
60
80
Temperature (°C)

Figure 9

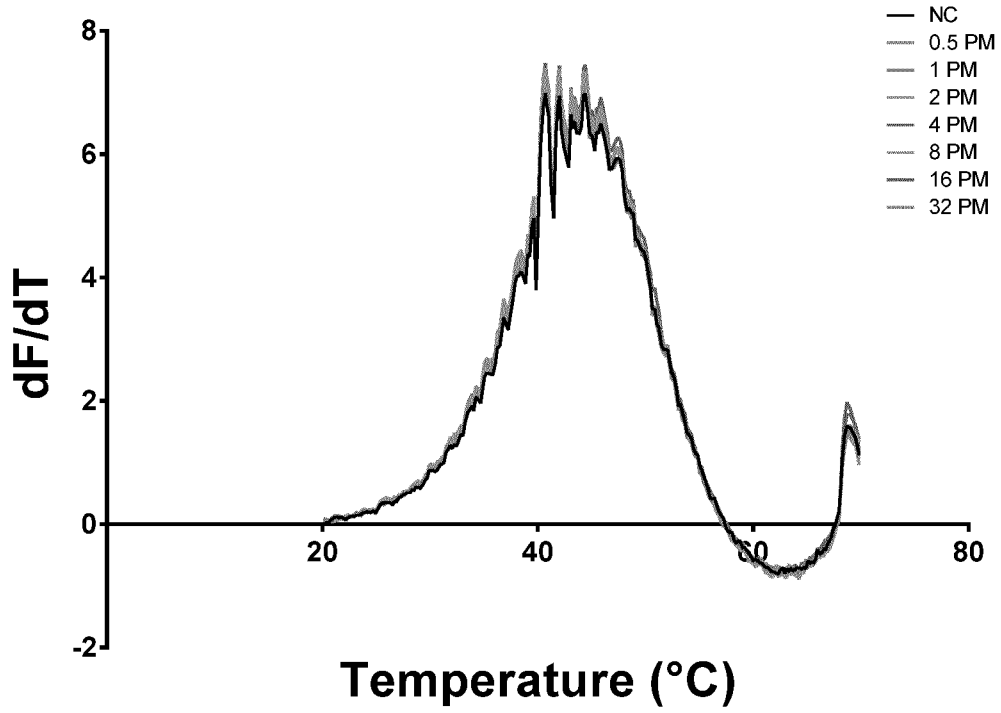
NC
0.5 PM
1 PM
2 PM
4 PM
8 PM
16 PM
32 PM
dF/dT
8
6
4
2
0
-2
20
40
60
80
Temperature (°C)

Figure 10

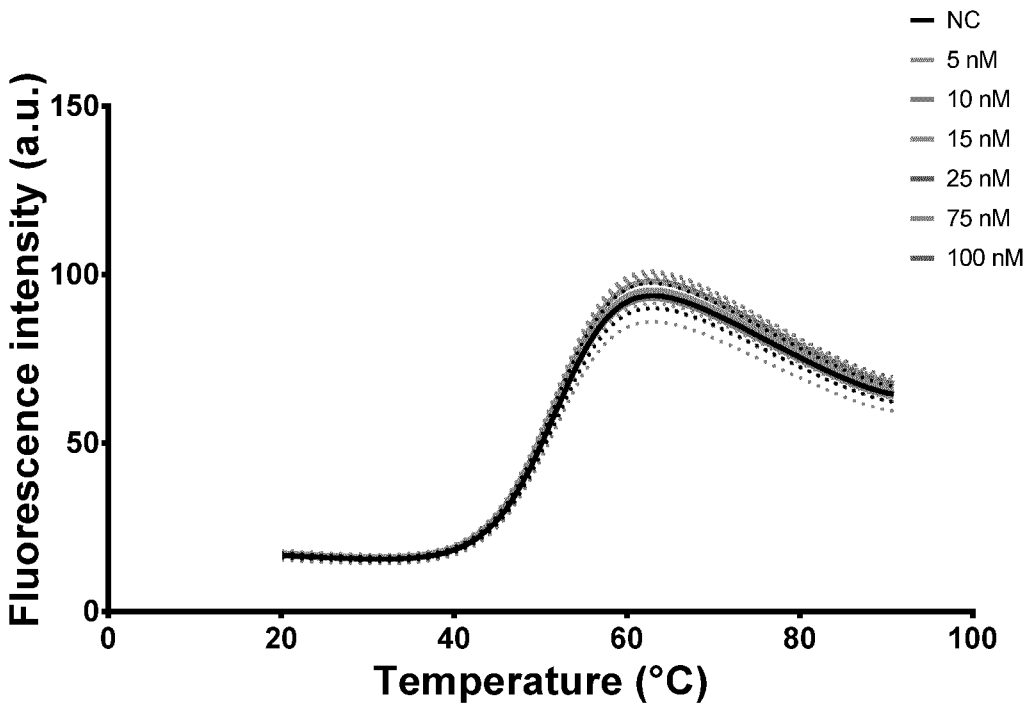
NC
5 nM
10 nM
15 nM
25 nM
75 nM
100 nM
Fluorescence intensity (a.u.)
150
100
50
0
0
20
40
60
80
100
Temperature (°C)

Figure 11

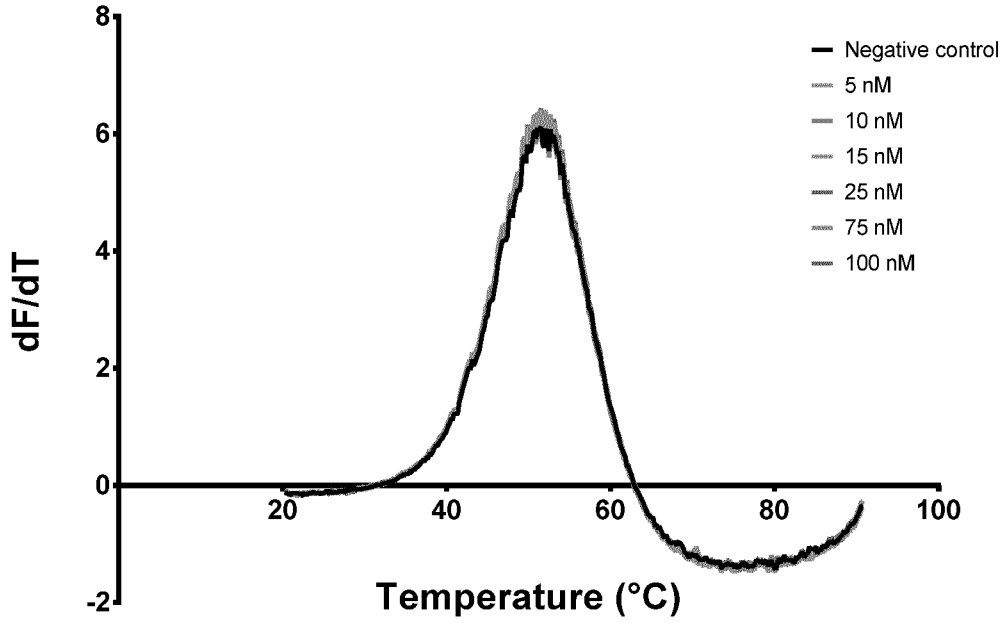
8
6
4
2
0
-2
dF/dT
20
40
60
80
100
Temperature (°C)
Negative control
5 nM
10 nM
15 nM
25 nM
75 nM
100 nM

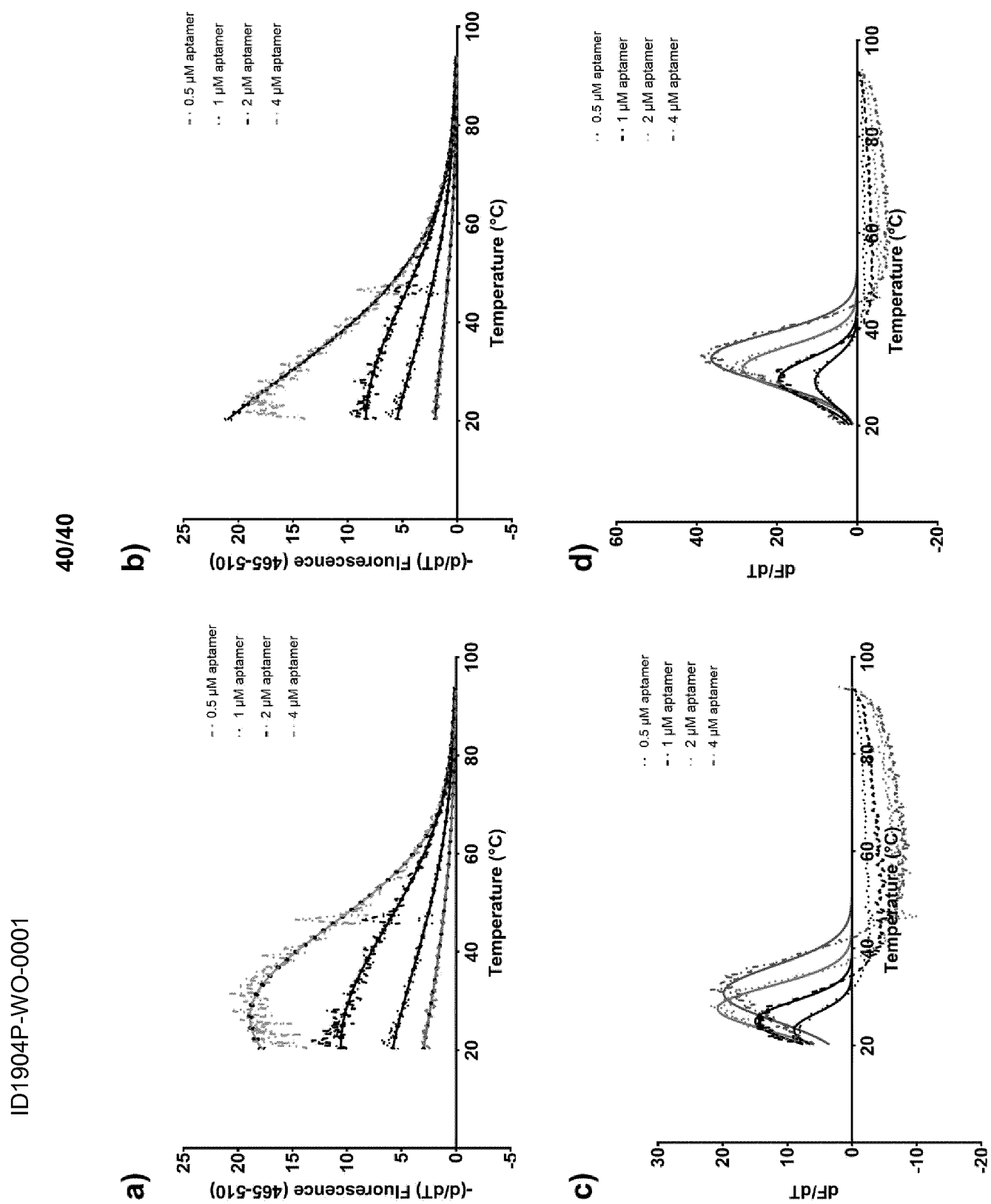
ID1904P-WO-0001
40/40
a)
b)
c)
d)
0.5 µM aptamer
1 µM aptamer
2 µM aptamer
4 µM aptamer
-(d/dT) Fluorescence (465-510)
dF/dT
Temperature (°C)

Figure 12

INTERNATIONAL SEARCH REPORT

International application No
PCT/EP2019/063828

A. CLASSIFICATION OF SUBJECT MATTER
INV. C12Q1/6818 C12N15/115
ADD.

According to International Patent Classification (IPC) or to both national classification and IPC

B. FIELDS SEARCHED

Minimum documentation searched (classification system followed by classification symbols)
C12Q C12N

Documentation searched other than minimum documentation to the extent that such documents are included in the fields searched

Electronic data base consulted during the international search (name of data base and, where practicable, search terms used)
EPO-Internal , WPI Data

C. DOCUMENTS CONSIDERED TO BE RELEVANT

Category*	Citation of document, with indication, where appropriate, of the relevant passages	Relevant to claim No.
X	JUAN HU ET AL: "Homogeneous Assays of Second Messenger Signaling and Hormone Secretion Using Thermofluorimetric Methods That Minimize Calibration Burden", ANALYTICAL CHEMISTRY, vol. 89, no. 16, 25 July 2017 (2017-07-25) , pages 8517-8523, XP055496862, US ISSN: 0003-2700, DOI: 10.1021/acs.analchem.7b02229	1-7,14, 16
Y	the whole document abstract, p. 8518, col. 1, para. 1-2; col. 2, para. 1-2	8-13,15

X	US 2015/140575 A1 (NORDLUND PÄR [SE]) 21 May 2015 (2015-05-21)	1-6, 14-16
Y	the whole document para. 11, 13-14, Examples 6, 7	7-13

	-/--	

[X] Further documents are listed in the continuation of Box C. [3] See patent family annex.

* Special categories of cited documents :

"A" document defining the general state of the art which is not considered to be of particular relevance

"E" earlier application or patent but published on or after the international filing date

"L" document which may throw doubts on priority claim(s) or which is cited to establish the publication date of another citation or other special reason (as specified)

"O" document referring to an oral disclosure, use, exhibition or other means

"P" document published prior to the international filing date but later than the priority date claimed

"T" later document published after the international filing date or priority date and not in conflict with the application but cited to understand the principle or theory underlying the invention

"X" document of particular relevance; the claimed invention cannot be considered novel or cannot be considered to involve an inventive step when the document is taken alone

"Y" document of particular relevance; the claimed invention cannot be considered to involve an inventive step when the document is combined with one or more other such documents, such combination being obvious to a person skilled in the art

"&" document member of the same patent family

Date of the actual completion of the international search	Date of mailing of the international search report
7 June 2019	18/06/2019

Name and mailing address of the ISA/	Authorized officer
European Patent Office, P.B. 5818 Patentlaan 2 NL - 2280 HV Rijswijk Tel. (+31-70) 340-2040, Fax: (+31-70) 340-3016	Sauer, Tincuta

1

Form PCT/ISA/210 (second sheet) (April 2005)

C(Continuation). DOCUMENTS CONSIDERED TO BE RELEVANT

Category*	Citation of document, with indication, where appropriate, of the relevant passages	Relevant to claim No.
X	CN 105 675 678 B (BEIJING AGRICULTURAL QUALITY & STANDARD AND DETECTION TECH RES CENTER) 5 January 2018 (2018-01-05)	12
Y	the whole document SEQ ID NO: 1	1-11, 13-16
Y	NOBUKO HAMAGUCHI ET AL: "Aptamer Beacons for the Direct Detection of Proteins", ANALYTICAL BIOCHEMISTRY, vol. 294, no. 2, 1 July 2001 (2001-07-01), pages 126-131, XP055367428, AMSTERDAM, NL ISSN: 0003-2697, DOI: 10.1006/abio.2001.5169 the whole document abstract, Fig. 1	1-16
Y	US 6 680 377 B1 (STANTON MARTIN [US] ET AL) 20 January 2004 (2004-01-20) the whole document col. 1, l. 64 - col. 2, l. 20	1-16
Y	JUAN HU ET AL: "Quantifying aptamer-protein binding via thermofluorimetric analysis", ANALYTICAL METHODS, vol. 7, no. 17, 1 January 2015 (2015-01-01), pages 7358-7362, XP055496564, GBR ISSN: 1759-9660, DOI: 10.1039/C5AY00837A the whole document abstract, p. 3, first full para.	1-16
Y	TULSI RAM DAMASE ET AL: "Application of the Open qPCR Instrument for the in Vitro Selection of DNA Aptamers against Epidermal Growth Factor Receptor and Drosophila C Virus", ACS COMBINATORIAL SCIENCE, vol. 20, no. 2, 17 January 2018 (2018-01-17), pages 45-54, XP055497006, US ISSN: 2156-8952, DOI: 10.1021/acscombsci.7b00138 the whole document p. 48, col. 1	1-16

1

INTERNATIONAL SEARCH REPORT

Information on patent family members

International application No
PCT/EP2019/063828

Patent document cited in search report	Publication date	Patent family member(s)	Publication date
US 2015140575 A1	21-05-2015	AU 2012246069 A1	31-10-2013
		CA 2833076 A1	26-10-2012
		CN 103733067 A	16-04-2014
		DK 2699910 T3	18-04-2016
		EP 2699910 A1	26-02-2014
		ES 2566637 T3	14-04-2016
		GB 2490404 A	31-10-2012
		HK 1192612 A1	12-05-2017
		JP 6032715 B2	30-11-2016
		JP 2014513293 A	29-05-2014
		KR 20140033366 A	18-03-2014
		SG 194137 A1	29-11-2013
		US 2014057368 A1	27-02-2014
		US 2015140575 A1	21-05-2015
		WO 2012143714 A1	26-10-2012
CN 105675678 B	05-01-2018	NONE	
US 6680377 B1	20-01-2004	US 6680377 B1	20-01-2004
		US 2005100919 A1	12-05-2005
		US 2008020939 A1	24-01-2008

(19) Europäisches Patentamt
European Patent Office
Office européen des brevets

(11) **EP 3 597 775 A1**

(12) **EUROPEAN PATENT APPLICATION**

(43) Date of publication:
22.01.2020 Bulletin 2020/04

(21) Application number: **18184111.5**

(22) Date of filing: **18.07.2018**

(51) Int Cl.:
C12Q 1/6823 *(2018.01)* ***C12Q 1/6825*** *(2018.01)*
C12Q 1/6834 *(2018.01)* ***C12N 15/115*** *(2010.01)*

(84) Designated Contracting States:
AL AT BE BG CH CY CZ DE DK EE ES FI FR GB GR HR HU IE IS IT LI LT LU LV MC MK MT NL NO PL PT RO RS SE SI SK SM TR
Designated Extension States:
BA ME
Designated Validation States:
KH MA MD TN

(71) Applicant: **Hochschule Furtwangen**
78120 Furtwangen im Schwarzwald (DE)

(72) Inventors:
- **Deigner, Hans-Peter**
  68623 Lampertheim (DE)
- **Mahmoud, Mostafa Mohamed Safwat Ahmed**
  78054 Villingen-Schwenningen (DE)

(74) Representative: **Müller-Boré & Partner**
Patentanwälte PartG mbB
Friedenheimer Brücke 21
80639 München (DE)

(54) **METHOD FOR THE DETECTION AND QUANTIFICATION OF SMALL MOLECULES AND FLUIDIC PLATFORM FOR PERFORMING THE SAME**

(57) The present invention relates to methods for the detection and/or quantification of an analyte of interest in a fluid sample, comprising the use of analyte-specific RNA or DNA aptamers and displaceable oligonucleotides that bind to the binding region of said aptamers. The present invention further relates to microfluidic devices that can be used in said methods.

EP 3 597 775 A1

Description

[0001] The present invention relates to methods for the detection and/or quantification of an analyte of interest in a fluid sample, comprising the use of analyte-specific RNA or DNA aptamers and displaceable oligonucleotides that bind to the binding region of said aptamers. The present invention further relates to microfluidic devices that can be used in said methods.

[0002] The detection and quantification of small molecule analytes in fluid samples remains a considerably challenging task that requires bulky and complex instruments as well as well-trained personnel, e.g. in the case of mass spectrometry. Their detection is hampered by the intrinsic properties of small molecule analytes, such as their small size and the availability of only one epitope for binding. Thus, most immunoassays still do not provide fast results and lack the sensitivity required for diagnostics. Moreover, the tedious steps included, e.g. washing, blocking and signal development, hinders the transfer of these assays to Point-of-Care (POC) devices.

[0003] Oligonucleotide aptamers stand out as a promising alternative to antibodies and similar specific proteinaceous binding molecules due to their stability, fast binding kinetics and reversibility of the binding. Aptamers are single stranded DNA or RNA sequences selected *in vitro* for binding to a target analyte, e.g. through a process known as SELEX (Systematic Evolution of Ligands by EXponential Enrichment). The fast binding kinetics and the easy functionalization of aptamers enables the development of non-conventional POC devices.

[0004] Magnetic beads are micro- or nano-sized particles containing iron or iron oxide. Magnetic mono-sized particles provide a large and uniform surface area for attaching functional molecules, such as antibodies, enzymes, DNA or aptamers. This can be achieved through various covalent and non-covalent strategies. The uniqueness of magnetic beads is the exceptionally fast separation of the same in fluid media using external magnetic forces. This allows for a hybrid assay which is fast due to the easy and efficient mixing and allows including washing steps when needed. These properties made magnetic beads suitable for use in various applications, such as cell preparation, immunoassays, bioseparation and targeted drug delivery.

[0005] Lateral flow assays are a class of paper or fiber based POC assays. Lateral flow immunoassays (LFIA) are simple, fast and can provide reliable results within a few minutes. Thus, lateral flow assays (LFA) or similar fluidic assays provide a rapid and cost-effective means to detect targets *in situ.* However, producing these type of test strips requires immobilization of antibodies or antigens on the surface of the test strips which can affect the conformation and stability of the reagents. Further, the commonly used sandwich or competitive formats are unsuitable for the detection of small molecules. This is due to the small size of the target molecules, hindering the efficient labeling for a competitive assay and the unavailability of two different binding epitopes required for sandwich assays.

[0006] Recently, a LFA system for small molecules based on adsorption and desorption on gold nanoparticles has been described. This assay made use of the fact that single stranded DNA adsorbs onto the surface of gold nanoparticles and when the target analyte is introduced, this ssDNA binds to it and desorbs from the surface. However, this assay, as well as other assay systems known in the art, is based on complex detection techniques and methodology.

[0007] Thus, there is a need to provide fast, easy, accurate and sensitive assay systems for the detection and quantification of small molecule analytes. These systems should not require the immobilization of proteins or any of the assay components, allow for easy detection by both visual and instrumental means, allow for regeneration of the assay components, and provide means for the detection and quantification of multiple different target analytes.

[0008] Therefore, the technical problem underlying the present invention is the provision of respective methods and devices for the detection and quantification of small molecule analytes.

[0009] The solution to the above technical problem is achieved by the embodiments characterized in the claims.

[0010] In particular, in a first aspect, the present invention relates to a method for the detection and/or quantification of an analyte of interest in a fluid sample, comprising the steps of:

(a) providing a fluid sample in a reaction vessel, wherein said fluid sample is to be analyzed for the presence and/or quantity of the analyte of interest;
(b) adding to said sample in said reaction vessel, either subsequently in any order, or concurrently,

(i) an RNA or DNA aptamer, and
(ii) an oligonucleotide,

wherein
said RNA or DNA aptamer is coupled to a magnetic bead and said oligonucleotide is coupled to a detectable marker; or said RNA or DNA aptamer is coupled to a detectable marker and said oligonucleotide is coupled to a magnetic bead,
said RNA or DNA aptamer comprises a binding region that is capable of binding the analyte of interest with a first affinity, and
said oligonucleotide comprises a nucleotide sequence that is complementary to a nucleotide sequence of said RNA

or DNA aptamer that forms at least a part of the aptamer's binding region, wherein said nucleotide sequences bind to each other via Watson-Crick pairing with a second affinity, wherein said second affinity is lower than said first affinity;
(c) subjecting the reaction vessel to a magnetic field, so that said magnetic bead-coupled RNA or DNA aptamers or magnetic bead-coupled oligonucleotides are sequestered to an inner surface of the reaction vessel;
(d) detecting the presence or absence and/or determining the amount of the detectable marker in the sample supernatant; and
(e) determining the presence or absence and/or the amount of the analyte of interest in the sample, wherein
the presence of detectable marker in the sample supernatant indicates that the RNA or DNA aptamer has bound the analyte of interest, so that the oligonucleotide has been displaced by the analyte of interest from the RNA or DNA aptamer or has been prevented from binding to the same, the magnetic bead-coupled RNA or DNA aptamer or the magnetic bead-coupled oligonucleotide has been sequestered to an inner surface of the reaction vessel, and the detectable maker-coupled oligonucleotide or the detectable maker-coupled RNA or DNA aptamer remains in the sample supernatant, thus indicating the presence of the analyte of interest in the sample, and
the amount of detectable marker in the sample supernatant positively correlates with the amount of the analyte of interest in the sample.

[0011] As used herein, the term "detection" with regard to the analyte of interest relates to the mere determination of whether said analyte of interest is present or absent in the sample, whereas the term "quantification" with regard to said analyte relates to the determination of the actual amount of analyte in the sample.

[0012] The analyte of interest to be detected and/or quantified with the methods of the present invention is not particularly limited in any way, provided that it is an analyte for which an RNA or DNA aptamer binding specifically to it can be generated. Considering the fact that such aptamers can be generated for a wide range of targets, including small molecules, proteins, nucleic acids, and even cells, tissues and organisms, this does not constitute a significant restriction. In preferred embodiments, the analyte of interest is a small molecule, e.g. a low molecular weight organic compound, e.g. having a molecular weight of below about 900 Da. In further embodiments, the target analyte is a small molecule analyte selected from the group consisting of drugs, metabolites, toxins, environmental pollutants, and food contaminants, including target analytes of clinical and non-clinical relevance. In this context, the terms "analyte of interest", "target analyte" or simply "target" are used synonymously herein.

[0013] The fluid sample to be used in the present invention is not particularly limited. Suitable samples can be diluted or undiluted samples that are natively fluid, e.g. blood, blood serum, blood plasma, urine, cerebrospinal fluid, saliva, semen, environmental samples such as water samples, and fluid comestibles. Further, suitable samples can also derive from non-fluid samples that have been dissolved in a suitable solvent to bring them into a fluid state. Respective non-fluid sample materials include e.g. fecal matter, environmental samples such as soil samples, and solid comestibles. Suitable diluents and solvents are not particularly limited and are known in the art, wherein aqueous diluents and solvents, in particular water, are preferred.

[0014] In step (a) of the methods of the present invention, a fluid sample that is to be analyzed for the presence and/or quantity of the analyte of interest is provided in a reaction vessel. Suitable reaction vessels are not particularly limited, and include e.g. standard micro reaction tubes ("Eppendorf" tubes), microtiter plates, and the like.

[0015] In a specific embodiment, the reaction vessel is a microfluidic device, preferably a microfluidic device comprising:

(i) a fluid inlet and a fluid outlet,
(ii) a sequestering zone between the inlet and the outlet that is to be subjected to the magnetic field in step (c),
(iii) a detection zone between the sequestering zone and the outlet, comprising an absorbing pad, wherein step (d) is performed in said detection zone, and
(iv) microfluidic channels placing the inlet and the sequestering zone, the sequestering zone and the detection zone, and the detection zone and the outlet in fluid communication.

[0016] In embodiments using a respective microfluidic device, fluid flow from the fluid inlet towards the fluid outlet can be either controlled actively, e.g. by using respective pumps known in the art, or passively using capillary forces.

[0017] In preferred embodiments, the microfluidic device used in the methods of the present invention is the microfluidic device according to the second aspect of the present invention as defined hereinafter.

[0018] In step (b) of the methods of the present invention, an RNA or DNA aptamer and an oligonucleotide are added to the sample in the reaction vessel either subsequently, in any order, or concurrently, *i.e.,* either the RNA or DNA aptamer is added first, and then the oligonucleotide, the oligonucleotide is added first, and then the RNA or DNA aptamer, or both the RNA or DNA aptamer and the oligonucleotide are added concurrently. In specific embodiments, the RNA or DNA aptamer and the oligonucleotide are combined with each other, optionally incubated with each other for a brief time, and then concurrently added to the sample in the reaction vessel.

[0019] According to the present invention, one of the RNA or DNA aptamer and the oligonucleotide is coupled to a

magnetic bead, and the other is coupled to the detectable marker, *i.e.,* said RNA or DNA aptamer is coupled to a magnetic bead and said oligonucleotide is coupled to a detectable marker; or said RNA or DNA aptamer is coupled to a detectable marker and said oligonucleotide is coupled to a magnetic bead. In preferred embodiments, the RNA or DNA aptamer is coupled to a magnetic bead and the oligonucleotide is coupled to a detectable marker. Methods of coupling aptamers and oligonucleotides to magnetic beads or detectable markers are not particularly limited and are known in the art. Coupling includes direct coupling, *i.e.,* forming a covalent or non-covalent (e.g. ionic, van der Waals or hydrogen) bond between the coupling partners, or indirect coupling via the use of binding systems known in the art, e.g. the biotin-streptavidin system. In specific embodiments, the RNA or DNA aptamers and oligonucleotides employed in the present invention are biotinylated, e.g. in the 3' position, and the magnetic beads and detectable markers are coated with streptavidin, thus facilitating binding of the former to the latter.

[0020] Further, said RNA or DNA aptamer comprises a binding region that is capable of binding the analyte of interest with a first affinity, and said oligonucleotide comprises a nucleotide sequence that is complementary to a nucleotide sequence of said RNA or DNA aptamer that forms at least a part of the aptamer's binding region, wherein said nucleotide sequences bind to each other via Watson-Crick pairing with a second affinity, wherein said second affinity is lower than said first affinity. In this context, it should be noted that binding affinities of RNA or DNA aptamers to their binding partner are generally much larger than the Watson-Crick binding affinities of short oligonucleotide stretches to each other, so that the latter prerequisite is generally easily fulfilled. Methods of generating RNA or DNA aptamers binding to a desired analyte of interest are not particularly limited and are known in the art. They include the SELEX method known in the art. Further, the generation of oligonucleotides that comprise a nucleotide sequence that is complementary to a nucleotide sequence of said RNA or DNA aptamer that forms at least a part of the aptamer's binding region is known in the art. In preferred embodiments, the oligonucleotide is a DNA oligonucleotide.

[0021] Detectable markers that can be used in the methods of the present invention are not particularly limited and are known in the art. They include e.g. fluorophores, colored particles such as e.g. dyed microbeads, quantum dots, and chromogenic enzymes that catalyze a color reaction, such as e.g. horseradish peroxidase. In preferred embodiments, the detectable marker is a marker advantageously allowing visual detection, e.g. by the naked eye, such as e.g. dyed microbeads.

[0022] The oligonucleotide's nucleotide sequence that is complementary to a nucleotide sequence of the RNA or DNA aptamer that forms at least a part of the aptamer's binding region has preferably a length of 5 to 15, more preferably 6 to 14, 7 to 13, 8 to 12, or 9 to 11 nucleotides, most preferably of about 10 nucleotides. In specific embodiments, the oligonucleotide consists entirely of this nucleotide sequence, *i.e.,* the oligonucleotide has a length of 5 to 15, more preferably 6 to 14, 7 to 13, 8 to 12, or 9 to 11 nucleotides, most preferably of about 10 nucleotides. In this context, said length can vary depending on the used aptamer and the affinity to the target. Further, said length can be easily optimized to achieve the condition that the above second affinity is lower than the above first affinity. This can include by varying the above length and/or including nucleotide mismatches Methods to determine the respective binding strengths are known in the art and include e.g. the use of common DNA thermodynamics analysis in order to determine the affinity of the complementary oligonucleotide to the aptamer and optimize it.

[0023] Further, the part of the DNA or RNA aptamer's binding region to which the oligonucleotide is complementary preferably has a length of 3 to 20, more preferably 3 to 17, 4 to 16, 5 to 15, 6 to 14, 7 to 13, 8 to 12, or 9 to 11 nucleotides, most preferably of about 10 nucleotides.

[0024] In step (c) of the methods of the present invention, the reaction vessel is subjected to a magnetic field, e.g. by placing the reaction vessel in direct contact with a magnet or by placing the reaction vessel in the vicinity of a magnet, so that the magnetic bead-coupled moiety, i.e. the magnetic bead-coupled RNA or DNA aptamers or the magnetic bead-coupled oligonucleotides are sequestered to an inner surface of the reaction vessel.

[0025] In this manner, in case the analyte of interest is not present in the sample, the entire complex of magnetic bead-coupled moiety and detectable marker-coupled moiety, bound to each other via Watson-Crick pairing of the oligonucleotide to the RNA or DNA aptamer, is sequestered to the inner surface of the reaction vessel, so that no detectable marker remains in the sample supernatant. However, in case the analyte of interest is present in the sample, the analyte displaces the oligonucleotide from the aptamer, or the analyte prevents the oligonucleotide from binding to the aptamer in the first place, due to the higher binding affinity of analyte to aptamer as compared to the affinity of Watson-Crick pairing of oligonucleotide to aptamer, so that the magnetic bead-coupled moiety, *i.e.,* either magnetic bead-coupled aptamer with bound analyte or magnetic bead-coupled oligonucleotide, is sequestered to the inner surface of the reaction vessel, whereas the detectable marker-coupled moiety, *i.e.,* the detectable marker-coupled oligonucleotide or the detectable maker-coupled aptamer with bound analyte, remain in the sample supernatant and can be detected therein. In this context, the term "sample supernatant" refers to the fluid material in the reaction vessel from which the magnetic bead-coupled moieties have been removed by sequestering the same to an inner surface of the reaction vessel.

[0026] In step (d) of the methods of the present invention, the presence or absence of the detectable marker in the sample supernatant is detected and/or the amount of the detectable marker in the sample supernatant is determined. Means for detecting a given detectable marker are not particularly limited and are known in the art. They include any

suitable visual or instrumental means. In specific embodiments, the detectable marker is a dyed microbead, advantageously allowing visual detection of the marker in the sample supernatant, e.g. by the naked eye. In case the detectable marker is a chromogenic enzyme catalyzing a color reaction, step (d) of the methods of the present invention encompasses the addition of a suitable substrate, such as e.g. 3,3',5,5'-tetramethylbenzidin or o-phenylenediamine dihydrochloride in the case of horseradish peroxidase. Further, means for determining the amount of detectable marker in the sample supernatant for a given marker are not particularly limited and are known in the art. They include e.g. photometric (absorbance) measurements and the use of calibration curves using known amounts of analyte, the detection of light emission of fluorophores as detectable marker, as well as other suitable instrumental means known in the art.

[0027] In step (e) of the methods of the present invention, the presence or absence of the analyte of interest and/or the amount of the analyte of interest in the sample are determined, wherein the presence of detectable marker in the sample supernatant indicates that the RNA or DNA aptamer has bound the analyte of interest, so that the oligonucleotide has been displaced by the analyte of interest from the RNA or DNA aptamer or has been prevented from binding to the same, the magnetic bead-coupled RNA or DNA aptamer or the magnetic bead-coupled oligonucleotide has been sequestered to an inner surface of the reaction vessel, and the detectable maker-coupled oligonucleotide or the detectable maker-coupled RNA or DNA aptamer remains in the sample supernatant, thus indicating the presence of the analyte of interest in the sample. Further, the amount of detectable marker in the sample supernatant positively correlates with the amount of the analyte of interest in the sample.

[0028] So far herein, the methods of the present invention have been described for the detection of one analyte of interest, using one pair of RNA or DNA aptamer and oligonucleotide (oligonucleotide/aptamer pair). However, in specific embodiments, the methods of the present invention can be used for the concurrent detection and/or quantification of more than one analyte of interest in the fluid sample. In these embodiments, step (b) of the methods of the present invention comprises the addition of one oligonucleotide/aptamer pair for each analyte of interest, wherein the detectable markers of each oligonucleotide/aptamer pair can be distinguished from each other, step (d) of the methods of the present invention comprises the detection of the presence or absence and/or the determination of the amount of each detectable marker, and step (e) of the methods of the present invention comprises determining the presence or absence and/or the amount of each analyte of interest in the sample.

[0029] Means for the detection and/or quantification of more than one detectable markers in the sample supernatant are not particularly limited and are known in the art. They include e.g. photometric (absorbance) measurements at different wavelengths, the detection of light emission of different fluorophores as detectable marker as well as any other suitable instrumental means known in the art. Further, also visual detection of e.g. different dyed microbeads can be used in this respect, provided that these differ in a further characteristic allowing separation of different dyed microbeads from each other. This characteristic may be the size of the microbeads, allowing for embodiments including the separation of different sized microbeads, e.g. in the devices of the present invention. Respective separation methods are not particularly limited and are known in the art.

[0030] The methods of the present invention are preferably *in vitro* methods, *i.e.*, they are not performed on the human or animal body.

[0031] In a second aspect, the present invention relates to a microfluidic device, comprising

(i) a fluid inlet and a fluid outlet,
(ii) a sequestering zone between the inlet and the outlet that is to be subjected to the magnetic field in step (c),
(iii) a detection zone between the sequestering zone and the outlet, comprising an absorbing pad, wherein step (d) is performed in said detection zone, and
(iv) microfluidic channels placing the inlet and the sequestering zone, the sequestering zone and the detection zone, and the detection zone and the outlet in fluid communication.

[0032] The sequestering zone and the detection zone of the microfluidic device of the present invention are preferably fluid reservoirs formed within the device. Further, materials for forming the absorbing pad in the detection zone are not particularly limited and are known in the art. They include e.g. cellulose.

[0033] Fluid flow from the fluid inlet towards the fluid outlet can be either controlled actively, e.g. by using respective pumps known in the art, or passively using capillary forces.

[0034] The term "about" as used herein refers to a modification of the specified amount of ± 10%, preferably ± 5, 3, 2, or 1%. By way of example, the term "about 900 Da" can refer to a molecular weight of 810 to 990 Da, and the term "about 10" can refer to a range of 9 to 11.

[0035] The term "comprise(s)/comprising" as used herein is expressly intended to encompass the terms "consist(s)/consisting essentially of" and "consist(s)/consisting of".

[0036] The present invention provides an assay system based on strand displacement and a combination of magnetic and dyed microbeads. This system mimics a lateral flow system, however, there is no need to immobilize the reagents on a test strip or cassette and the assay allows for a combination of different detectable markers for multiplexing. In

contrast to most competitive assays known in the art, wherein the signal is inversely related to the concentration of the target, in the methods of the present inveniton, the signal intensity in the sample supernatant is positively correlated with the amount of target analyte.

[0037] The aim of the present invention was the development of a fast quantitive assay for small molecules such as drugs, metabolites, toxins and environmental pollutants. This assay is also able to work with minimum equipment or none equipment at all, and allows non-trained personnel and home users to use it through visual detection. Thus, it will have a great potential for various applications, such as e.g. the detection and quantification of drugs of abuse or intoxication, environmental or food contaminants and clinical applications in a simple POC format.

[0038] The principle of the assay of the present invention is making use of strand displacement, where an aptamer specific for a certain target analyte is used in combination with a complementary strand. This complementary strand competes with the target and thus can be used for quantification.

[0039] The assay principle is shown in detail in Figure 1. The detection molecule here is a blue micro bead that allows the quantification either visually or by measuring the absorbance. However, the assay is very flexible and can make use of other detection molecules such as quantum dots. This allows for easy multiplexing. The assay of the present invention can be used in connection with a microfluidic device (Figure 2) and combined with a POC detector for quantification. The parameters of such device and its design are adapted and optimized in such a way that no user interference is necessary.

[0040] In comparison to methods known in the art, the methods of the present invention do not require the immobilization of proteins or any of the assay components on e.g. a test strip. Moreover, the detection can be both visual and instrumental through measuring absorbance. The assay components can be regenerated, e.g. the sensor magnetic beads and the fluidic device after washing. The principle of the present invention allows for multiplexing through changing the label to e.g. quantum dots or similar or even using colored particles with different absorbance wavelength. The assay kinetics and flow speeds can be adapted through active fluidic control (pump) allowing faster results.

[0041] The figures show:

Figure 1:
Schematic illustration of one embodiment of the assay of the present invention. (A) represents the reaction in absence of the target molecules. The complementarity between the aptamer and the complementary strand leads to a clear solution when the beads are magnetically separated. (B) Upon addition of the target analyte, the complementary strand is displaced from the aptamer or is prevented from binding to the aptamer in the first place, leading to a concentration-dependent increase in the blue color of the solution.

Figure 2:
Schematic representation of the microfluidic device of the present invention. (A) represents the assay in presence of target analyte, the brown rectangle represents a permanent magnet to be placed below the device where the other rectangle is a cellulose or similar absorbing pad to be placed within the device. (B) represents the negative assay in absence of the target analyte. The flow could be either controlled actively (pumps) or passively using capillarity or similar means.

Figure 3:
The figure shows a control experiment to exclude non-specific adsorption. The right Eppendorf tube shows a negative control where the beads were functionalized by non-complementary oligonucleotides whereas the left one had an ethanolamine aptamer and its corresponding complementary strand. As seen in the right Eppendorf tube, the beads did not attach to each other and the solution remained blue. On the other hand, the complementarity between the aptamer and the short strand lead to the attachment of the beads together and the solution is clear.

Figure 4:
The assay of the present invention performed in Eppendorf tubes, wherein the right tube is the negative control (no target), the middle is 10 nM of ethanolamine (610 picograms/ml), and the left is 100 nM (6 ng/ml). The color intensity between the negative and positive assays could be clearly distinguished by the naked eye.

Figure 5:
Calibration curve for the absorbance of blue beads measured at a wavelength of 600 nm. The absorbance is plotted against the concentration and the line represents the best fitting line (r^2 =0.99). The error bars represent the standard deviation, n=3.

[0042] The present invention will be further illustrated by the following example without being limited thereto.

Example

Material

[0043] Aptamers and oligonucleotides were purchased from Integrated DNA Technology (Coralville, IA).

Name	Ethanolamine aptamer
Sequence	ATTCAATTTGAGGCGGGTGGGTGGGTTGAAT/3Bio/ (SEQ ID NO: 1)
5' Modification	none
3' Modification	Biotin
Supplier	Integrated DNA Technology (Coralville, IA)
Concentration	100 μM
Molecular weight	101 kDa

Name	Et 10_3 (complementary strand)
Sequence	CCACCCACCC/3Bio/ (SEQ ID NO: 2)
5' Modification	none
3' Modification	Biotin
Supplier	Integrated DNA Technology (Coralville, IA)
Concentration	100 μM
Molecular weight	33 kDa

[0044] The microparticles were supplied by Bangs Labs Inc., Indiana, USA as follows:

Name	Streptavidin Coated Magnetic Classical
Mean diameter	0.36 μm
Binding capacity	1.24 μM biotin/mg microspheres
Concentration	10 mg/ml

Name	Streptavidin Coated Microspheres (Cabo Blue)
Mean diameter	0.192 μm
Binding capacity	2.55 μM biotin/mg microspheres
Concentration	10 mg/ml

[0045] All other chemicals used herein were purchased from standard suppliers and used without further purification.
[0046] The functionalization of the beads was done according to the manufacturer's instructions.

Example:

[0047] First, streptavidin-coated beads were reacted with the corresponding biotinylated oligonucleotide, wherein the magnetic beads were functionalized with the ethanolamine aptamer and the blue beads with the complementary strand.
[0048] The aptamer was selected and optimized as known in the art. The respective aptamer is well characterized and is specific for ethanolamine which is a very small organic molecule (Mw = 61.08 g/mol) and represent one of the smallest aptamer targets so far which makes it a very suitable model to prove the feasibility of the concept underlying

the present invention.

[0049] To prove the success of the reaction and to exclude any non-specific adsorption, a negative control with the same exact beads and handling procedures was made. However, the beads were functionalized with non-complementary sequences and therefore should lack the ability to bind each other.

[0050] As shown in Figure 3, the beads were successfully functionalized and the non-specific adsorption was minimal. The results also revealed that the volume should be decreased in order to increase the color intensity.

[0051] Therefore, in order to develop the sensor, the functionalized magnetic beads and blue beads were allowed first to react together. Then, the supernatant was discarded to leave a magnetic beads-blue beads sensor. Then this was reacted with the target (50 μL) at 100 nM and 10 nM of ethanolamine.

[0052] As shown in Figure 4, the 10 nM concentration lead to a visual color change in comparison to the control. With this setup, 10 nM of ethanolamine which corresponds to a concentration of 610 picograms/ml could be detected.

[0053] Further, an absorption calibration curve for the blue beads was established (Figure 5). This means that the reaction could also be quantified through the use of a conventional absorbance detector.

SEQUENCE LISTING

<110> Hochschule Furtwangen

<120> Method for the Detection and Quantification of Small Molecules and Fluidic Platform for Performing the Same

<130> F 2335EU

<160> 2

<170> PatentIn version 3.5

<210> 1
<211> 31
<212> DNA
<213> Artificial sequence

<220>
<223> DNA aptamer

<220>
<221> misc_feature
<222> (31)..(31)
<223> 3' biotinylated

<400> 1
attcaatttg aggcgggtgg gtgggttgaa t 31

<210> 2
<211> 10
<212> DNA
<213> Artificial sequence

<220>
<223> complementary sequence

<220>
<221> misc_feature
<222> (10)..(10)
<223> 3' biotinylated

<400> 2
ccacccaccc 10

SEQUENCE LISTING

<110> Hochschule Furtwangen

<120> Method for the Detection and Quantification of Small Molecules and Fluidic Platform for Performing the Same

<130> F 2335EU

<160> 2

<170> PatentIn version 3.5

<210> 1
<211> 31
<212> DNA
<213> Artificial sequence

<220>
<223> DNA aptamer

<220>
<221> misc_feature
<222> (31)..(31)
<223> 3′ biotinylated

<400> 1
attcaatttg aggcgggtgg gtgggttgaa t 31

<210> 2
<211> 10
<212> DNA
<213> Artificial sequence

<220>
<223> complementary sequence

<220>
<221> misc_feature
<222> (10)..(10)
<223> 3′ biotinylated

<400> 2
ccacccaccc 10

Claims

1. A method for the detection and/or quantification of an analyte of interest in a fluid sample, comprising the steps of:

(a) providing a fluid sample in a reaction vessel, wherein said fluid sample is to be analyzed for the presence and/or quantity of the analyte of interest;
(b) adding to said sample in said reaction vessel, either subsequently in any order, or concurrently,

(i) an RNA or DNA aptamer, and
(ii) an oligonucleotide,

wherein
said RNA or DNA aptamer is coupled to a magnetic bead and said oligonucleotide is coupled to a detectable marker; or said RNA or DNA aptamer is coupled to a detectable marker and said oligonucleotide is coupled to a magnetic bead,
said RNA or DNA aptamer comprises a binding region that is capable of binding the analyte of interest with a first affinity, and
said oligonucleotide comprises a nucleotide sequence that is complementary to a nucleotide sequence of said RNA or DNA aptamer that forms at least a part of the aptamer's binding region, wherein said nucleotide sequences bind to each other via Watson-Crick pairing with a second affinity,
wherein said second affinity is lower than said first affinity;
(c) subjecting the reaction vessel to a magnetic field, so that said magnetic bead-coupled RNA or DNA aptamers or magnetic bead-coupled oligonucleotides are sequestered to an inner surface of the reaction vessel;
(d) detecting the presence or absence and/or determining the amount of the detectable marker in the sample supernatant; and
(e) determining the presence or absence and/or the amount of the analyte of interest in the sample, wherein the presence of detectable marker in the sample supernatant indicates that the RNA or DNA aptamer has bound the analyte of interest, so that the oligonucleotide has been displaced by the analyte of interest from the RNA or DNA aptamer or has been prevented from binding to the same, the magnetic bead-coupled RNA or DNA aptamer or the magnetic bead-coupled oligonucleotide has been sequestered to an inner surface of the reaction vessel, and the detectable maker-coupled oligonucleotide or the detectable maker-coupled RNA or DNA aptamer remains in the sample supernatant, thus indicating the presence of the analyte of interest in the sample, and the amount of detectable marker in the sample supernatant positively correlates with the amount of the analyte of interest in the sample.

2. The method of claim 1, wherein the analyte of interest is a small molecule analyte.

3. The method of claim 2, wherein the small molecule analyte is selected from the group consisting of drugs, metabolites, toxins, environmental pollutants, and food contaminants.

4. The method of any one of claims 1 to 3, wherein the fluid sample is selected from the group consisting of diluted or undiluted samples, selected from the group consisting of blood, blood serum, blood plasma, urine, cerebrospinal fluid, saliva, semen, environmental samples, and fluid comestibles, and dissolved non-fluid sample materials, selected from the group consisting of fecal matter, environmental samples, and solid comestibles.

5. The method of any one of claims 1 to 4, wherein the oligonucleotide is a DNA oligonucleotide.

6. The method of any one of claims 1 to 5, wherein the detectable marker is selected from the group consisting of fluorophores, colored particles, dyed microbeads, quantum dots, chromogenic enzymes, and quantum dots.

7. The method of any one of claims 1 to 6, wherein the oligonucleotide's nucleotide sequence that is complementary to a nucleotide sequence of said RNA or DNA aptamer that forms at least a part of the aptamer's binding region has a length of 5 to 15 nucleotides.

8. The method of any one of claims 1 to 7, wherein the part of the DNA or RNA aptamer's binding region to which the oligonucleotide is complementary has a length of 3 to 20 nucleotides.

9. The method of any one of claims 1 to 8, wherein the reaction vessel is a microfluidic device, said device comprising:

(i) a fluid inlet and a fluid outlet,
(ii) a sequestering zone between the inlet and the outlet that is to be subjected to the magnetic field in step (c),
(iii) a detection zone between the sequestering zone and the outlet, comprising an absorbing pad, wherein step (d) is performed in said detection zone, and
(iv) microfluidic channels placing the inlet and the sequestering zone, the sequestering zone and the detection zone, and the detection zone and the outlet in fluid communication.

10. The method of any one of claims 1 to 9, wherein more than one analyte of interest is detected and/or quantified in the fluid sample, wherein
step (b) comprises the addition of one oligonucleotide/aptamer pair for each analyte of interest, wherein the detectable

markers of each oligonucleotide/aptamer pair can be distinguished from each other,
step (d) comprises the detection of the presence or absence and/or the determination of the amount of each detectable marker, and
step (e) comprises determining the presence or absence and/or the amount of each analyte of interest in the sample.

11. The method of any one of claims 1 to 10, wherein said RNA or DNA aptamer is coupled to a magnetic bead and said oligonucleotide is coupled to a detectable marker.

12. A microfluidic device, comprising

(i) a fluid inlet and a fluid outlet,
(ii) a sequestering zone between the inlet and the outlet that is to be subjected to the magnetic field in step (c),
(iii) a detection zone between the sequestering zone and the outlet, comprising an absorbing pad, wherein step (d) is performed in said detection zone, and
(iv) microfluidic channels placing the inlet and the sequestering zone, the sequestering zone and the detection zone, and the detection zone and the outlet in fluid communication.

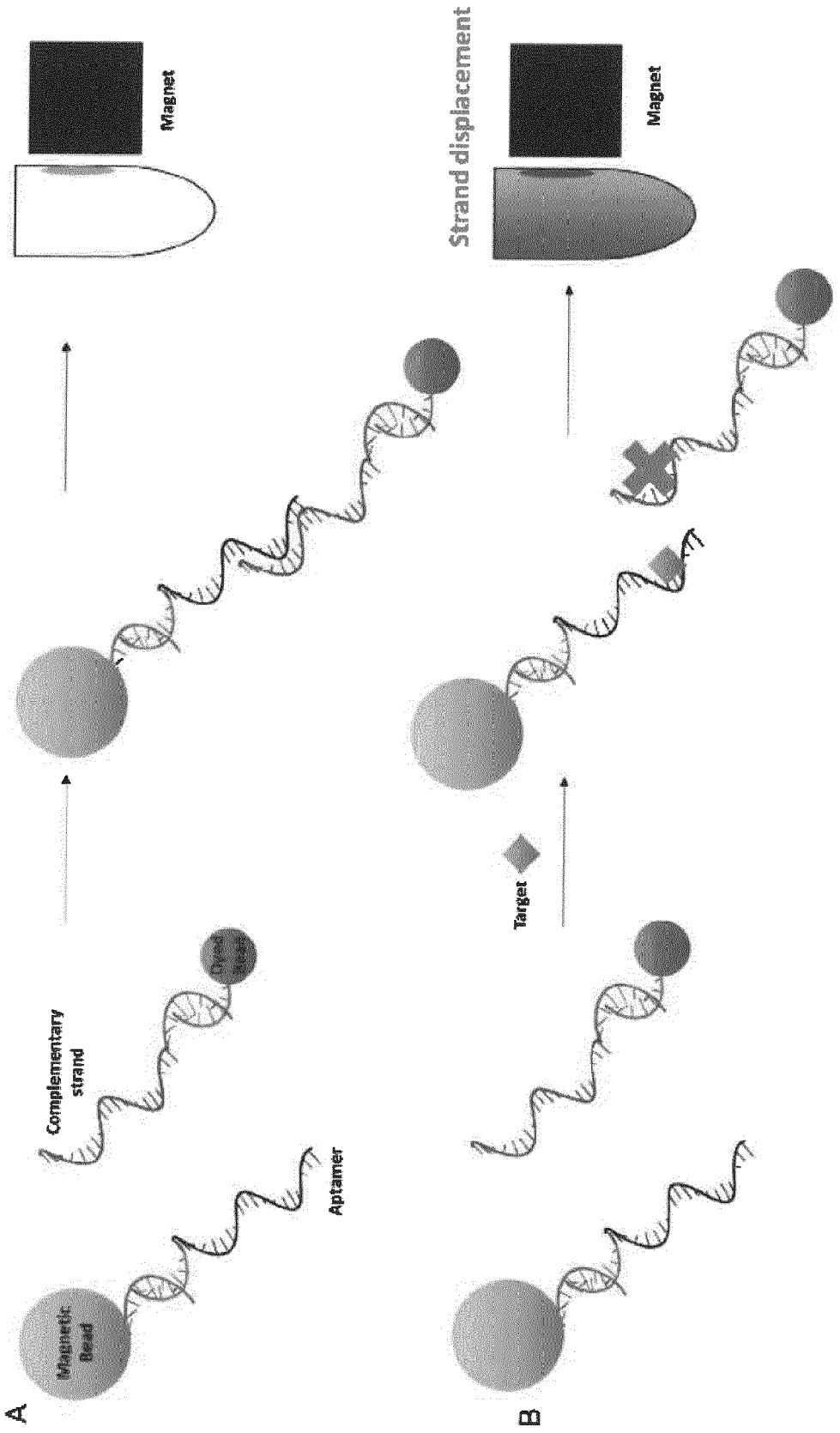
Magnet
Strand displacement
Magnet
Complementary strand
Aptamer
Target
A
B

Figure 1

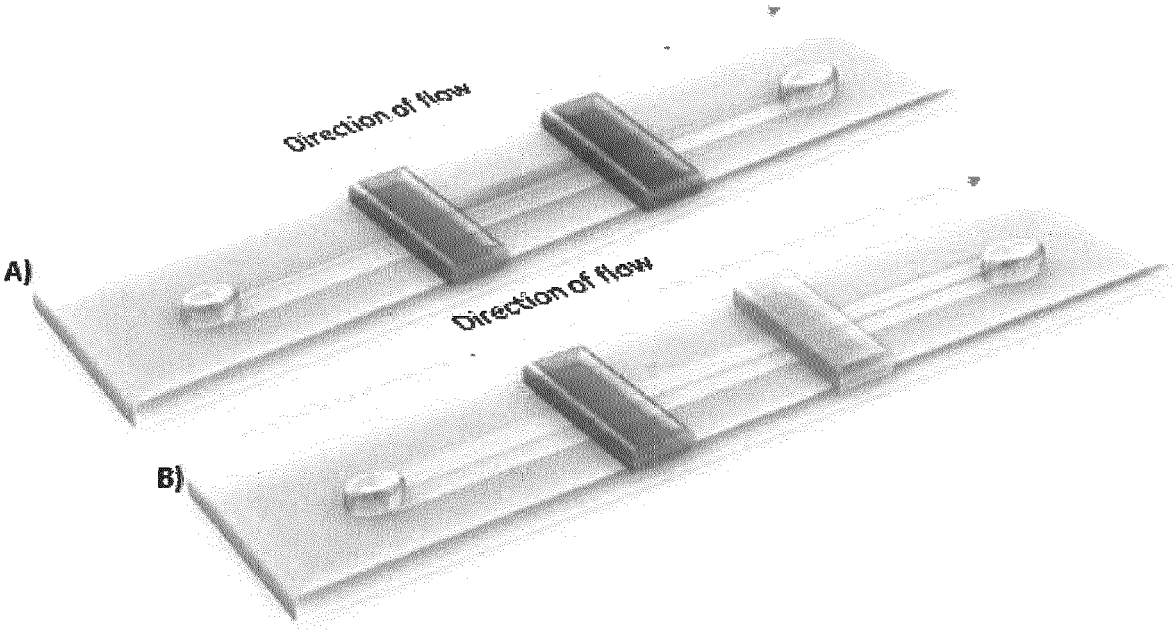

Figure 2

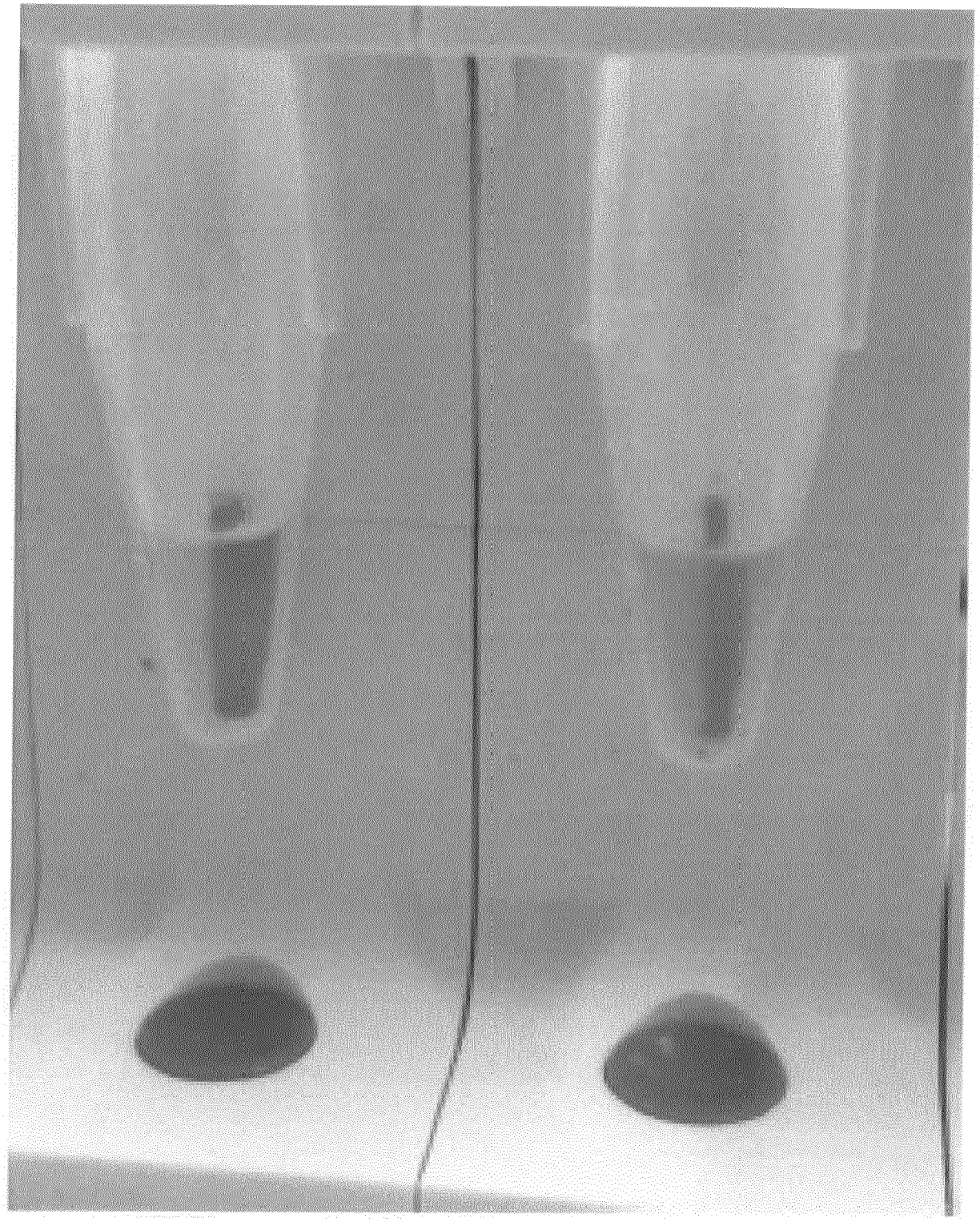

Figure 3

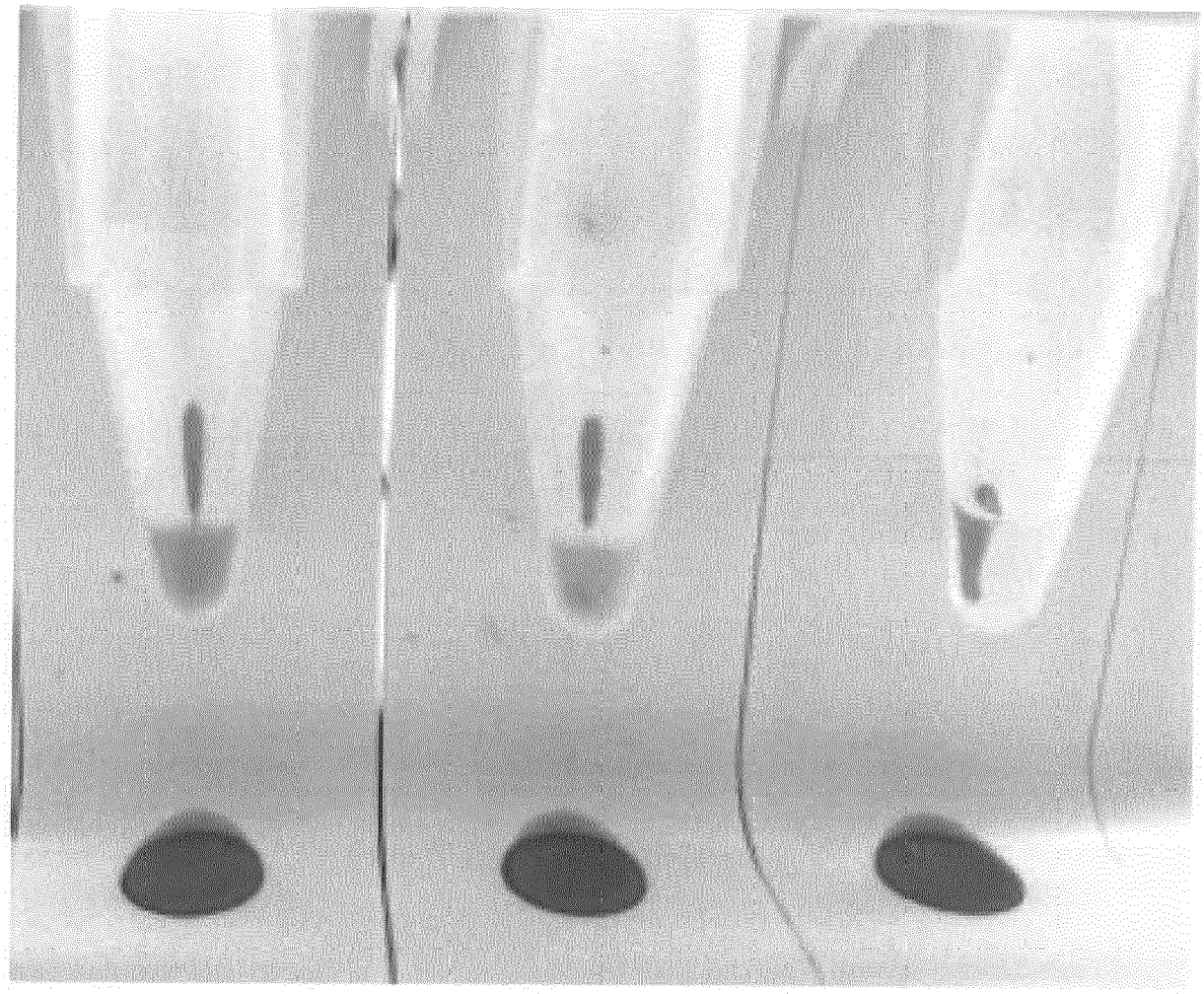

Figure 4

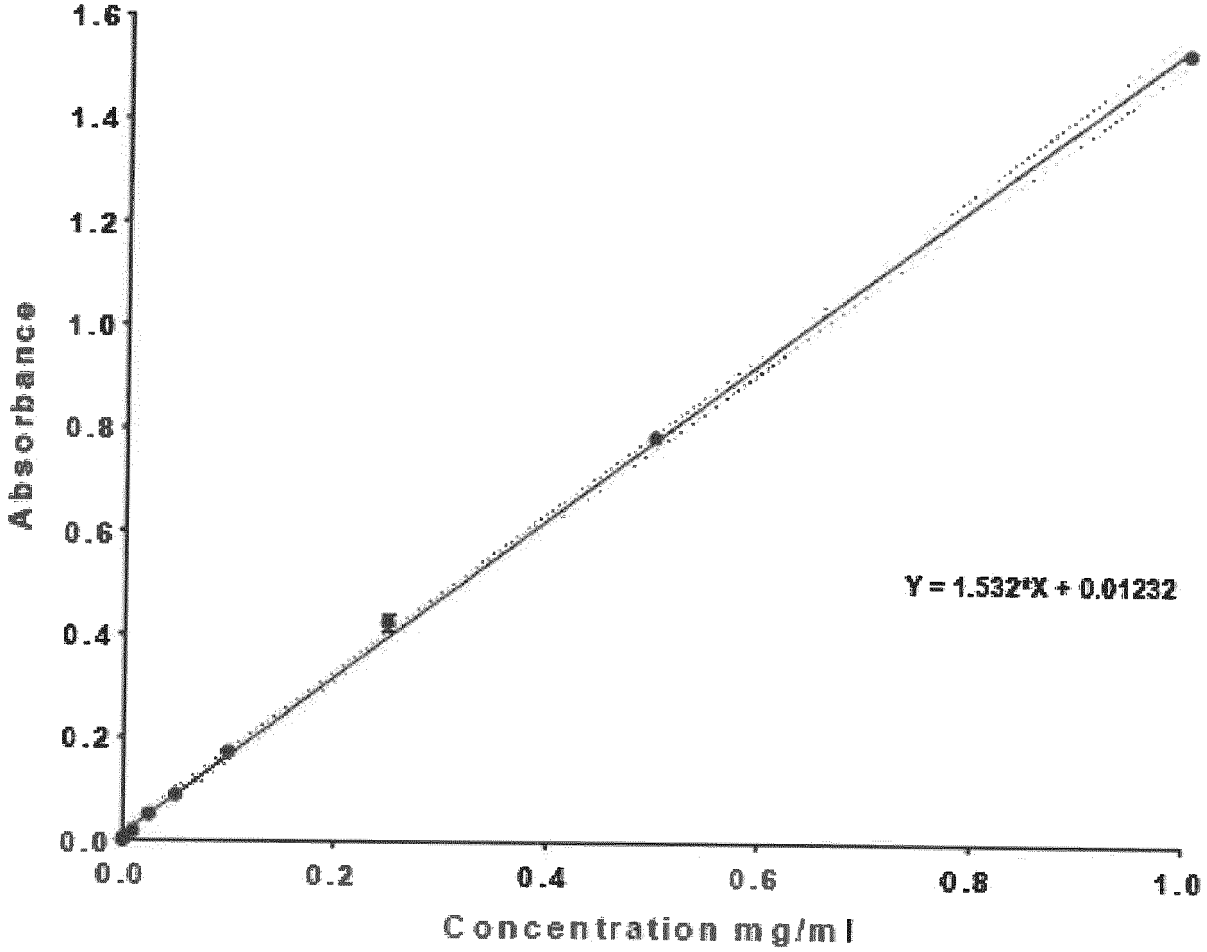
1.6
1.4
1.2
1.0
0.8
0.6
0.4
0.2
0.0
Absorbance
0.0
0.2
0.4
0.6
0.8
1.0
Concentration mg/ml
Y = 1.532*X + 0.01232

Figure 5

Europäisches Patentamt
European Patent Office
Office européen des brevets

EUROPEAN SEARCH REPORT

Application Number
EP 18 18 4111

DOCUMENTS CONSIDERED TO BE RELEVANT

Category	Citation of document with indication, where appropriate, of relevant passages	Relevant to claim	CLASSIFICATION OF THE APPLICATION (IPC)
X	WO 2018/089391 A1 (DOTS TECH CORP [US]) 17 May 2018 (2018-05-17) * abstract; claims 1-10,30-48; figures 1,3,6A-6B *	1-11	INV. C12Q1/6823 C12Q1/6825 C12Q1/6834 C12N15/115
X	WO 01/40790 A1 (QUANTUM DESIGN INC [US]) 7 June 2001 (2001-06-07) * abstract; claims 52-59; figures 7-9 *	12	
X	WO 2017/074658 A1 (UNIV PENNSYLVANIA [US]) 4 May 2017 (2017-05-04) * claims 1-12,15 *	12	
Y	WO 2009/104075 A2 (OTC BIOTECHNOLOGIES LLC [US]) 27 August 2009 (2009-08-27) * abstract; claims 1-8; figure 1 *	1-11	
Y	WO 2017/180549 A1 (DOTS TECH CORP [US]) 19 October 2017 (2017-10-19) * abstract; claims 1-22; figure 1 * * paragraph [0130] *	1-11	
			TECHNICAL FIELDS SEARCHED (IPC) C12Q C12N

The present search report has been drawn up for all claims

Place of search	Date of completion of the search	Examiner
Munich	7 September 2018	Costa Roldán, Nuria

CATEGORY OF CITED DOCUMENTS

X : particularly relevant if taken alone
Y : particularly relevant if combined with another document of the same category
A : technological background
O : non-written disclosure
P : intermediate document

T : theory or principle underlying the invention
E : earlier patent document, but published on, or after the filing date
D : document cited in the application
L : document cited for other reasons

& : member of the same patent family, corresponding document

EPO FORM 1503 03.82 (P04C01)

ANNEX TO THE EUROPEAN SEARCH REPORT ON EUROPEAN PATENT APPLICATION NO. EP 18 18 4111

This annex lists the patent family members relating to the patent documents cited in the above-mentioned European search report. The members are as contained in the European Patent Office EDP file on
The European Patent Office is in no way liable for these particulars which are merely given for the purpose of information.

07-09-2018

Patent document cited in search report	Publication date	Patent family member(s)	Publication date
WO 2018089391 A1	17-05-2018	NONE	
WO 0140790 A1	07-06-2001	AT 522805 T	15-09-2011
		AU 775690 B2	12-08-2004
		CA 2394857 A1	07-06-2001
		CN 1402833 A	12-03-2003
		EP 1240509 A1	18-09-2002
		ES 2372475 T3	20-01-2012
		JP 4657552 B2	23-03-2011
		JP 2003515743 A	07-05-2003
		US 6437563 B1	20-08-2002
		US 2001052769 A1	20-12-2001
		US 2001052770 A1	20-12-2001
		US 2004150396 A1	05-08-2004
		WO 0140790 A1	07-06-2001
WO 2017074658 A1	04-05-2017	NONE	
WO 2009104075 A2	27-08-2009	AU 2009215342 A1	27-08-2009
		CA 2684875 A1	27-08-2009
		CN 102165071 A	24-08-2011
		EP 2255015 A2	01-12-2010
		JP 2011527745 A	04-11-2011
		JP 2014131512 A	17-07-2014
		KR 20100126758 A	02-12-2010
		US 2011065086 A1	17-03-2011
		WO 2009104075 A2	27-08-2009
WO 2017180549 A1	19-10-2017	NONE	

EPO FORM P0459

For more details about this annex : see Official Journal of the European Patent Office, No. 12/82

Abbreviations

3-D	Three dimensional
DNA	Deoxyribonucleic acid
EA	Ethanolamine
ELISA	Enzyme-linked immunosorbent assay
IL-6	Interleukin-6
LC	Liquid chromatography
LF(I)A	Lateral flow (immuno)assay
LOD	Limit of detection
MEA	Mono ethanolamine
MRE	Molecular recognition element
MS	Mass spectrometry
NMR	Nuclear magnetic resonance
nt	Nucleotide
PDB	Protein Data Bank
PDB	Protein data bank
PE	Phosphatidylethanolamine
POC	Point-of-care
QD	Quantum dot
RNA	Ribonucleic acid
SELEX	Systematic evolution of ligands by exponential enrichment
STAT-3	Signal transducer and activator of transcription 3
TBA	Thrombin binding aptamer
UV	Ultraviolet
kDa	Kilo Dalton
qPCR	quantitative polymerase chain reaction